



*ugr* | Universidad  
de Granada

TELECOMMUNICATIONS ENGINEERING  
DEGREE

DEGREE THESIS

***“UHF-VHF Cubesat Antennas Design”***

ACADEMIC YEAR: 2013/2014

Teresa Lucía Aparicio Jiménez





TELECOMMUNICATIONS ENGINEERING DEGREE

***“UHF-VHF Cubesat Antennas Design”***

REALIZADO POR:

**Teresa Lucía Aparicio Jiménez**

THESIS DIRECTOR:

**Andrés María Roldán Aranda**

DEPARTAMENT:

**Electronic and Computer Technologies**



The undersigned authorizes the document submitted to be at the university library and/or at the department so it can be consulted by the public.

Granada, July, 2014

Signed.



# **UHF-VHF Cubesat Antennas Design**

**Teresa Lucía Aparicio Jiménez**

## **KEYWORDS:**

Cubesat, GranaSAT, UHF-VHF, Antenna, Feko, Computational electromagnetic techniques, Transponder, Network analyser, Spectrum analyser, PCB, Quadrifilar Helix Antenna, Turnstile, Bodipole, Circular polarization.

## **Resumen:**

Este proyecto tendrá como objetivo la comprensión de las antenas usadas en los Cubesats, un tipo de picosatélite desarrollado mayormente en universidades. El trabajo se concentrará en el análisis de sistemas usados en misiones previas dentro del ámbito de los picosatélites, recepción de señales de otros satélites y diseño de un prototipo de modelado de antenas para la misión GranaSAT.

## **Abstract:**

The main objective of this Thesis is to understand the antennas used in Cubesats (a satellite type becoming very popular among universities for teaching their students space related skills while improving their background) and to develop a prototype for future development in the GranaSAT mission. This Thesis aims to be a future reference for students developing Cubesat antennas for GranaSAT.

For start, a brief introduction on antenna theory will be made for readability purposes, introducing all the terms and the fundamental parameters necessary for understanding the Thesis like scattering parameters, standing wave ratio, input impedance of an antenna, an analysis of the radiation pattern , directivity, polarization and a brief analysis on considerations for space communications. In space communications it is fundamental to achieve circular polarization because of the effect of the ionosphere in the electromagnetic waves. The strong electric charge can change the polarization in a way that is impossible to predict, so at the ground station it is mandatory to have a circular polarized antenna.

After this introduction on antenna matters, an analysis of the solutions used in the previous mission will be developed, specially considering different approaches, as well as the study of the State of the Art solution. A popular receiving antenna called Quadrifilar Helix Antenna will be simulated with the Feko software in order to understand its behaviour. After simula-

tion, it will be built for obtaining the "know-how" about working with this kind of electronic devices, attempting to receive NOAA (National Oceanic and Atmospheric Administration from United States of America) satellites.

Once this antenna has been built and tested, a study of the chosen solution for Cubesats will be performed in order to achieve working prototypes of a bodipole an antenna designed in Standford and Turnstile antenna. Simulations for obtaining the feeding conditions depending on the fabrication purposes (like a substrate of FR4) were performed obtaining the input impedance. A study of the conditions of each antenna lead to choosing among different baluns (balanced-unbalanced lines transformer) for impedance matching and feeding purposes. A Printed Circuit Board (PCB) that could attach the balun coaxial configurations as well as the antennas all in a double layer was designed. The antennas were built and tested to compare them with the theoretical resonance frequency.

The test results were not satisfactory, as the antennas resonated at different frequencies, obtainint unexpected results. A new analysis and a new solution is proposed for the Turnstile antenna, achieving the expected frequency. The bodipole results were analysed and the reason for having a different resonant frequency is explained.

A PCB that could integrate both antenna solutions will be proposed as future working lines for persisting with the design of the antennas for GranaSAT.

*Dedicado a:*

*Mi familia, que siempre creyó en mi. A las personas que me hacen querer ser mejor cada día. Sin vuestro apoyo este sueño no sería posible.*



## ***Agradecimientos:***

Para empezar este mérito no es solo mío. Mi familia ese bastión de refugio que me ha dado tantas oportunidades como estaban en su mano tiene gran culpa de esto. En especial me gustaría agradecer a mis padres su apoyo y confianza. Gracias a Juan por ser tan buen hermano, siempre sonriente y preparado para lo que la vida le depare. En extensión este trabajo no es solo mío, si no de toda mi familia. No hay nada mejor en esta vida que tener una familia grande y saber que todos ellos están contigo, aunque se hayan marchado hace tiempo.

En especial gracias a mi abuela Justa, por preocuparse siempre de mí y hacerme sentir tan orgullosa de ser su nieta. Es una superviviente, siempre preparada para todo y dispuesta a disfrutar de la vida.

Me gustaría agradecer a Andres María Roldán Aranda su dedicación como profesor, dispuesto a afrontar los mayores retos y con una inventiva tremenda para solucionar cualquier problema, siempre siendo de gran ayuda e inspiración.

Todos son igualmente partícipes de este trabajo.



# INDEX

<b>Library Deposit Authorization</b>	v
<b>Summary</b>	vii
<b>Dedication</b>	ix
<b>Acknowledgments</b>	xi
<b>Index</b>	xiii
<b>Figure Index</b>	xix
<b>List of Tables</b>	xxv
<b>1 Introduction</b>	1
1.1 Context . . . . .	1
1.2 Prior knowledge . . . . .	3
1.3 Main bibliography . . . . .	3

<b>2 Project goals</b>	<b>5</b>
2.1 Objectives . . . . .	5
2.2 Achieved objectives . . . . .	6
2.3 Workflow and brief summary . . . . .	6
<b>3 Antenna theory introduction</b>	<b>9</b>
3.1 Introduction . . . . .	9
3.2 Scattering parameters . . . . .	10
3.3 Standing Wave Ratio . . . . .	11
3.4 Impedance . . . . .	11
3.5 Radiation pattern . . . . .	12
3.5.1 Beamwidth . . . . .	13
3.5.2 Examples . . . . .	13
3.6 Directivity . . . . .	14
3.7 Polarization . . . . .	14
3.7.1 Axial ratio . . . . .	15
3.8 Antenna system for space communication . . . . .	15
3.8.1 Azimuth and elevation angle . . . . .	15
3.8.2 Van Allen radiation belt . . . . .	16
<b>4 Previous missions</b>	<b>17</b>
4.1 Cubesat Antennas approaches . . . . .	17
4.1.1 Dipole . . . . .	18
4.1.1.1 Theory . . . . .	18
4.1.1.2 Radiation Pattern . . . . .	20
4.1.2 Folded dipole . . . . .	21
4.1.2.1 Theory . . . . .	21
4.1.2.2 Radiation Pattern . . . . .	23
4.1.3 Patch antenna . . . . .	24

4.1.3.1	Theory . . . . .	24
4.1.3.2	Radiation Pattern . . . . .	25
4.2	Comparative table . . . . .	26
4.2.1	Stanford University solution . . . . .	28
4.3	Gpredict . . . . .	31
4.3.1	Setting the ground station . . . . .	31
4.3.2	Cubesat tracking . . . . .	32
4.3.3	Transponders . . . . .	33
<b>5</b>	<b>Ground Antenna: Introductory Model</b>	<b>35</b>
5.1	Ultra High Frequency (UHF) and Very High Frequency (VHF) antennas used by FM operators . . . . .	35
5.1.1	The Yagi-Uda . . . . .	35
5.1.2	Ground-plane Antennas . . . . .	36
5.1.3	Quadrifilar Helix Antenna . . . . .	37
5.2	QHA antenna . . . . .	37
5.2.1	Far field region . . . . .	38
5.2.2	Antenna Simulations . . . . .	38
5.2.2.1	3D Antenna . . . . .	38
5.2.2.2	Single bent dipole . . . . .	38
5.2.2.3	Two bent dipoles . . . . .	40
5.3	QHA Building . . . . .	42
5.3.1	Materials . . . . .	42
5.3.2	Procedure . . . . .	42
5.3.2.1	Balun description . . . . .	43
5.3.2.2	Final Antenna . . . . .	44
5.4	QHA Characterisation . . . . .	44
5.4.1	Agilent's Network Analyser E5071C . . . . .	45

5.4.2	Determining measurement conditions . . . . .	46
5.4.3	Calibration . . . . .	46
5.4.4	Measurement setup in the Electronics Laboratory . . . . .	47
5.5	Reception with QHA . . . . .	48
5.5.1	Decoding the signal . . . . .	51
<b>6</b>	<b>Cubesat antenna design</b>	<b>55</b>
6.1	Antenna selection . . . . .	55
6.2	Antenna design . . . . .	55
6.2.1	Mechanical design . . . . .	56
6.2.1.1	3D printed Cubesat . . . . .	56
6.2.1.2	Antenna arrangement . . . . .	59
6.2.2	Matching networks and baluns . . . . .	59
6.2.2.1	Bodipole . . . . .	59
6.2.2.1.1	Using a coaxial balun . . . . .	61
6.2.2.1.2	Using passive components . . . . .	61
6.2.2.2	Tunstile . . . . .	62
6.2.2.2.1	Using a coaxial balun . . . . .	64
6.2.2.2.2	Using passive components . . . . .	65
6.2.3	PCB design for coaxial baluns . . . . .	65
6.2.4	PCB design with passive components . . . . .	68
6.3	Antennas fabrication . . . . .	72
6.3.1	PCB fabrication . . . . .	72
6.3.2	Antenna implementation on the PCB . . . . .	73
6.4	Antenna tests . . . . .	73
6.4.1	Bodipole . . . . .	74
6.4.2	Turnstile . . . . .	74
6.5	Turnstile antenna with different length . . . . .	76

6.5.1	Circular polarization . . . . .	78
<b>7</b>	<b>Conclusion and plans for the future</b>	<b>81</b>
<b>Appendix</b>		<b>83</b>
A.1	Feko Guide step by step . . . . .	83
A.1.1	Feko® overview . . . . .	83
A.1.2	Feko® user interface . . . . .	84
A.1.2.1	CADFEKO . . . . .	84
A.1.2.1.1	Selecting the model unit . . . . .	85
A.1.2.1.2	Creating variables . . . . .	85
A.1.2.1.3	Creating 3D models . . . . .	86
A.1.2.1.4	Creating ports . . . . .	87
A.1.2.1.5	Excitations . . . . .	88
A.1.2.1.6	Solution frequency . . . . .	88
A.1.2.1.7	Far field request . . . . .	89
A.1.2.1.8	Meshing . . . . .	90
A.1.2.1.9	Validating the model . . . . .	91
A.1.2.2	Feko Solver . . . . .	91
A.1.2.3	POSTFEKO . . . . .	92
A.1.2.3.1	3D Far field model . . . . .	93
A.1.2.3.2	Working with the scattering parameters . . . . .	94
A.1.2.3.3	Source data graph . . . . .	95
<b>Bibliography</b>		<b>97</b>
<b>Acronyms</b>		<b>99</b>



# FIGURE INDEX

1.1	Interconnection of satellite subsystems [1] . . . . .	2
1.2	An artists rendition of Montana State University's Explorer-1 CubeSat. . . . .	2
1.3	(a) Granasat and (b) REXUS/BEXUS logos . . . . .	3
2.1	Work flow chart . . . . .	7
3.1	Antenna as a transition device [2] . . . . .	10
3.2	Two port general network . . . . .	11
3.3	An equivalent impedance of an antenna . . . . .	12
3.4	Impedance matching of an antenna to a source . . . . .	12
3.5	Spherical coordinates [3] . . . . .	12
3.6	2D radiation pattern examples [3] . . . . .	13
3.7	(a) Isotropic, (b)omnidirectional and (c) directive radiation patterns [3] . . .	14
3.8	Polarized electromagnetic wave [4] . . . . .	14
3.9	Axial ratio in dB shown by Feko® . . . . .	15
3.10	Azimuth-Altitude schematic [4] . . . . .	16

4.1	Half wave dipole and its parasitic capacitance . . . . .	18
4.2	Elemental dipole [3] . . . . .	19
4.3	Half wave dipole designed with Feko® . . . . .	20
4.4	3D Far field radiation pattern of a dipole . . . . .	20
4.5	Far field radiation pattern of a dipole . . . . .	20
4.6	Decomposition of a folded dipole into line mode and antenna mode [5] . . . . .	21
4.7	3D folded dipole model built on Feko . . . . .	23
4.8	3D gain pattern . . . . .	23
4.9	Far field radiation patterns of a folded dipole depending on (a) $\theta$ and (b) $\phi$ . . . . .	23
4.10	The basic structure of the microstrip patch antenna [6] . . . . .	24
4.11	Four common feeding methods of microstrip patch antenna [6] . . . . .	24
4.12	Patch antenna designed with Feko . . . . .	25
4.13	Results for a far field analysis for a single frequency . . . . .	25
4.14	Far field radiation pattern of a patch antenna depending on (a) $\theta$ and (b) $\phi$ . . . . .	26
4.15	bodipole model from SNAPS [7] . . . . .	28
4.16	Dimensions of the bodipole designed by SNAPS [7] . . . . .	29
4.17	bodipole model built in Feko . . . . .	29
4.18	3D radiation pattern of the bodipole . . . . .	30
4.19	Far field radiation pattern of the bodipole depending on (a) $\theta$ and (b) $\phi$ . . . . .	30
4.20	(a) Axial ratio on dB of the bodipole at 435 MHz and (b) Handedness . . . . .	31
4.21	Setting Granada as the ground station . . . . .	31
4.22	Different groups of satellites available in Gpredict . . . . .	32
4.23	Gpredict positioning the satellites under study . . . . .	33
4.24	Vermont Lunar Cube orbit information . . . . .	33
4.25	Beesat-1 Transponder information on Gpredict® . . . . .	34
5.1	Two-element Yagi systems using a single parasitic element [8] . . . . .	36
5.2	Ground plane antenna example for 222 MHz [8] . . . . .	36

5.3	Quadrifilar Helix Antenna . . . . .	37
5.4	Bigger loop of the QHA . . . . .	39
5.5	3D radiation pattern of QHA bigger loop . . . . .	39
5.6	Far field radiation pattern at 137.5 MHz depending on (a) $\theta$ and (b) $\phi$ . . . . .	39
5.7	Complete QHA . . . . .	40
5.8	First case of QHA polarization . . . . .	40
5.9	Results of the first case of polarization (a) gain (dB) and (b) Handedness . . . . .	40
5.10	Second case of QHA polarization . . . . .	41
5.11	Results of the second case of polarization (a) gain (dB) and (b) Handedness . . . . .	41
5.12	Far field radiation pattern at 137.5 MHz depending on (a) $\theta$ and (b) $\phi$ . . . . .	41
5.13	Copper tubes and bents . . . . .	42
5.14	(a) Drilling the PVC tube and (b) assembling the tubes . . . . .	43
5.15	Built balun . . . . .	44
5.16	Antenna built . . . . .	44
5.17	E5071C Front panel [9] . . . . .	45
5.18	a) OPEN calibration, b) SHORT calibration and c) LOAD calibration. . . . .	47
5.19	<i>SWR</i> measurement of the built QHA . . . . .	47
5.20	Gpredict positioning NOAA satellites with future passes . . . . .	48
5.21	Set up for receiving at the terrace . . . . .	49
5.22	Spectrum of the signal received . . . . .	49
5.23	Reception of FM signals with a QHA . . . . .	50
5.24	Checking the polarization of the antenna. . . . .	50
5.25	(a) Phase difference between two connections (b) Phase difference between the other two connections . . . . .	51
5.26	a) Black & White image b) False colour image c) Ocean temperature . . . . .	52
5.27	Decoded picture of the audio captured with the sdr-rtl . . . . .	53
6.1	Cubesat standard [10] . . . . .	57
6.2	Cubesat model (a) in SolidWorks® . . . . .	58

6.3	3D printed Cubesat . . . . .	58
6.4	On the left Cubesat before launch and on the right with antennas deployed [11]	59
6.5	Bodipole with FR4 PCB in Feko® . . . . .	60
6.6	(a) Gain of the bodipole and (b) with FR4 substrate . . . . .	60
6.7	Bodipole impedance (a) real part and (b) imaginary part . . . . .	60
6.8	Bodipole VSWR . . . . .	61
6.9	Balun with impedance matching in AppCAD . . . . .	62
6.10	Crossed dipoles with FR4 PCB in Feko® . . . . .	62
6.11	(a) Gain of the turnstile antenna (b) with FR4 substrate . . . . .	63
6.12	Impedance (a) real part and (b) imaginary part . . . . .	63
6.13	Turnstile SWR . . . . .	64
6.14	Balun normally used for turnstile configuration . . . . .	64
6.15	Turnstile with impedance matching in AppCAD . . . . .	65
6.16	Top layer of the PCB . . . . .	66
6.17	Bottom layer of the PCB . . . . .	67
6.18	Impedance of the tracks with the design conditions . . . . .	68
6.19	PCB with passives . . . . .	69
6.20	Top layer of the PCB with passive components . . . . .	70
6.21	Bottom layer of the PCB with passive components . . . . .	71
6.22	Creating a new fabrication output . . . . .	72
6.23	Requesting the gerber files and NC drills . . . . .	72
6.24	Selecting the minimum resolution available . . . . .	72
6.25	Turnstile antenna mounted with the coaxial balun . . . . .	73
6.26	Bodipole mounted with the coaxial balun . . . . .	73
6.27	Bodipole <i>SWR</i> measurements . . . . .	74
6.28	Turnstile <i>SWR</i> measurements . . . . .	75
6.29	<i>SWR</i> of the turnstile made with wires . . . . .	75
6.30	Turnstile with copper pour . . . . .	76

6.31 <i>SWR</i> of the turnstile with copper pour . . . . .	76
6.32 Original antenna with copper pour and double size antenna . . . . .	77
6.33 <i>SWR</i> of the double size antenna . . . . .	77
6.34 Monopole working at 433 MHz . . . . .	78
6.35 Setup for measuring circular polarization of the turnstile antenna . . . . .	78
6.36 Spectrum analyser configured at 433 MHz and receiving trough the monopole	79
6.37 Monopole receiving in all angles at 433 MHz . . . . .	79
A.1 Feko workflow . . . . .	84
A.2 CADFEKO screen on startup . . . . .	85
A.3 Selecting the unit for the enviroment . . . . .	85
A.4 Defining the frequency under study . . . . .	86
A.5 Creating a variable from other variables . . . . .	86
A.6 Menu for creating a line and a polyline . . . . .	87
A.7 Selection for defining a wire port . . . . .	87
A.8 Defining the wire port parameters . . . . .	88
A.9 Selecting a voltage source . . . . .	88
A.10 Defining the voltage source parameters . . . . .	88
A.11 Selecting the frequency analysis . . . . .	89
A.12 Setting a single frequency . . . . .	89
A.13 Requesting a far field calculation . . . . .	89
A.14 Setting the far field request to cover all the points . . . . .	90
A.15 Accesing the mesh options . . . . .	90
A.16 Setting the mesh parameters . . . . .	91
A.17 Validation of the parameters . . . . .	91
A.18 POSTFEKO and Run FEKO® button . . . . .	92
A.19 POSTFEKO main window . . . . .	92
A.20 Exporting data from simulation . . . . .	93

A.21 Far field options and results . . . . .	93
A.22 (a) Axial ratio and (b) handedness of a dipole . . . . .	94
A.23 S-parameter graph options . . . . .	94
A.24 Calculations for the VSWR . . . . .	94
A.25 Source data graph options . . . . .	95

# LIST OF TABLES

4.1	Different Cubesat antenna aproaches . . . . .	18
4.2	Comparison of different missions and their antenna approach . . . . .	27
4.3	Alive/Dead Cubesats listed on Table 4.2 . . . . .	32
4.4	Actual state of the Cubesat listed on Table 4.2 . . . . .	34



# CHAPTER

## 1

# INTRODUCTION

### 1.1 Context

On my last year of the Degree in Telecommunication Technologies, I intended to do a study of how other Cubesat missions have handled the communications of their picosatellite, and perform a preliminary design for GranaSAT. GranaSAT is an academic design project from the University of Granada consisting of the development of a picosatellite. A picosatellite is an artificial satellite with the mass between 0.1 and 1 kg. The Cubesat with a mass approximately of 1.33 kg is an example of a large picosatellite.

A Cubesat is a type of satellite that is becoming very popular among universities for teaching their students space related skills while improving their background. The Cubesat program was developed by research laboratories at California Polytechnic State University and Stanford University in 1999. The purpose of the project is to provide a standard for design of picosatellites to reduce costs and development time, increase accessibility to space, and sustain frequent launches. An example of a Cubesat architecture is shown in Figure 1.1.

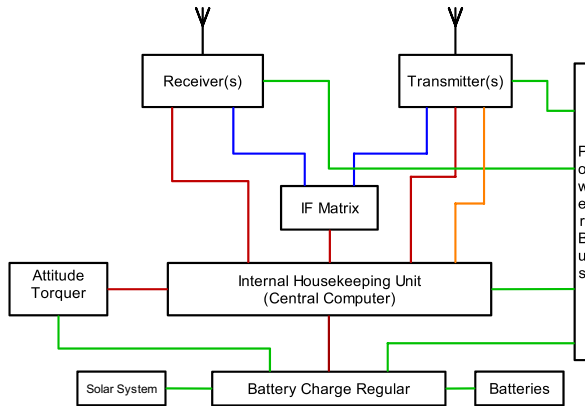


**Figure 1.1 – Interconnection of satellite subsystems [1]**

Developers benefit from the sharing of information within the community. The aim of this project is to create "educational opportunities for future leaders of industry" in their own words. Following the same model over all the different missions and programs, more than 200 Cubesat have been created around the world [10].



**Figure 1.2 – An artists rendition of Montana State University's Explorer-1 CubeSat.**

In this context, a considerable amount of universities have joined the spatial career and are developing this type of picosatellites. The University of Granada wants to be a part of this new wave of educational background so the program GranaSAT was created by the Electronics and Computer Technologies department.

The GranaSAT mission aims to design a Cubesat step by step, without the need for experts. At the moment, there are different Degree and Master Thesis being developed for this mission. Also it is participating in the BEXUS/REXUS program. The REXUS/BEXUS program is realized under a bilateral Agency Agreement between the German Aerospace Center (DLR) and the Swedish National Space Board (SNSB). The Swedish share of the payload has been made available to students from other European countries through a collaboration with the European Space Agency (ESA). This project in which I also take part leading the mechanical department, is allowing us to learn the know-how about space missions and their future applications in the GranaSAT program. The logos of both missions can be seen in Figure 1.3.

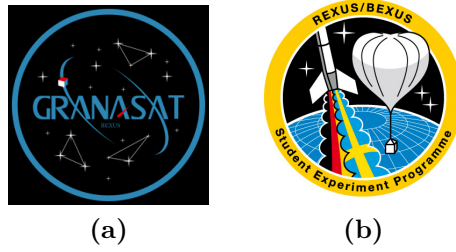


**Figure 1.3 – (a) GranaSAT and (b) REXUS/BEXUS logos**

In parallel with the REXUS/BEXUS project, the technical parts of GranaSAT are being developed following the standards [10]. Cubesat standard dimensions for the 1U model are 10x10x10 cm<sup>3</sup> and in the standard the radio-communication systems propose the use of the VHF, UHF, S- and X-band. These systems must be much smaller than what is used in conventional satellites due to space constraints.

With the help of other missions as well as the constraints from the standard [10], this Degree Thesis aims to perform an overview of antennas used in Cubesats choosing between the different approaches followed by other experiments. This Degree Thesis is intended to be a guide for future students working in GranaSAT to implement the antenna system in the picosatellite.

The laboratories dependent on the Electronics and Computer Technologies department of Granada University will be used. In that environment, the possibility to use a network analyser, a PCB milling machine and the different materials will help the creation of the Hardware of this Degree Thesis.

## 1.2 Prior knowledge

This Degree Thesis needs some prior knowledge before being faced. A background on electromagnetism is necessary for understanding the antenna related theory and being able to explain their behaviour. Also, a certain knowledge about space communications is needed for a comprehensive approach of what is happening between the transmission and reception on satellites. Advanced electronics and PCB design are important for understanding the impedance matching as well as the process of design and fabrication of the PCBs. Some other competences for having a correct development of the Thesis are self learning capacity and autonomous organization.

## 1.3 Main bibliography

The main bibliography used for documenting this Degree Thesis is the following:

- [2] Constantine A. Balanis. Antenna Theory: Analysis and Design. Wiley, 2005. ISBN 978-0471667827.

[3] Lluís Jofre Roca, Ángel Cardama Aznar. Antenas. Edicions UPC, 2002. ISBN 84-8301-625-7.

[8] American Radio Relay League. The ARRL Antenna Book. ARRL, 2000. ISBN 0-87259-804-7.

[12] Feko. Reference guide. 2014.

With the books from C. Balanis [2] and A. Cardama [3], the antenna theory was approached. They are the theoretical reference for understanding how the antennas are working. The ARRL book [8] is the reference for passing from theory to practice, explaining problems that can appear when building antennas and solutions to them. The Feko® reference guide is the pillar for performing the simulations before approaching the building of the antennas, understanding how they work and how the FR4 substrate of the PCB will change its behaviour.

## CHAPTER

# 2

## PROJECT GOALS

The requirements and constraints of this Thesis Degree will be presented as well as the achieved results. The different project chapters will be described.

### 2.1 Objectives

The main objective of this Degree Thesis is to set a base for future working in the design of GranaSAT antennas, understanding satellite communications, choosing the solution to implement and test it in a preliminary design. This objective was divided when the project was set out in February of 2014 in the following objectives:

- (1) To understand the main antenna parameters used for building antennas.
- (2) To study the most common approaches to antennas followed by other Cubesats.
- (3) To perform and understand electromagnetic simulations with a software used in industry.
- (4) To build a receiver antenna in the UHF-VHF band.
- (5) To receive signals from already existing satellites.
- (6) To study antenna polarization with a built model.
- (7) To design a prototype of a working antenna with circular polarization to implement in GranaSAT.

- (8) To build a prototype of a working antenna with circular polarization to implement with an easy deployment method, without the need of a mechatronics expert.

## 2.2 Achieved objectives

The 1st and 2nd goals correspond with a documentation stage. This stage was one of the longest because of the lack of knowledge about antennas when facing the project. These goals were all achieved as can be seen in Chapter 3, and in Chapter 4.

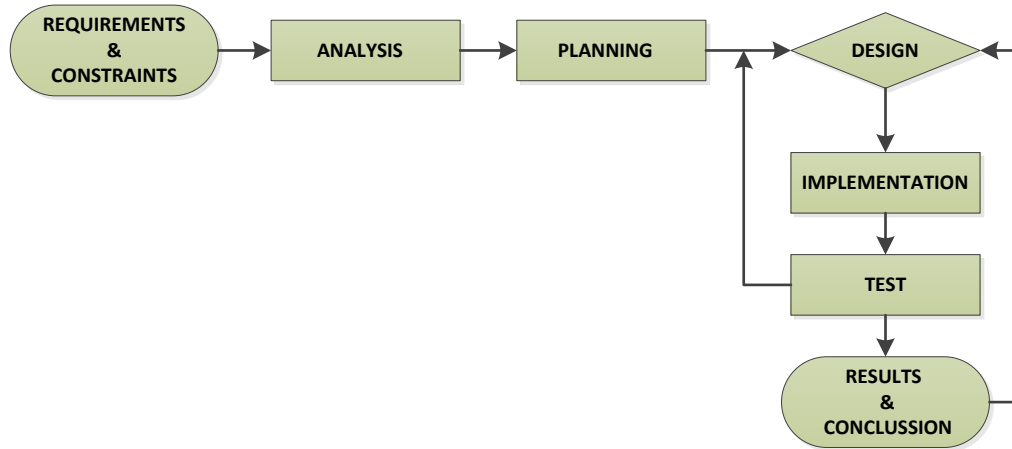
The 3rd goal was essential for understanding all the simulations performed during this whole Degree Thesis. In Appendix A.1 there is a step by step guide of how to perform and explain the simulation results, and in Chapter 4, Chapter 5 and Chapter 6 there are a large number of simulations with Feko®, a piece of software largely used in the industry. This objective was completely achieved.

Objectives 4, and 5 are concerned with the fabrication of a Quadrifilar Helix Antenna for receiving NOAA satellites in Chapter 5. The antenna was built, fully achieving the 4th objective and a noisy signal is received with a software defined radio, but not good enough to obtain all the information the satellite sent. Objective 5 is partially achieved, and solutions are proposed on the same chapter for receiving a clean signal.

The 6th, 7th and 8th objectives are met in Chapter 6, where an antenna system is proposed with the mechanical restriction of their deployment. One antenna is made of tape measure, allowing a simple deployment and another is integrated in the Cubesat. Two designs of this system are proposed, building the simpler one (made with coaxial baluns) as a prototype and proposing the second (with a balun composed of passive elements) for further work on the development of GranaSAT antennas. The antennas built are tested and circular polarization is achieved. This objective is fully achieved.

## 2.3 Workflow and brief summary

Once the context and the scope of this Degree Thesis is described, we can observe in Figure 2.1 the work flow chart followed.

**Figure 2.1 – Work flow chart**

Based on the diagram, the chapters will be numbered with the common thread being the understanding of Cubesat antennas.

- **Chapter 3:** A brief introduction on antenna theory with the description of all the parameters used during this Degree Thesis. The antennas will be modelled as impedances and studied like a circuit.
- **Chapter 4:** An analysis of the antennas in previous missions as well as a description of the State of the Art in Cubesat antennas will be performed. A software for satellite tracking will be described and used for positioning the different satellites in their orbits.
- **Chapter 5:** There will be a presentation of some ground antennas used for receiving satellites. An antenna for receiving the weather satellites of the National Oceanic and Atmospheric Administration of the United States will be built and tested.
- **Chapter 6:** A 3D model of the Cubesat will be built for the antenna mechanical constraints. Using the model developed and the analysis of Chapter 2 a prototype PCB will be designed for mounting a turnstile antenna and a bodipole. Antennas are built and tested. After obtaining results different than expected, an explanation of the behaviour and a new model of PCB is designed.
- **Chapter 7:** Brief conclusion and future development.



## CHAPTER

# 3

# ANTENNA THEORY INTRODUCTION

In this chapter, a brief introduction of the main antenna parameters will be made. The antennas will be analysed from a circuital point of view in this Degree Thesis. This analysis will be focused on enumerating the essential parameters of an antenna to understand its behaviour as well as on the parameters used during this thesis.

### 3.1 Introduction

Antennas belong to a class of electronic devices called transducers. This term is derived from two Latin words, meaning literally “to lead across” or “to transfer.” Thus, a transducer is a device that transfers, or converts, energy from one form to another. The purpose of an antenna is to convert radio-frequency electric current to electromagnetic waves, which are then radiated into space. The IEEE Standard Definitions of terms for Antennas (IEEE Std 145–1983) defines the antenna or aerial as “a means for radiating or receiving radio waves”. The guiding device or transmission line may take the form of a coaxial line or a hollow pipe (waveguide), and it is used to transport electromagnetic energy from the transmitting source to the antenna, or from the antenna to the receiver. In the former case, we have a transmitting antenna and in the latter a receiving antenna [2].

The main difference between an antenna and an ordinary electronic circuit is that normally the dimensions of the components are small compared to the wavelength. In antenna theory

the wavelength ( $\lambda$ ) is defined as:

$$\lambda = \frac{c}{f} \quad (3.1.1)$$

Where in Equation 3.1.1  $c$  is the speed of light and  $f$  the working frequency.

When circuit dimensions are small compared to  $\lambda$ , most of the electromagnetic energy is confined to the circuit itself, and is used up either performing useful work or is converted into heat. However, when the dimensions of wiring or components become significant compared with the wavelength, some of the energy escapes through radiation in the form of electromagnetic waves [8]. The electric field in a transition device can be seen in Figure 3.1.

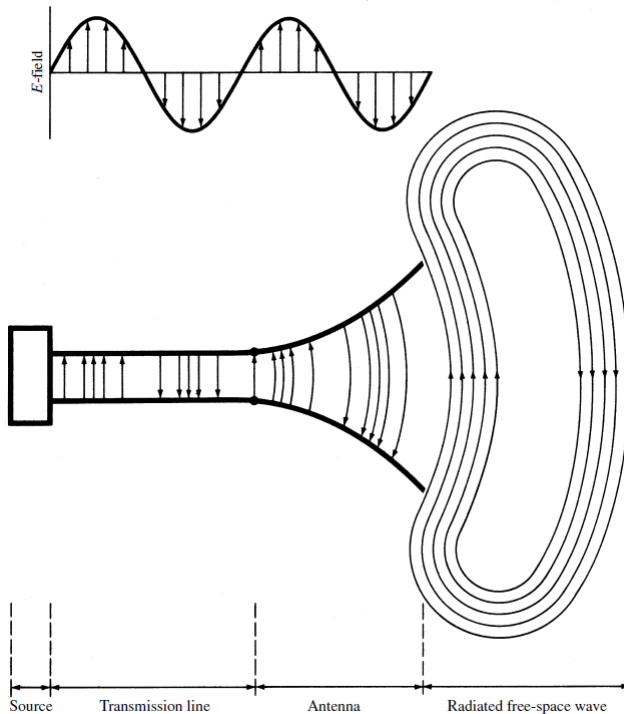


**Figure 3.1 – Antenna as a transition device [2]**

In this Degree Thesis the antennas will be considered from an electronic point of view. The antenna will be considered as an impedance that will be feed by a source. For obtaining the radiation pattern of them Feko® will be used for performing simulations.

## 3.2 Scattering parameters

Linear two-port (and multi-port) networks are characterized by a number of equivalent circuit parameters such as the scattering matrix. Figure 3.2 shows a typical two port network.

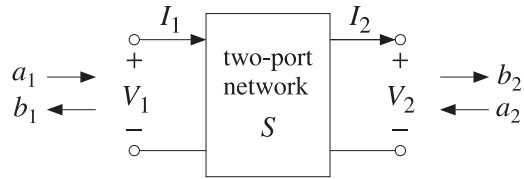


**Figure 3.2 – Two port general network**

The scattering parameters of the two port network are defined in Equations 3.2.1, 3.2.2, 3.2.3 and 3.2.4.

$$S_{11} = \frac{b_1}{a_1} \Big|_{Z_L=Z_0} \quad (3.2.1)$$

$$S_{12} = \frac{b_1}{a_2} \Big|_{Z_s=Z_0} \quad (3.2.2)$$

$$S_{21} = \frac{b_2}{a_1} \Big|_{Z_L=Z_0} \quad (3.2.3)$$

$$S_{22} = \frac{b_2}{a_2} \Big|_{Z_s=Z_0} \quad (3.2.4)$$

The parameter  $S_{11}$  is known as the input reflection coefficient,  $S_{22}$  as the output reflection coefficient. The scattering parameters will be used for characterising different antenna configurations under this thesis.

### 3.3 Standing Wave Ratio

The SWR is the ratio comparing the maximum value of a partial standing wave in comparison with the minimum in an electrical transmission line. It is usually defined as a voltage ratio, called Voltage Standing Wave Ratio. The definition of this parameter is in Equation 3.3.1.

$$\text{SWR} = \frac{1 + \|S_{11}\|}{1 - \|S_{11}\|} \quad (3.3.1)$$

### 3.4 Impedance

The input impedance of an antenna  $Z_{in}$  will have a real part  $R_{in}(\omega)$  and an imaginary part  $X_{in}(\omega)$  defined by the voltage-current relations on the input.  $Z_{in}$  allows to obtain a circuital model as seen in Figure 3.3. The antenna will be connected to a transmitter in order to radiate the maximum power with the minimum loss possible. This can be achieved by doing complex impedance matching (Figure 3.4).

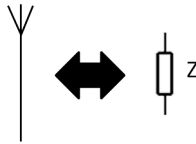


**Figure 3.3 – An equivalent impedance of an antenna**

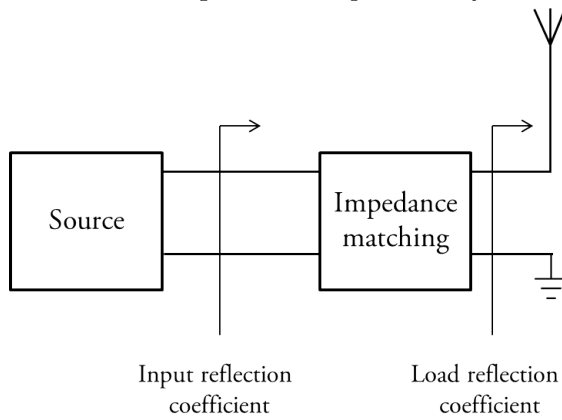


**Figure 3.4 – Impedance matching of an antenna to a source**

### 3.5 Radiation pattern

A Radiation pattern defines the variation of the power radiated by an antenna as a function of the angles  $\theta, \phi$  at a fix distance. The antenna is positioned at the origin of the spherical coordinate axis (Figure 3.5).

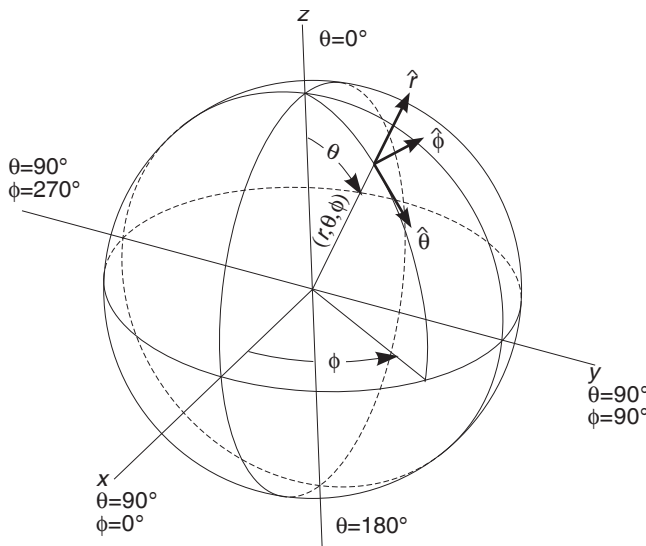


**Figure 3.5 – Spherical coordinates [3]**

If the antenna is observed from a long distance, the radiation will be seen as coming from a single point. Very far from a point source the wave fronts are essentially plane waves. This

is called the Fraunhofer regime, and the diffraction pattern is called Fraunhofer diffraction. For antennas physically larger than a half-wavelength of the radiation they emit, the near and far fields are defined in terms of the Fraunhofer distance following Equation 3.5.1.

$$d_f = \frac{2D^2}{\lambda} \quad (3.5.1)$$

Where,  $D$  is the largest dimension of the radiator.

Although a 3D radiation pattern can be useful for studying near and far field, for engineering purposes it is better to have the information on 2D by making a cross-section diagram. There are two main drawings:

- Cross-section with  $\phi$  constant.
- Cross-section with  $\theta$  constant.

3

An example of 2D diagram can be seen in Figure 3.6.

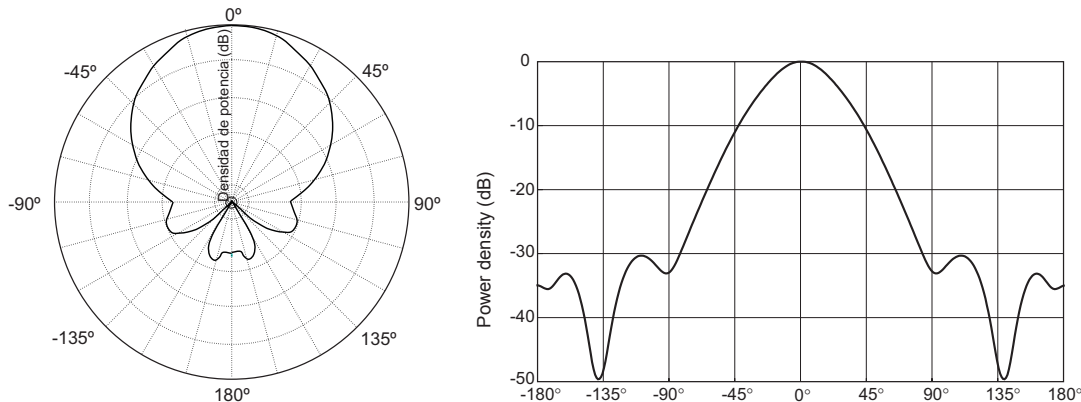


**Figure 3.6 – 2D radiation pattern examples [3]**

### 3.5.1 Beamwidth

The *beamwidth* ( $\Delta\theta_{-3dB}$ ), is the distance in degrees between the points where the transmitted power is the half of its maximum (3dB).

### 3.5.2 Examples

There are three radiation patterns used as a base reference for understanding other radiation pattern. They can be seen in Figure 3.7.

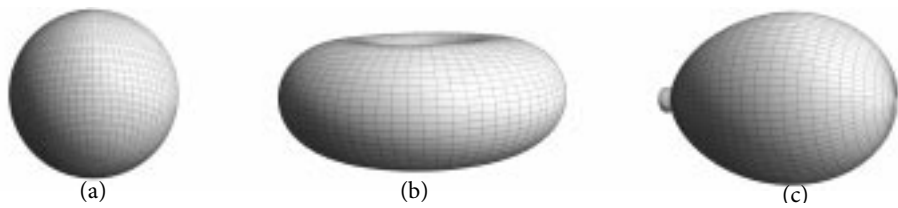


**Figure 3.7 – (a) Isotropic, (b) omnidirectional and (c) directive radiation patterns [3]**

An *isotropic* antenna is an antenna that delivers the same power into all space directions. An *omnidirectional* antenna radiates its power uniformly in a plane. A *directive* antenna directs its energy in a narrow beam.

## 3.6 Directivity

The *directivity* of an antenna is equal to power radiated in a direction divided by the power density radiated at the same distance by an isotropic antenna (Equation 3.6.1).

$$D(\theta, \phi) = \frac{P(\theta, \phi)}{P_r / 4\pi r^2} \quad (3.6.1)$$

## 3.7 Polarization

An antenna's polarization is that of its electric field, in the direction where the field strength is maximum.

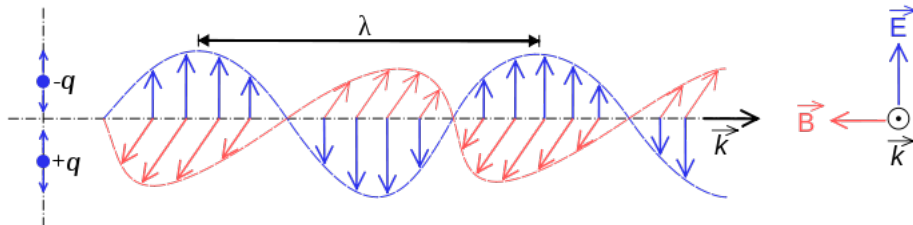


**Figure 3.8 – Polarized electromagnetic wave [4]**

Lineal polarization is achieved when the electric field and the magnetic field are perpendicular to each other and to the direction the plane wave is propagating. If vertical and horizontal elements in the same plane are fed out of phase (where the beginning of the RF period applied to the feed point of the vertical element is not in time phase with that applied to the horizontal), the resultant polarization is elliptical. Circular polarization is a special case of elliptical polarization. The wave front of a circularly polarized signal appears (in passing a fixed observer) to rotate every 90° between vertical and horizontal, making a complete 360° rotation once every period. Field intensities are equal to all instantaneous polarizations. Circular polarization is frequently used for space communications [8].

### 3.7.1 Axial ratio

The *axial ratio* is the ratio of orthogonal components of an E-field. When there is circular polarization, the axial ratio is 0 dB. If the axial ratio is larger than 0 dB, we will have an elliptical polarisation [2]. The axial ratio for lineal polarisation is infinite.

In Feko®, we can observe the polarization of an antenna using the *axial ratio* parameter as shown in Figure 3.9.

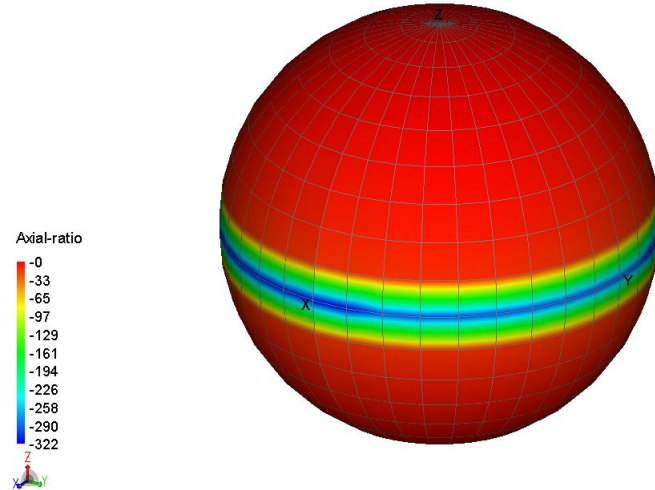


**Figure 3.9 – Axial ratio in dB shown by Feko®**

## 3.8 Antenna system for space communication

There are two basic modes of space communications: satellite and earth-moon-earth (EME also referred to as moonbounce). Both require consideration of the effects of polarization and elevation angle which were commented on in Section 2, along with the azimuth directions of transmitted and received signals. In this Degree Thesis, satellite communications will be considered.

### 3.8.1 Azimuth and elevation angle

The azimuth (az) angle is the compass bearing, relative to geographic north, of a point on the horizon directly beneath an observed object. The elevation (el) angle, also called the altitude, of an observed object is determined by first finding the compass bearing on the horizon relative to true north, and then measuring the angle between that point and the object, from the reference frame of the observer. It is easier to understand these concepts by looking at Figure 3.10.

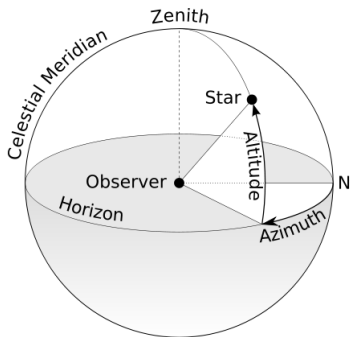


**Figure 3.10 – Azimuth-Altitude schematic [4]**

### 3.8.2 Van Allen radiation belt

The Low Earth Orbit (LEO) and Medium Earth Orbit (MEO) satellites orbit in the Van Allen belt, which lie between the magnetosphere and ionosphere. The Van Allen Belt is formed by two zones encircling the earth in which there are relatively large numbers of high-energy charged particles. LEO satellites are orbiting under the most intense and damaging portions of the lower Van Allen belts. The energetic particles can damage the exposed antenna components. Due to this effect, the electromagnetic wave can change its plane of polarization. Receiver antennas on Earth should always have circular polarization for receiving from Space.

## CHAPTER

# 4

## PREVIOUS MISSIONS

Regarding the Cubesat programme, as the information is shared, an analysis of previous educational missions can be made. The Cubesat antennas description are not only available on educational papers, a big number of enterprises and spin-offs have started selling technology related to this field after a Cubesat development in different universities. The analysis will be focused specially on 1U Cubesat (same size as GranaSAT). Their dimensions are 10x10x10 cm<sup>3</sup>, so for an antenna bigger than 10 cm long a deployment method will be needed.

This chapter starts with a small introduction to those antennas most used in Cubesat applications. After describing the most common antennas, a comparison chart of the technology used will be presented. Using a free software real-time satellite tracking and orbit prediction application we can check the frequencies used on each satellite and their position at the moment, this software will be used for positioning the selected satellites still alive in their trajectory.

### 4.1 Cubesat Antennas approaches

As mentioned before, our focus is on 1U Cubesats [10]. Following the standard design requirements described in Chapter 2 different solutions are presented in different universities, pursuing an evolution aiming for higher data rate. The different approaches considered for space exploration are described on the following subsections, but as a starter, we can consider the Table 4.1.

Antenna type	Frequency range in satellites	Configuration	Deployment	Gain [dB]	Beamwith [°]
Half wave dipole	VHF [30MHz,300MHz]	Unfolt	Yes	2	78
	UHF [300MHz,3GHz]				
Folded dipole	VHF [30MHz,300MHz]	Bent	No	2	78
	UHF [300MHz,3GHz]				
Patch	S-band [1.5GHz,5.2GHz]	Sticker	No	7-9	65

**Table 4.1 – Different Cubesat antenna approaches**

#### 4.1.1 Dipole

A dipole antenna is a vertical radiator fed in the centre which consists of two terminals. The length of the radiating element determines many of the properties of the antenna like impedance, working frequency, radiation pattern, etc.

##### 4.1.1.1 Theory

Historically, the  $\lambda/2$  dipole is one of the most used by amateurs worldwide [8] because of its easiness to build and its effective performance. A dipole is normally feed in the centre, but there are as well *off-centre-fed-dipoles*.

The current is driven into a dipole with open circuit end. To understand how the current can close its path we need to consider the parasitic capacitance between the arms of the dipole which will generate a return path for the current as seen in Figure 4.1

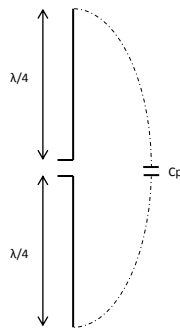


**Figure 4.1 – Half wave dipole and its parasitic capacitance**

As mentioned in Chapter 3, we are interested in the antenna circuital analysis. For this purpose, we are interested in obtaining the equivalent impedance of the antenna at the feed point.

The radiation resistance is defined by Equation 4.1.1

$$R_r = \frac{P_r}{I(0)^2} \quad (4.1.1)$$

$P_r$  is the total power radiated. It is obtained integrating the power density created by an antenna in a completely covered closed surface. For obtaining  $I(0)$  we can consider an ideal rectilinear wire with an small radius compared to wave length as seen in Figure 4.2

4

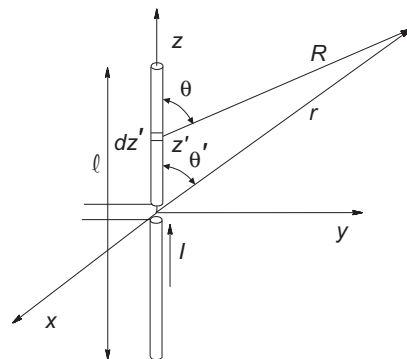


**Figure 4.2 – Elemental dipole [3]**

The current at the feed point is defined by Equation 4.1.2, if we consider the dipole as a transmission line of parallel wires open-ended.

$$I_0 = I_m \sin kH \quad (4.1.2)$$

Where  $I_m$  is the current maximum and  $k = \frac{2\pi}{\lambda}$ . Using a theoretical analysis we can determine the impedance of the dipole as seen on [3]. The real part of the half wave dipole is then  $R_r = 73\Omega$ .

The imaginary part is calculated considering a transmission line open-ended.

$$X_e = -jZ_0 \cot kH \quad (4.1.3)$$

Considering  $Z_0$  as the characteristic impedance of the transmission line formed by the dipole,  $X_e = j21\Omega$ .

$$Z_{in} = 73 + j21\Omega \quad (4.1.4)$$

#### 4.1.1.2 Radiation Pattern

Using Feko® as described in the Appendix A.1, we developed a 3D model of a half wave dipole at 75 MHz to obtain its radiation pattern. The results can be seen in Figure 4.3 with the feeding port placed in the middle.

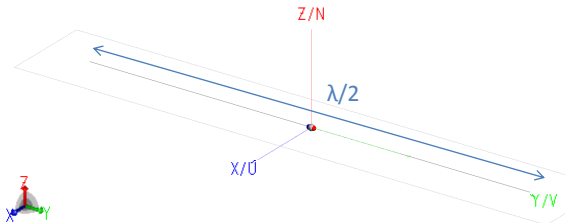


**Figure 4.3 – Half wave dipole designed with Feko®**

The solution frequency was set to 75 MHz and the segment radius to 1 mm for meshing. The results obtained in POSTFEKO are shown in the Figures 4.4 and Figure 4.5.

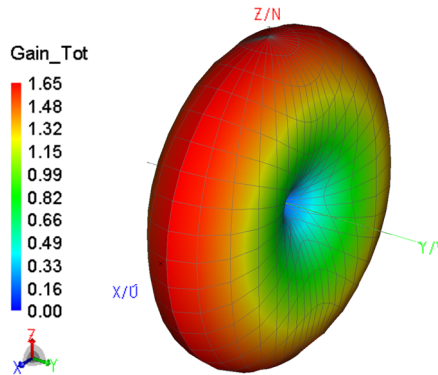


**Figure 4.4 – 3D Far field radiation pattern of a dipole**

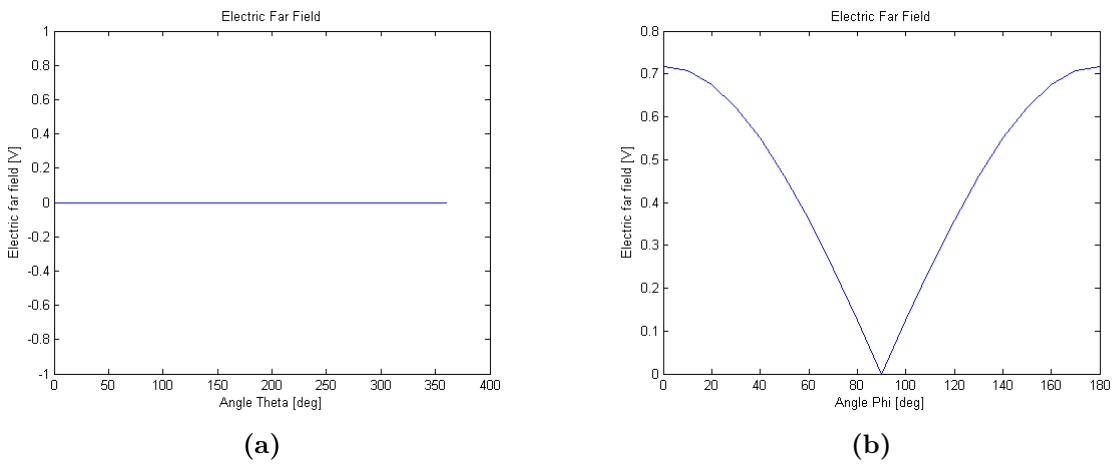


**Figure 4.5 – Far field radiation pattern of a dipole**

### 4.1.2 Folded dipole

The folded dipole consists of two conductors each of  $\lambda/2$  length, connected. It has a wider bandwidth than a fundamental dipole and a better mechanical strength.

#### 4.1.2.1 Theory

The folded dipole input impedance is four times bigger than the normal dipole, this can be proven if we assume the folded dipole to be as an unbalanced transmission line. the current that circulates on the antenna under analysis is split into two different modes (Figure 4.6).

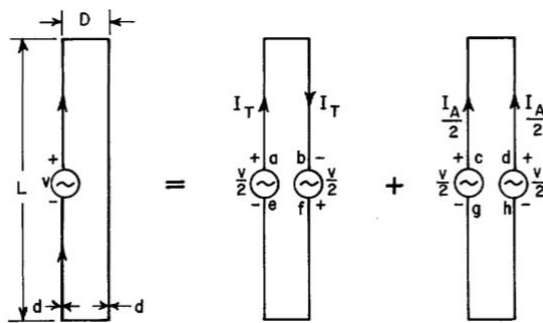


**Figure 4.6 – Decomposition of a folded dipole into line mode and antenna mode [5]**

A first mode in which we consider the folded dipole into line mode as defined in Figure 4.6. The line impedance is defined by Equation 4.1.5

$$Z_T = Z_0 * \frac{Z_L + jZ_0 \tan(kl')}{Z_0 + jZ_L \tan(kl')} \quad (4.1.5)$$

For the folded dipole we consider:

$$l' = \frac{l}{2} \quad (4.1.6)$$

In line mode we consider the input impedance seen from the points *a* and *b* as a short-circuit, obtaining:

$$Z_L = 0 \quad (4.1.7)$$

Replacing the values defined in Equations 4.1.6 and 4.1.7 into Equation 4.1.5:

$$Z_T = jZ_0 \tan k \frac{l}{2} \quad (4.1.8)$$

The voltage difference between *a* and *b* is equal to  $\frac{V}{2}$ , so the current that flows into the line is in Equation 4.1.9.

$$I_T = \frac{V/2}{Z_T} \quad (4.1.9)$$

In the antenna mode the current  $I_A$  (Equation 4.1.10) depends on the dipole's input impedance, which we will define as  $Z_D$ .

$$I_A = \frac{V/2}{Z_D} \quad (4.1.10)$$

The radius used for computing  $Z_D$  will be an equivalent wire radius defined in Equation 4.1.11.

$$\ln a_e = \ln a + \frac{1}{2} \ln \frac{D}{a} \quad (4.1.11)$$

Once decomposed the model, we can compute the final value of the current:

$$I_{in} = I_T + \frac{I_A}{2} = \frac{V(2Z_D + Z_T)}{4Z_T Z_D} \quad (4.1.12)$$

$$Z_{in} = \frac{V}{I_{in}} = \frac{4Z_T Z_D}{2Z_D + Z_T} \quad (4.1.13)$$

Equation 4.1.13 can be used for computing the input impedance of a folded dipole of any length. In this case we have the conditions defined in Equation 4.1.6, so then we can assume that the current distribution on the folded dipole added together  $I_{in}$  will be the same as on the half-wave dipole  $I_D$ . The radiating power should be the same in both cases:

$$P_D = P_F \quad (4.1.14)$$

$$\frac{1}{2} Z_D I_D^2 = \frac{1}{2} Z_{in} I_{in}^2 \quad (4.1.15)$$

$$\frac{1}{2} Z_D I_D^2 = \frac{1}{2} Z_{in} \frac{I_D^2}{2} \quad (4.1.16)$$

$$4Z_D = Z_{in} \quad (4.1.17)$$

### 4.1.2.2 Radiation Pattern

Using the Feko Software we designed a 3D model of a Folded dipole at a frequency of 137.5 MHz fed in the centre with a radius of 1 mm.

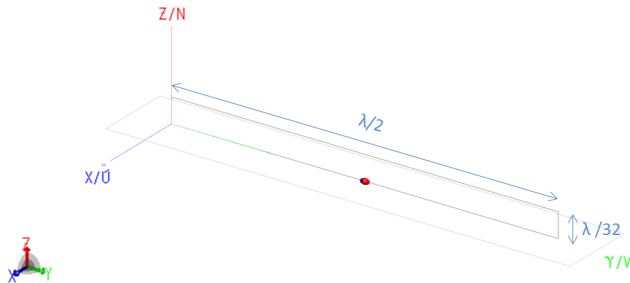


**Figure 4.7 – 3D folded dipole model built on Feko**

The results of the simulation for the radiation pattern are shown in Figure 4.8 and Figure 4.9.

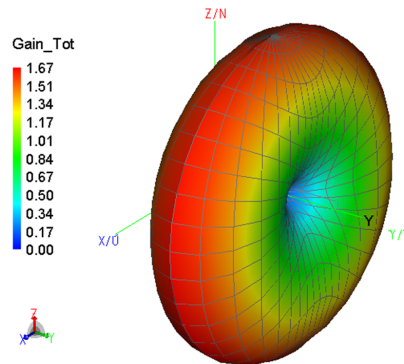


**Figure 4.8 – 3D gain pattern**

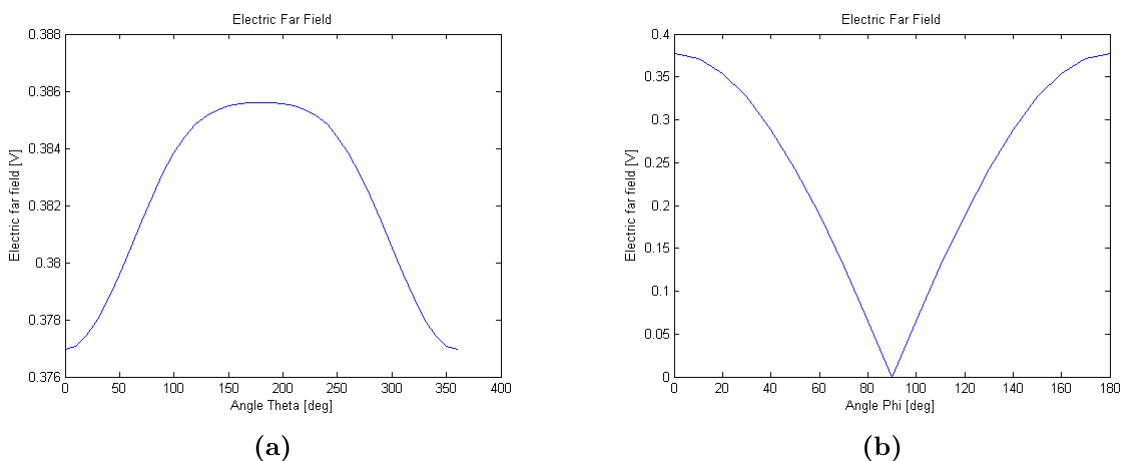


**Figure 4.9 – Far field radiation patterns of a folded dipole depending on (a)  $\theta$  and (b)  $\phi$**

This antenna has largely been used in radio applications as it can be seen in chapter 5 in [8].

### 4.1.3 Patch antenna

#### 4.1.3.1 Theory

The idea of microstrip patch antennas arose from using printed circuit technology not only for the circuit components and transmission lines but also for the radiating elements of an electronic system. It was first proposed by Deschamps [13] in 1953, but did not become practical until 1970 when this antenna was developed into more details.

The basic structure is described in Figure 4.10. It has a thin dielectric substrate above a ground plane. The patch shape can be really different, but on the right of Figure 4.10 there is a representation of the most common shapes.

A patch antenna is normally feed by either coaxial probe, microstrip line feed, aperture-coupled feed and proximity feed (Figure 4.11).

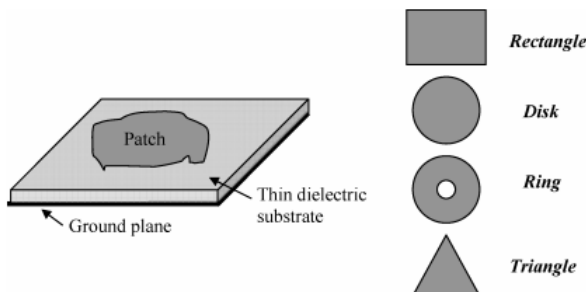


**Figure 4.10 – The basic structure of the microstrip patch antenna [6]**

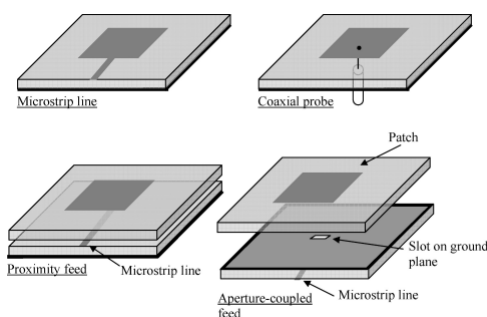


**Figure 4.11 – Four common feeding methods of microstrip patch antenna [6]**

This kind of antennas are available off-the-shelf, but for omnidirectional coverage we would require multiple patch antennas. A patch antenna can be produced by printed circuit technology and does not need a deploy method. It has a greater gain than the dipole and folded dipole antenna as described in Table 4.1.

### 4.1.3.2 Radiation Pattern

We can design a 3D model of a patch antenna working on 7.5 GHz. We will create a perfect electric conductor polygon that is supported in a dielectric substrate. In Figure 4.12 the antenna can be seen in the middle of free space, marked on red.

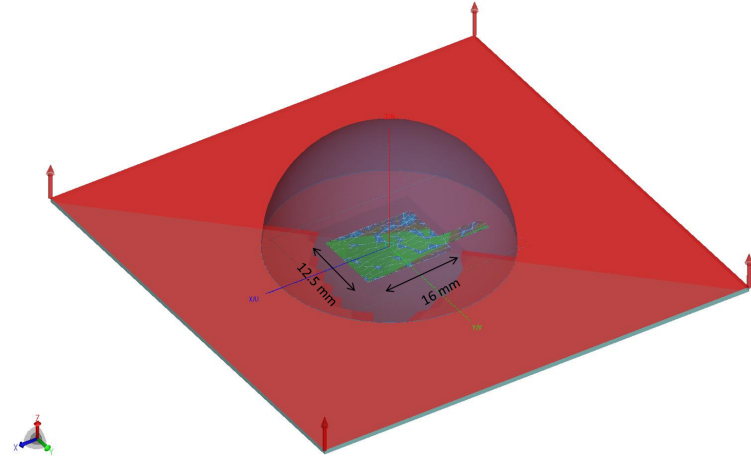


**Figure 4.12 – Patch antenna designed with Feko**

The simulation results are in Figures 4.14.

4

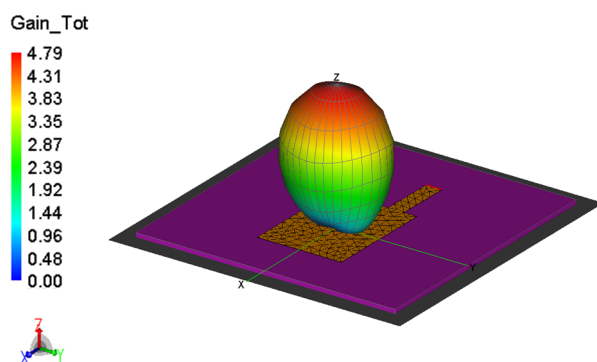


**Figure 4.13 – Results for a far field analysis for a single frequency**

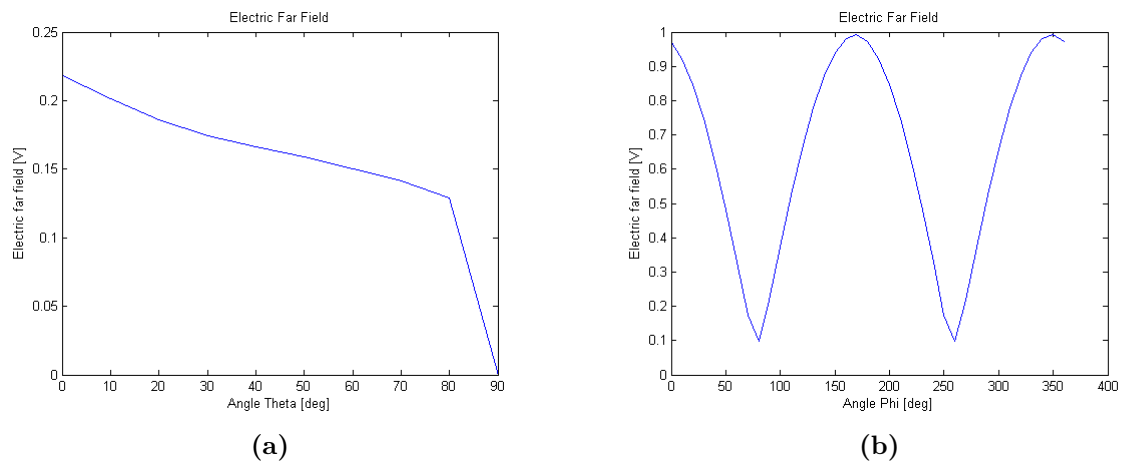


**Figure 4.14 – Far field radiation pattern of a patch antenna depending on (a)  $\theta$  and (b)  $\phi$**

## 4.2 Comparative table

In the next table, an analysis of the previous missions is performed with its more important parameters. Not all the Cubesat missions are described since that would be a complete Bachelor Thesis on its own, but we have chosen different examples of antennas used for a comparison.

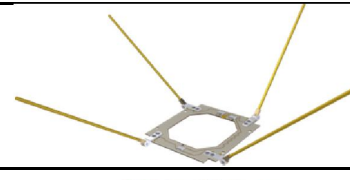
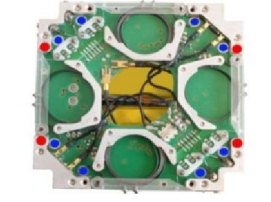
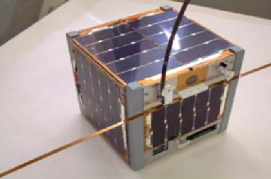
Mission	Support	Launch date	Estimated life span	Antenna development	Antenna type	Working frequency	Positioning
<a href="#">AAU1 Cubesat</a>	Aalborg University (Denmark)	30/06/2003	3 months	Comercial from OSS (price not available)	Dipole	437.425 MHz [Half duplex]	
<a href="#">DTUsat-1</a>	Technical University of Denmark	01/07/2003	0 days	Designed at University	Canted turnstile [Half duplex]	437.475 MHz [Half duplex]	
<a href="#">ArduSat-1</a>	Kickstarter	19/10/2013	2+ months	Comercial from GomSpace (5.550 €)	Turnstile Antenna	437.325 MHz [Half duplex]	
<a href="#">Vermont Lunar Cube</a>	Vermont Technical College (USA)	20/10/2013	1+ month	Commercial from ISIS (4.500 €)	Crossed dipoles	DL: 437.305 MHz UL: 150 MHz	
BEESAT1	Technical University of Berlin (Germany)	23/07/2009	43+ months	Designed at University	Quarter-wave monopole antennas with toroidal radiation pattern.	436 MHz [Half duplex]	
BEESAT2	Technical University of Berlin (Germany)	19/04/2013	2+ weeks	Designed at University	2xMonopole	435.95 MHz [Half duplex]	
BEESAT3	Technical University of Berlin (Germany)	19/04/2013	2+ weeks	Designed at University	UHF Monopole & S Patch antenna	DL: 435.950 MHz UL: 2.263 MHz	
<a href="#">CUTE-1</a>	Tokyo Institute of Technology (TITech) and SRTL (Space Robotics and Teleoperations Laboratory) of Tokyo (Japan)	30/06/2013	118+ months	Designed at University	3xMonopole	DL & CW: 430 MHz UL: 144 MHz	

Table 4.2 – Comparison of different missions and their antenna approach

As it can be seen in the comparative table, there are some commercial solutions starting at a few thousand euros [14]. There are more than fifty enterprises that commercialise antennas for Cubesats, and most of them come from a Cubesat project at University. Having the whole communication system developed at the University allows the student to face a real engineering challenge. In GranaSAT, we decide to develop the antenna at the university, following the path of many universities like the Technical University of Berlin and Tokyo Institute Technology among others.

The antenna approaches are different, but they all fit into the requirements established in [10]. All of them are deployable, making the mechanics of the satellite more difficult and error-prone.

#### 4.2.1 Stanford University solution

As the engineering evolves within the Cubesat technologies, there are other solutions avoiding deployable methods. The solution developed by the Space and System Development Laboratory of Stanford requires a special mention. They developed a miniature satellite (2.5x10x10cm) capable of imaging, on-board photo processing and analysis as well as down-link. The Stanford Nano Picture Satellite (SNAPS) architecture is open and well documented, and allows end users to tailor hardware and software to their application [7].

SNAPS utilizes a “BodiPole” UHF antenna, which is integrated into the body of the space-craft, avoiding deployable methods. It is a folded, bent dipole with a length of  $\sim 30\text{cm}$  working at 435 MHz.

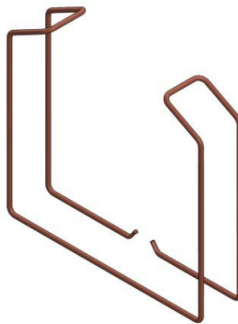


**Figure 4.15 – bodipole model from SNAPS [7]**

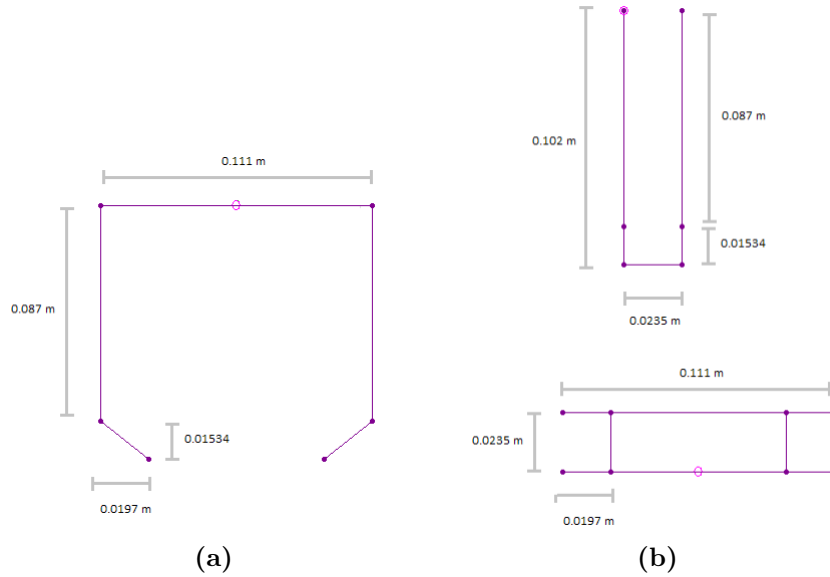


**Figure 4.16 – Dimensions of the bodipole designed by SNAPS [7]**

The antenna gives an omnidirectional radiation pattern according to theory. A 3D model design was built with Feko® (Figure 4.17) to gain a deeper knowledge about how the antenna works. The obtained radiation pattern can be seen in Figure 4.18 and Figure 4.19.

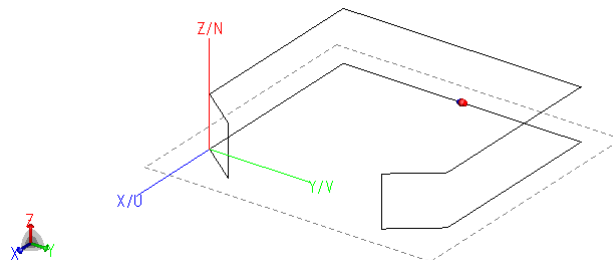


**Figure 4.17 –** *bodipole model built in Feko*

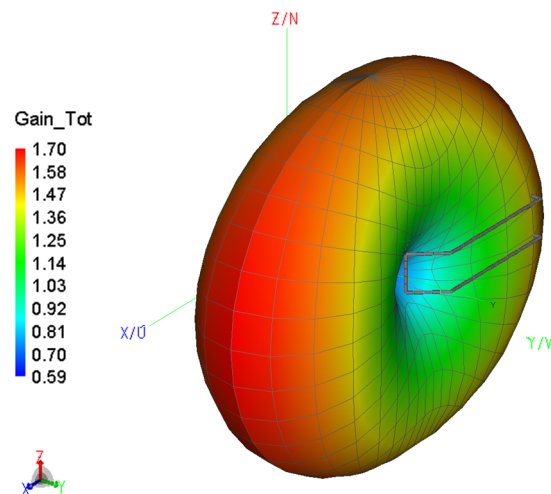


**Figure 4.18 – 3D radiation pattern of the bodipole**

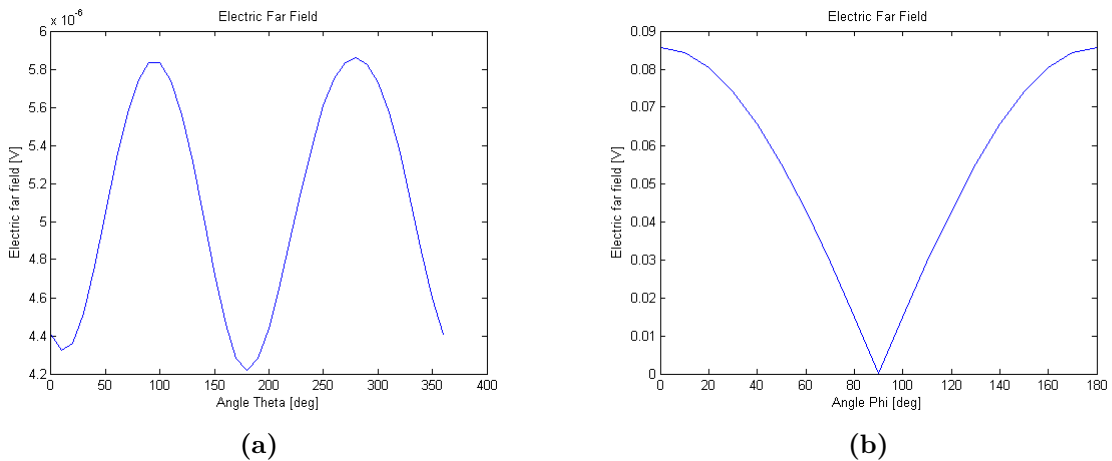


**Figure 4.19 – Far field radiation pattern of the bodipole depending on (a)  $\theta$  and (b)  $\phi$**

This antenna has the advantage of achieving circular polarization as shown with Feko® with simulations. The results of this simulation are shown in Figure 4.20.

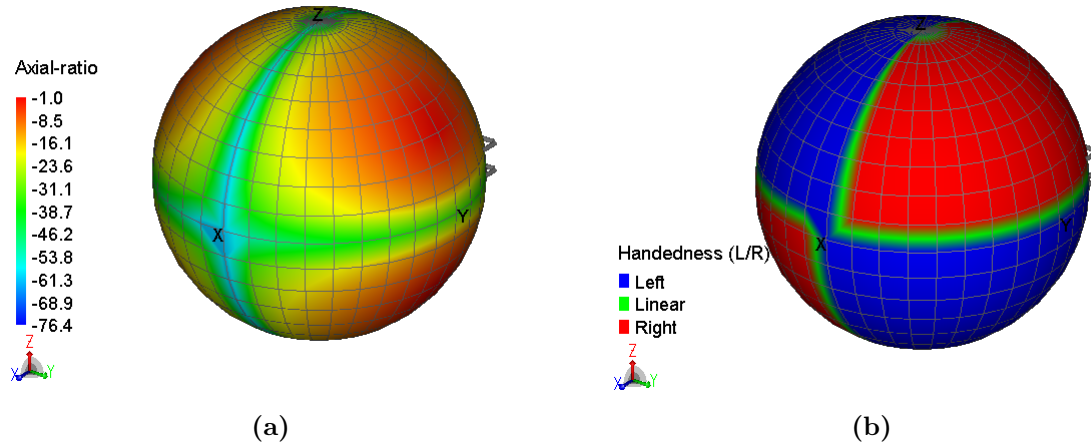


**Figure 4.20 – (a) Axial ratio on dB of the bodipole at 435 MHz and (b) Handedness**

## 4.3 Gpredict

Gpredict is a real-time satellite tracking and orbit prediction application. It can track an unlimited number of satellites and display their position and other data in lists, tables, maps, and polar plots (radar view). Gpredict is free software licensed under the GNU General Public License. Gpredict is different from other satellite tracking programs in that it allows you to group the satellites into visualisation modules, for example, Cubesats.

For downloading it we only need to go to <http://gpredict.oz9aec.net/> and download the version for the operative system used.

### 4.3.1 Setting the ground station

On a first step, we can set the ground station to Granada to be able to know when different satellites will pass above the city. For doing so we need to select the city or either introduce the coordinates.

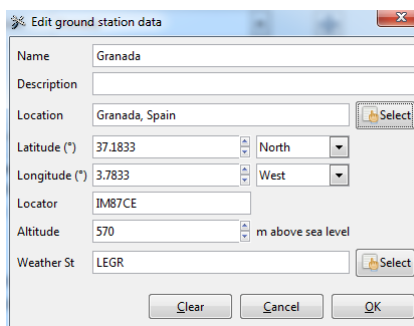


**Figure 4.21 – Setting Granada as the ground station**

### 4.3.2 Cubesat tracking

There are different group of satellites to select available since we open the program for the first time as seen in Figure 4.22.

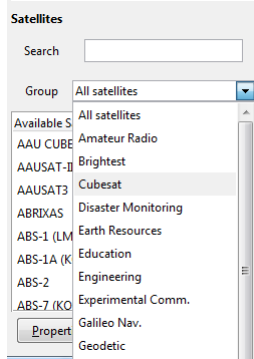


**Figure 4.22 – Different groups of satellites available in Gpredict**

Selecting Cubesat we access to a big database of available satellites that are working at the moment. From the comparison Table 4.2 we find the following satellites available on the software:

Mission	Status
AAU1 Cubesat	Dead
DTUsat-1	Dead
ArduSat	Dead
Vermont Lunar Cube	Alive
BEESAT1	Alive
BEESAT2	Alive
BEESAT3	Alive
CUTE-1	Dead

**Table 4.3 – Alive/Dead Cubesats listed on Table 4.2**

The trajectory of different satellites can be observed, like Vermont Lunar Cube marked in red in Figure 4.23.

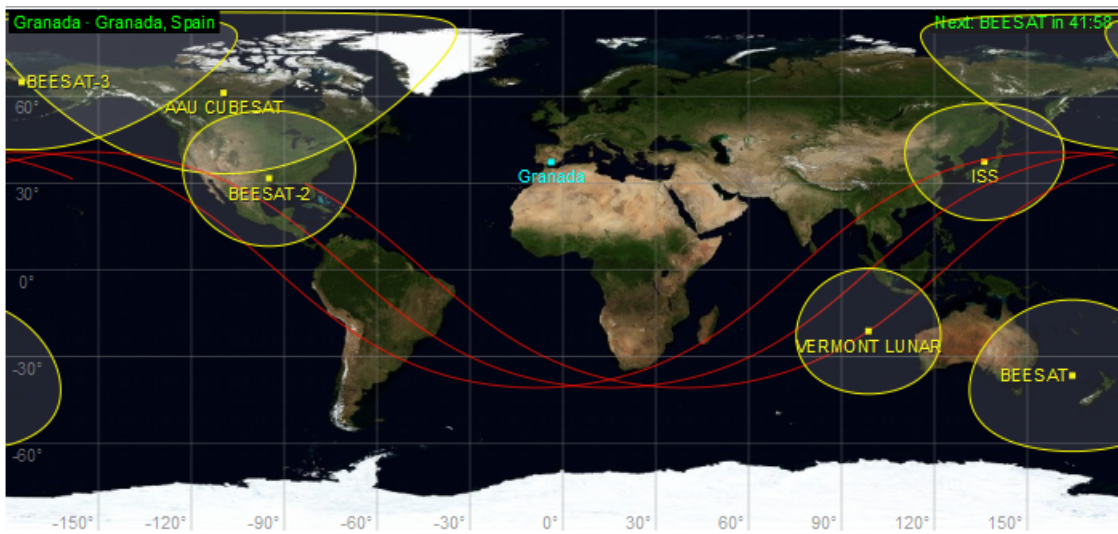


**Figure 4.23 – Gpredict positioning the satellites under study**

Orbit information can be accessed directly from the program (Figure 4.24).

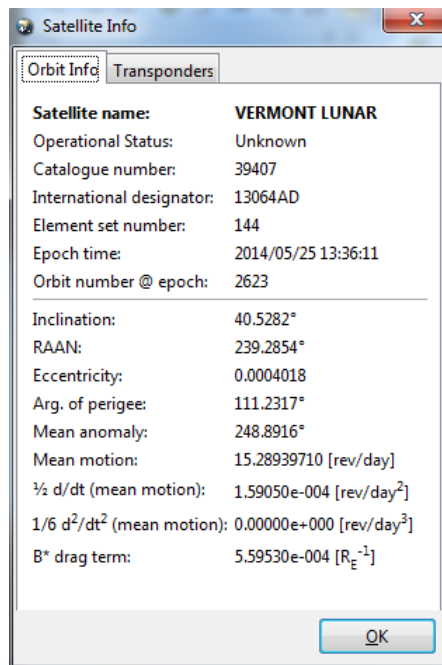


**Figure 4.24 – Vermont Lunar Cube orbit information**

### 4.3.3 Transponders

The program allows to consult the frequencies of the transponders available for some satellites as extracted from AMSAT Cubesat list.

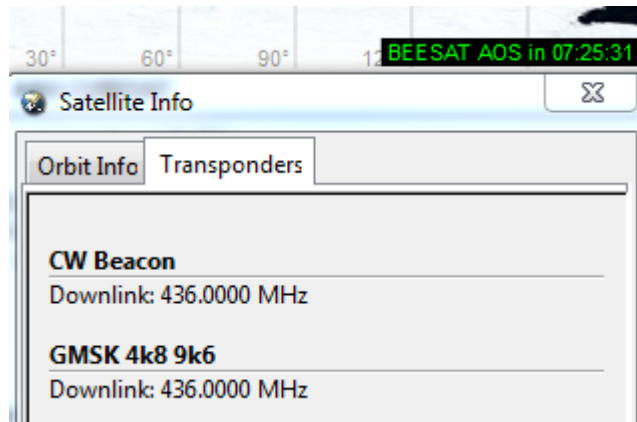


**Figure 4.25 – Beesat-1 Transponder information on Gpredict®**

By checking the AMSAT database we can complete the information available on Gpredict® with the information provided by the IARU:

Mission	Actual State	Transponder
AAU1 Cubesat	Dead	437.425 MHz
DTUsat-1	Dead	Information not available
ArduSat	Dead	437.325 MHz
Vermont Lunar Cube	Alive	437.305 MHz
BEE-SAT1	Alive	436.000 MHz
BEE-SAT2	Alive	435.950 MHz
BEE-SAT3	Alive	435.950 MHz
CUTE-1	Dead	Information not available

**Table 4.4 – Actual state of the Cubesat listed on Table 4.2**

## CHAPTER

# 5

## GROUND ANTENNA: INTRODUCTORY MODEL

In [8] VHF and UHF antenna system are described as followed “Even with high gain antennas, experimentation is greatly simplified at VHF and UHF because the antennas are a physically manageable size. Setting up a home antenna range is within the means of most amateurs, and much can be learned about the nature and adjustment of antennas”. The aim of this chapter is to describe the main receiver antennas used for UHF and VHF communications to obtain more knowledge about how they work. After the analysis of the different options, an antenna will be built step by step and its functionality will be checked.

### 5.1 Ultra High Frequency (UHF) and Very High Frequency (VHF) antennas used by FM operators

#### 5.1.1 The Yagi-Uda

Developed by Hidetsugu Yagi and Shintaro Uda in the 1920s, this antenna is a multielement array widely used for amateur radio and distribution systems like television, as well as for receiving LEO satellites. At the minimum, it consists of a single driven element (dipole) and a single parasitic element, depending on the positioning of the parasitic element it is called a *director* or a *reflector* as seen in Figure 5.1.

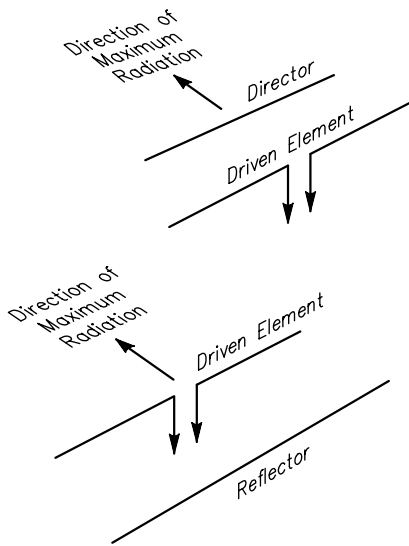


**Figure 5.1 – Two-element Yagi systems using a single parasitic element [8]**

Yagis employing 30 or more elements are not uncommon because one of its major advantages is the possibility of increasing its gain by adding more numbers of directors. Nevertheless, if the number of directors is increased, the directivity will increase as well. This directiviness creates the necessity of a rotor to follow the satellites during its trajectories.

### 5.1.2 Ground-plane Antennas

A ground-plane antenna is a variant of the dipole antenna, designed for use with an unbalanced feed line such as coaxial cable. The main element of a ground-plane antenna is almost always oriented vertically.

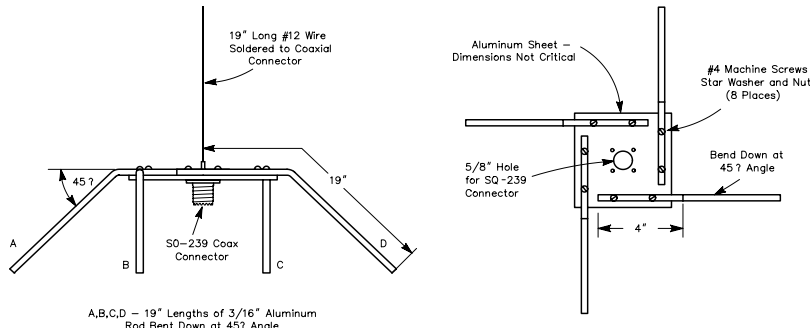


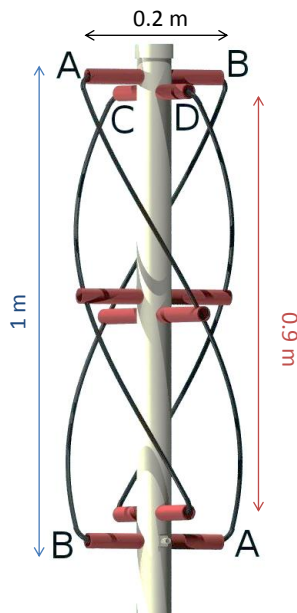
**Figure 5.2 – Ground plane antenna example for 222 MHz [8]**

It is really simple to mount, but it has lineal polarization, normally horizontal.

### 5.1.3 Quadrifilar Helix Antenna

The QHA represents one specific form of helical antenna, commonly used for receiving data from different satellites due to its hemispheric radiation pattern. It is normally used LEO satellite communications, handsets of global positioning system receivers and satellite mobiles as it is omnidirectional and circularly polarized.

It was developed by Kilgus in 1968 [15]. It is demonstrated that two bifilar helices with orthogonal radials fed in phase quadrature produce a cardioid pattern shape ( $130^\circ$  3 dB beamwidth,  $180^\circ$  6 dB beamwidth) with less than 3 dB axial ratio over the hemisphere. The form of the antenna is shown in Figure 5.3 for 137.5 MHz. Kilgus achieved to approximate the QHA for two orthogonal dipole antennas, a bigger dipole marked on blue, and a smaller one on red [15].



5

**Figure 5.3 – Quadrifilar Helix Antenna**

One of the major drawbacks of this type of antenna is the complex feed network required because of the phase shift necessary, but it performs an isotropic omnidirectional radiation pattern which makes it ideal for receiving satellites, without the need of a rotor.

## 5.2 QHA antenna

On section 5.1 we have just seen some examples of antennas used for receiving UHF-VHF signals. Signals become circularly polarized while passing through the ionosphere as seen in Chapter 3. Therefore, we need a circular polarization antenna for receiving the signals.

As there is a lot of information about the building and tuning of the QHA and it has an omnidirectional pattern allowing to receive almost during all the pass of the satellite, this is

the antenna chosen to use as an introductory model.

### 5.2.1 Far field region

As this antenna will be used for receiving satellites, it will be working on far field, also called Fraunhofer region as seen in Chapter 3, this region is determined by Equation 5.2.1:

$$d_f = \frac{2D^2}{\lambda} \quad (5.2.1)$$

It must satisfy these two conditions:

$$d_f \gg D \quad (5.2.2)$$

$$d_f \gg \lambda \quad (5.2.3)$$

Using Equation 5.2.1, and considering the physical length of the antenna as the loop formed by its biggest conductor:

$$d_f = \frac{22.3974^2}{2.18} = 5.27\text{m} \quad (5.2.4)$$

## 5

### 5.2.2 Antenna Simulations

Once we know the electric field we should expect from a QHA antenna, some simulations can be performed in order to know the expected results after building the antenna. For this purpose Feko® will be used as described in Appendix A.1.

#### 5.2.2.1 3D Antenna

A QHA is based in two folded dipoles of different size connected in parallel. As this model is more complicated than others already simulated with Feko® in this Degree Thesis, a step by step approach for understanding the results of this antenna will be made.

#### 5.2.2.2 Single bent dipole

The first model designed is a single folded dipole with the QHA bigger loop dimensions (0.9x0.2m), seen in Figure 5.4.

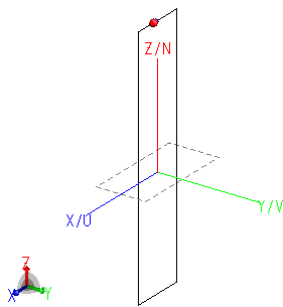


**Figure 5.4 – Bigger loop of the QHA**

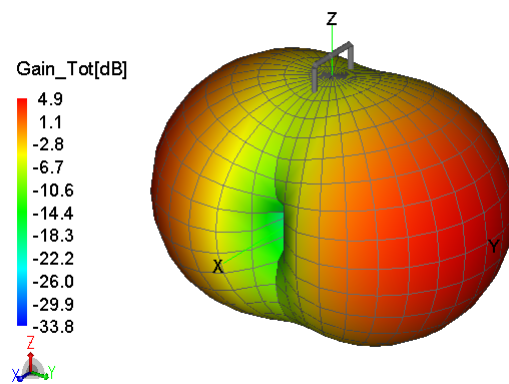


**Figure 5.5 – 3D radiation pattern of QHA bigger loop**

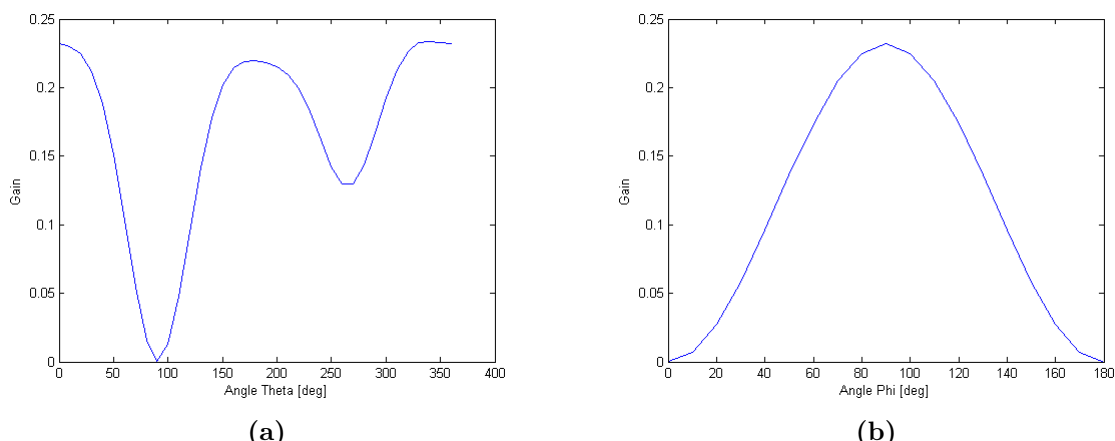


**Figure 5.6 – Far field radiation pattern at 137.5 MHz depending on (a)  $\theta$  and (b)  $\phi$**

The radiation pattern shows a healthy gain in the horizontal direction perpendicular to the plane of the loop.

### 5.2.2.3 Two bent dipoles

An omnidirectional antenna in the horizontal plane can be achieved by using a second loop perpendicular to the first (Figure 5.7). The second loop should be feed with a  $90^\circ$  phase difference.

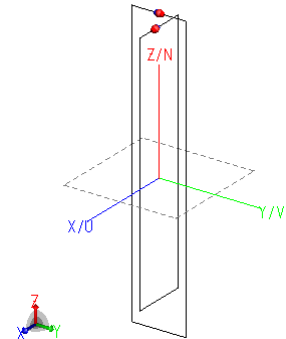


**Figure 5.7 – Complete QHA**

The polarization changes the results of simulation. In Figure 5.8 a first case and its results are shown in Figure 5.9. In Figure 5.10 and Figure 5.11, the second case of polarization is shown.

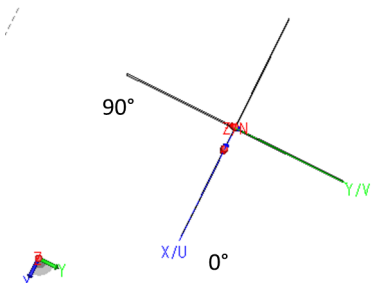


**Figure 5.8 – First case of QHA polarization**

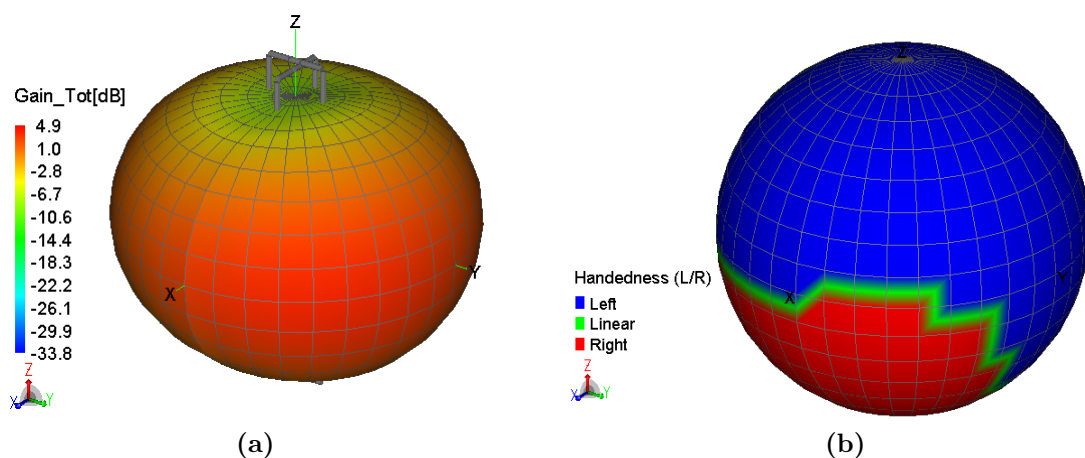


**Figure 5.9 – Results of the first case of polarization (a) gain (dB) and (b) Handedness**

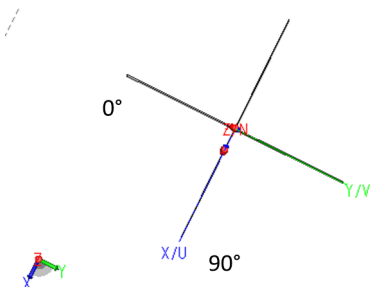


**Figure 5.10 – Second case of QHA polarization**

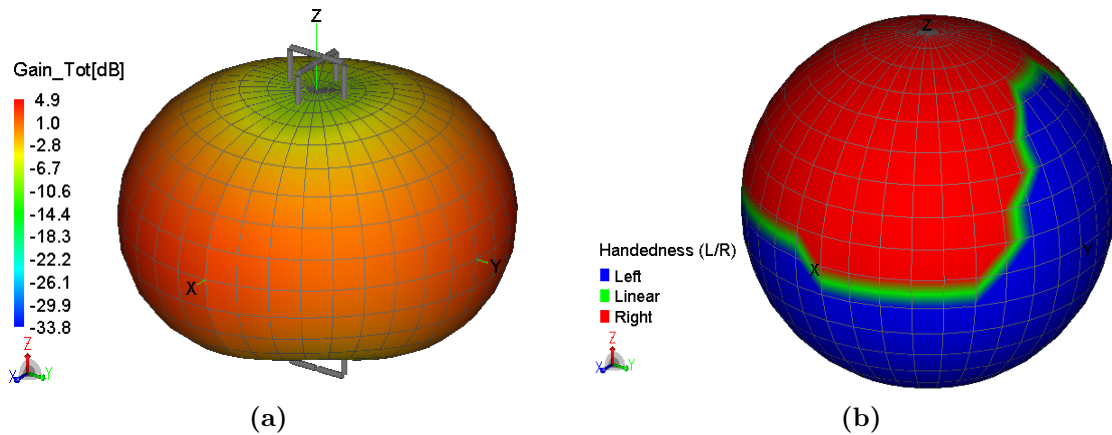


**Figure 5.11 – Results of the second case of polarization (a) gain (dB) and (b) Handedness**

NOAA satellites are right handed polarized, therefore the solution chosen should be the one shown in Figure 5.10. The 2D far field graphs are detailed in Figure 5.12. The gain has decreased in comparison with the single bent dipole, but circular polarization for receiving the satellite can be achieved.

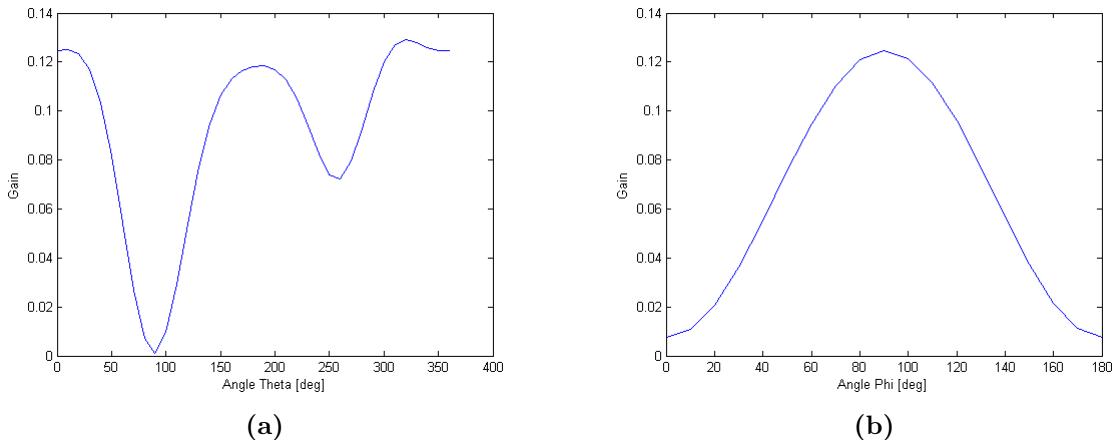


**Figure 5.12 – Far field radiation pattern at 137.5 MHz depending on (a)  $\theta$  and (b)  $\phi$**

## 5.3 QHA Building

Following the experimental information available online [16], an easy to build but performing antenna for receiving at 137.5 MHz will be presented.

### 5.3.1 Materials

Following the requirements, a 137.5 MHz QHA was built. The material needed for doing so is [16]:

- 1.) 1.5 meters of 32mm PCV pipe.
- 2.) 4.6 m of soft copper tube.
- 3.) 8 copper elbows for corners.
- 4.) Suitable coaxial line.

### 5.3.2 Procedure

- 1.) Cut the soft copper in appropriated lengths as seen in Figure 5.13, it is needed:
  - A.) 2x190mm bottom horizontal tubes
  - B.) 2x903mm short helix elements
  - C.) 2x1002mm long helix element tubes
  - D.) 2x90mm top horizontal elements
- 2.) Drill 4x8 mm holes at 90 degrees each other, a detailed picture of how this was done is provided in Figure 5.14
- 3.) Assemble tubes as in Figure 5.14.
- 4.) Use the coaxial line to fabricate a choke balun as analysed and performed in Section 5.3.2.1.

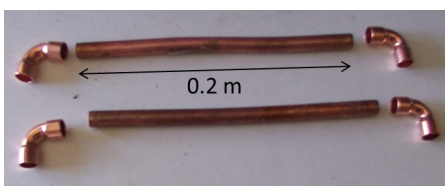


**Figure 5.13 – Copper tubes and bents**

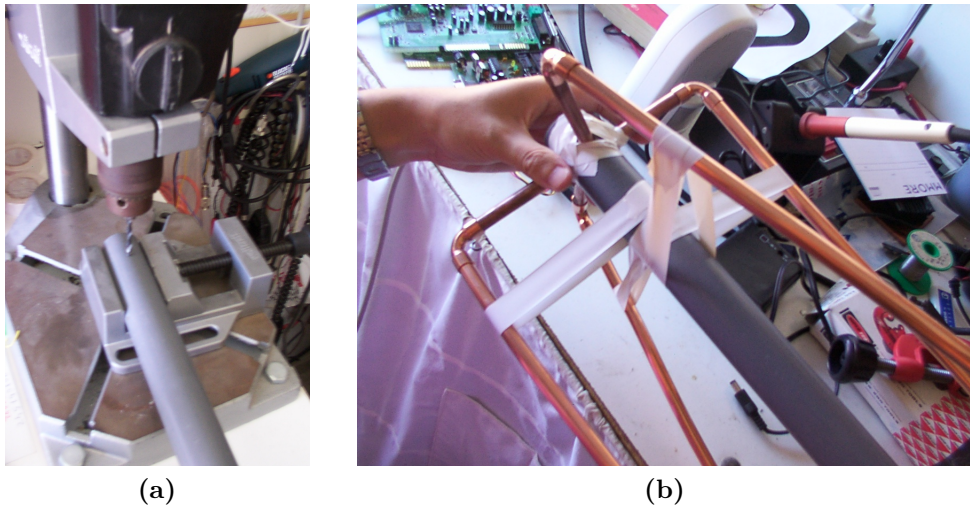


**Figure 5.14 – (a) Drilling the PVC tube and (b) assembling the tubes**

### 5.3.2.1 Balun description

A balun properly connects a balanced transmission line to an unbalanced transmission line. It serves to maximize the impedance on the outside surface of the transmission line and to decrease the amount of electrical field generated where the transmission line is attached to the transmission line of the antenna [17].

In a coaxial cable, the currents on the inner conductor and the inside of the shield are equal and opposite. This is because the fields from the two currents are confined to the same space. If we fed an antenna with a coaxial without a balun, the current on the outer conductor splits between the antenna conductor and the outside conductor.

This is why a balun is more than necessary when considering antennas design. To recall, what we want for a balun is to cause the currents in the feed line conductors to be equal in magnitude and opposite in phase resulting in a zero imbalance current.

For the QHA, we will use a choke balun. This type of balun is a coil in the coaxial feeding the antenna as close to the feed point as possible. It will prevent the common mode currents to propagate.

This is accomplished by presenting a high impedance to RF currents flowing outside the coaxial shield, which forces currents in each side of a driven element to be equal. Using this type of balun, the coaxial line will be differenced from the antenna itself.

For finishing the QHA building, the coaxial line will be wrapped around the mast four times making the desired balun as seen in Figure 5.15:



**Figure 5.15 – Built balun**

### 5.3.2.2 Final Antenna

The antenna built can be seen on the Figure 5.16:



**Figure 5.16 – Antenna built**

## 5.4 QHA Characterisation

After building the antenna, its characteristics have to be measured. For doing so, we will use the Network Analyser E5071C from Agilent available at the laboratory.

We will be specially interested in measuring the  $S_{11}$  parameter and the Standing Wave Ratio[SWR]:

$$S_{11} = \Gamma = \frac{Z_L - Z_0}{Z_L + Z_0} \quad (5.4.1)$$

$$SWR = \frac{V_{max}}{V_{min}} = \frac{1 + |\Gamma|}{1 - |\Gamma|} \quad (5.4.2)$$

Ideally, if the impedance is matched:

$$S_{11} = 0 \Rightarrow SWR = 1 \quad (5.4.3)$$

#### 5.4.1 Agilent's Network Analyser E5071C

The Network Analyser E5071C belongs to medium class electronic instrumentation device. It has flexible configurations letting the user to choose the number of ports to be used, frequency and bias tees.

The one in the lab has 4 ports and a frequency range from 100 kHz to 8.5 GHz. One of its more stunning capabilities is the high temperature stability (0.005 dB/°C). It also has a wide dynamic range bigger than 123 dB.

The front panel is shown in Figure 5.17.

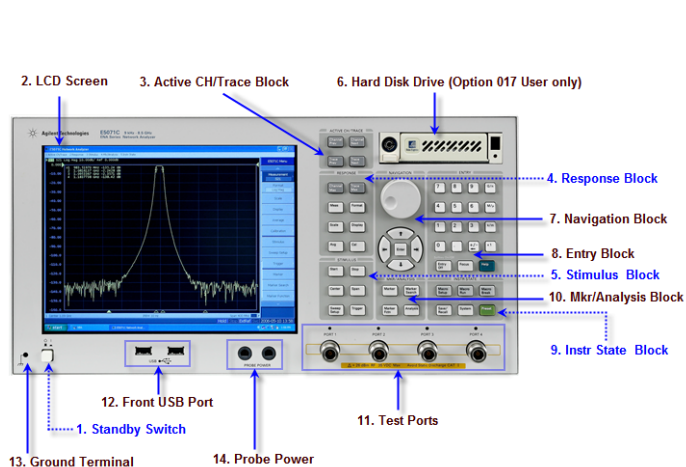


**Figure 5.17 – E5071C Front panel [9]**

There are two main parts, the *Stimulus Block* for defining signal sources and trigger and the *Response Block* for setting the parameters of the measurement as well as the format in which they data will be presented.

The values can be stored in *csv* format allowing to represent the data with Matlab or any other processing tool. We can as well export the information displayed on the screen as an image.

### 5.4.2 Determining measurement conditions

The QHA built is made for 137.5 MHz. We will set this value as the centre frequency in our Network Analyser, also a span of 50 MHz will be specified to have a complete view of our antenna at frequencies of interest.

One of the most important parameters to define is the Intermediate Frequency Bandwidth [IFB]. It determines the selectivity of the instrument, a narrow IF bandwidth configuration requires more spectrum acquisitions for a given span and led to longer measurement times. Although the drawback of a narrow IF bandwidth is longer measurement times, it can significantly improve the instruments performance. Decreasing the bandwidth of an IFB filter decreases the measured noise floor. The sweep time[ST] is defined in Equation 5.4.4:

$$ST = \frac{Span}{IFB^2} \quad (5.4.4)$$

This parameter should be taken into account when performing the measurements.

### 5.4.3 Calibration

The first step is to calibrate our device. For doing so we used the calibration kit available and followed the recommended instruction from the user manual (insertar referencia?).

In this case we will use only one port for our QHA, so we will calibrate port 1. The steps followed are:

- 1.) Specify calibration Kit.
- 2.) Select the number of ports that will be used.
- 3.) Measure the calibration for the OPEN standard.
- 4.) Measure the calibration for the SHORT standard.
- 5.) Measure the calibration for the LOAD standard.

The results of this calibration are presented in Figure 5.18

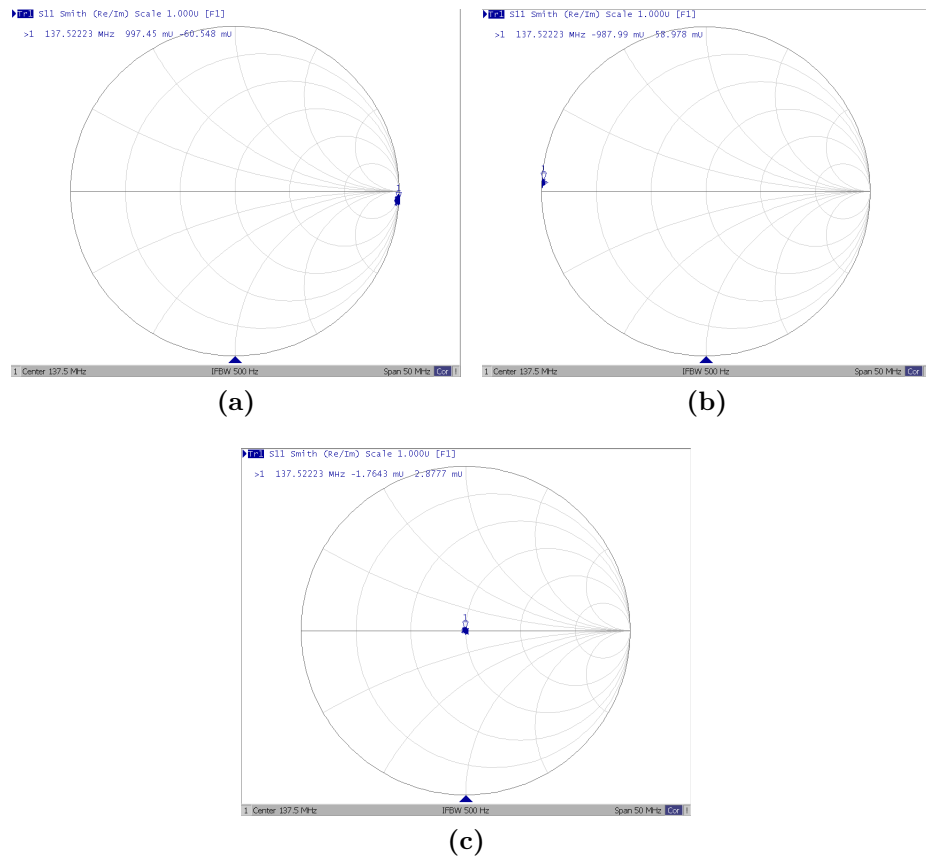


**Figure 5.18 – a) OPEN calibration, b) SHORT calibration and c) LOAD calibration.**

#### 5.4.4 Measurement setup in the Electronics Laboratory

The antenna was positioned in the laboratory connected to the Network Analyser, the measured SWR is shown in Figure 5.19.



**Figure 5.19 – SWR measurement of the built QHA**

The *SWR* is a good indicator that the antenna has a good impedance matching.

## 5.5 Reception with QHA

The NOAA satellites only pass overhead at certain times of the day, broadcasting a signal. At the moment NOAA 15, 17, 18 and 19 are operational. Using Gpredict® it is possible to know in advance when the satellites will pass over the ground station (Figure 5.20).

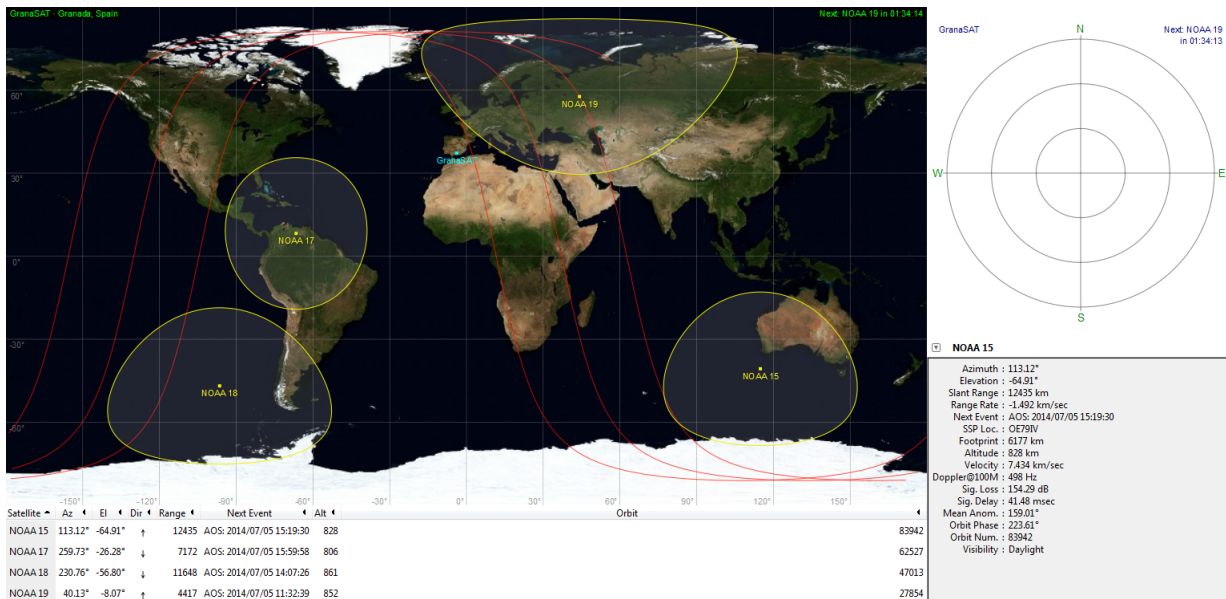


**Figure 5.20 – Gpredict positioning NOAA satellites with future passes**

To set up a NOAA weather satellite at a receive station it is needed:

- 1.) An rtl-sdr dongle (DVB-T USB receiver) working with SDRSharp.
- 2.) An audio piping method.
- 3.) A right hand circularly polarized antenna tuned at 137 MHz.
- 4.) Software for decoding the APT signal.

The DVB-T USB receiver is already available in the Electronic Engineering Laboratory, as well as the antenna just built. For the audio piping method, the free software VB-Audio will be set up and configured.

There is a lot of information online about setting the computer ready for reception, but the fundamental is to have SDRSharp configured with an audio piping method for sending the data directly to the signal decoder, in this case WXtoImg.

The setup configured with spectrum analyser the computer and the antenna is in Figure 5.21.

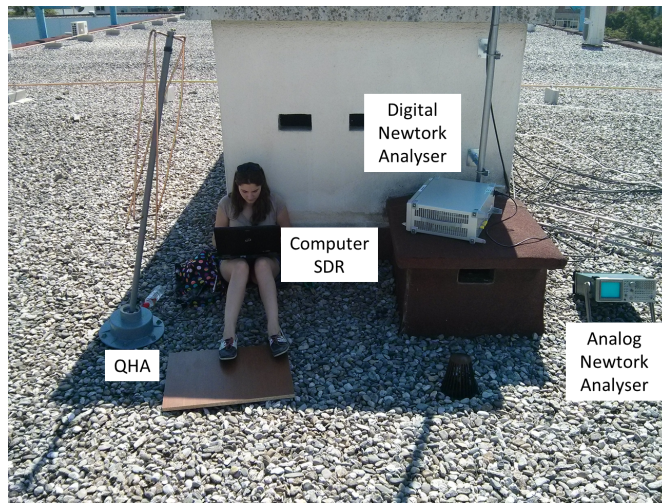


**Figure 5.21 – Set up for receiving at the terrace**

When satellites were passing, it was possible to observe the signal with the spectrum analyser Figure 5.22.

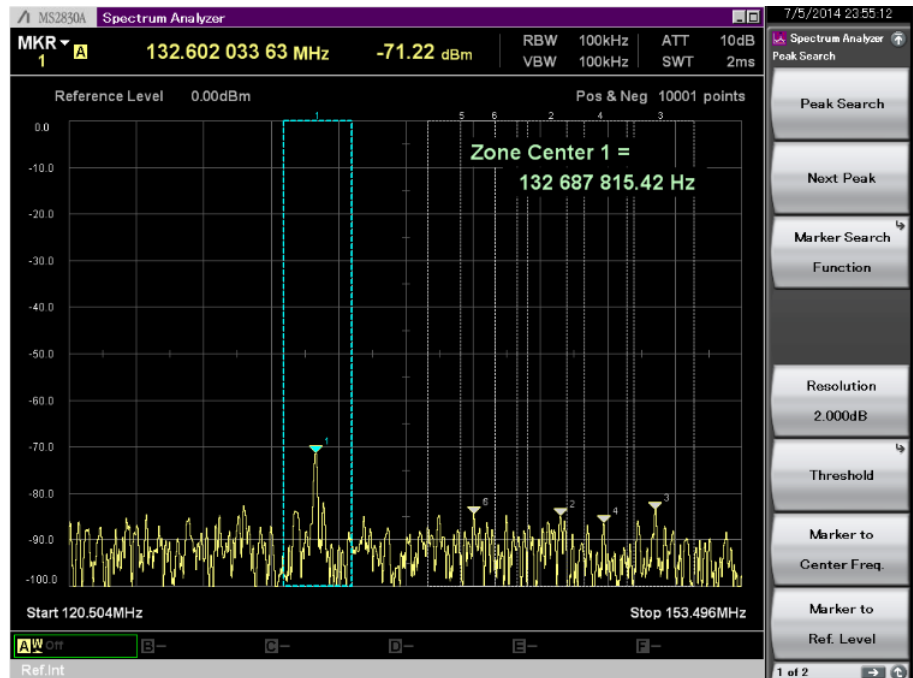


**Figure 5.22 – Spectrum of the signal received**

When connecting the antenna to the rtl-sdr dongle, we check first if the antenna is properly connected to the computer. The reception of FM was achieved as seen in Figure 5.23.

When setting the rtl-sdr dongle to receive at the NOAA frequency with a bandwidth large enough for not losing the signal due to doppler effect (40 KHz) there is a small signal shown in the computer meanwhile there is something at the spectrum analyser. This test were repeated obtaining the same results each time.

(Loading Video...)

**Figure 5.23 – Reception of FM signals with a QHA**

As the *SWR* of the antenna is good enough for receiving in normal conditions, the problem was coming from the polarization. If an antenna is badly polarized, the losses can be between 18 and 20 dB. The polarization was checked using a high frequency source and an oscilloscope (Figure 5.24). A closed loop was used for measuring.



**Figure 5.24 – Checking the polarization of the antenna.**

The results obtained are a phase difference of  $70^\circ$  instead of  $90^\circ$  (Figure 5.25).

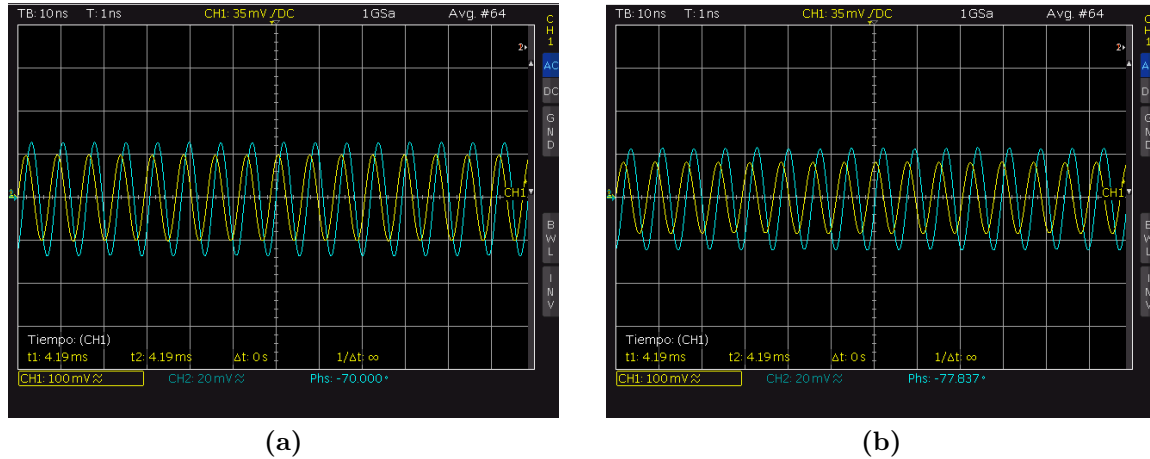


**Figure 5.25 – (a) Phase difference between two connections (b) Phase difference between the other two connections**

Not having a correct polarization is due to the choke balun. To fix this the choke balun should be built again.

### 5.5.1 Decoding the signal

Using the software WxtoImg it is possible to obtain the image from an audio file. For example, with the following attached file as an example we can obtain different results, depending on the options of the software (Figure 5.26).



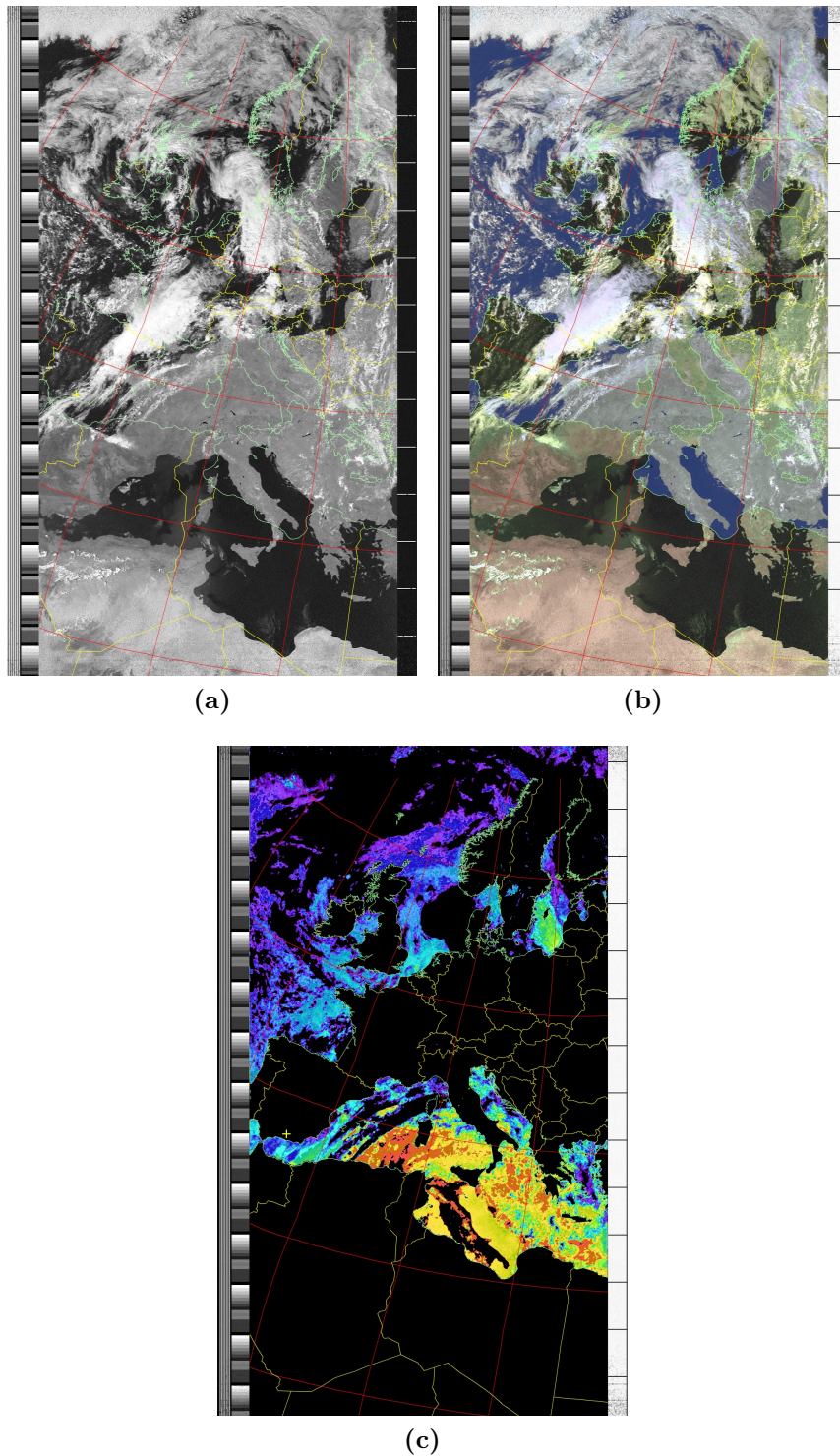


**Figure 5.26 – a) Black & White image b) False colour image c) Ocean temperature**

The data obtained with our set up is:



The decoded picture is shown in Figure 5.27.

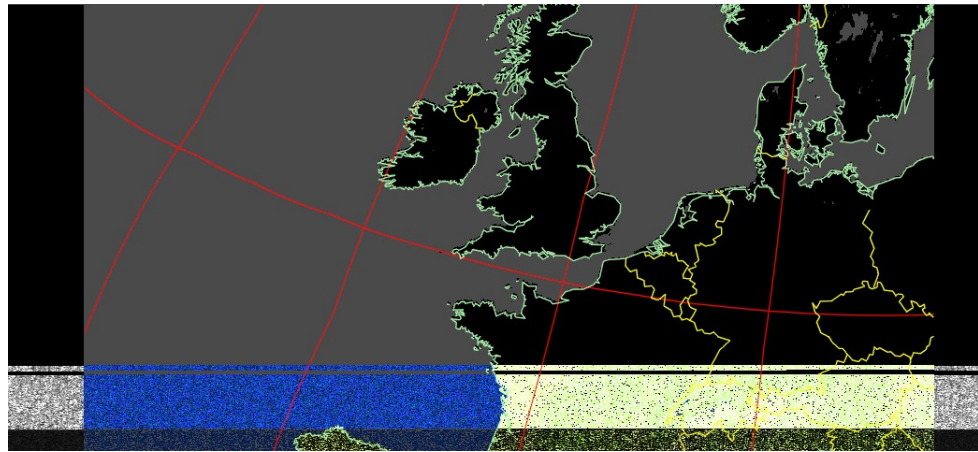


**Figure 5.27 – Decoded picture of the audio captured with the sdr-rtl**

There is no telemetry data downloaded and the data is too noisy for a correct conversion. The antenna should be made again, but for knowing the number of turns the balun should have it is recommended to use the setup of Figure 5.24.



# CHAPTER

## 6

# CUBESAT ANTENNA DESIGN

### 6.1 Antenna selection

Once we have made a carefully comparison of different antennas in Chapter 4 and have overcome the main steps to build and characterise an antenna in Chapter 5 , it is the time to choose the antenna to build for GranaSAT. As this is an introduction to the antenna design of a Cubesat, we would like to test two different antennas.

In the first step, we would like to test the State of the Art solution, the one developed by SNAPS [7].

In the second step, we would like to develop a model based on two crossed dipoles, obtaining the gain of only one dipole but with circular polarization.

### 6.2 Antenna design

Antennas need a matching network for maximum power transfer. A balun is also necessary for connecting from a balance signal to an unbalanced signal. Both can be combined in one solution, implemented in a PCB fitting in the mechanical constraints of the Cubesat Manual [10].

### 6.2.1 Mechanical design

A PCB in a FR4 substrate through milling will be made. The antennas will be connected to it. This PCB will be attached to the top part of the Cubesat, so it was necessary to define the mechanical boundaries before working on the PCB.

#### 6.2.1.1 3D printed Cubesat

The first step to start the design of Cubesat antennas in this Degree Thesis is to obtain the dimensions from the Cubesat manual [10] as seen in Figure 6.1.

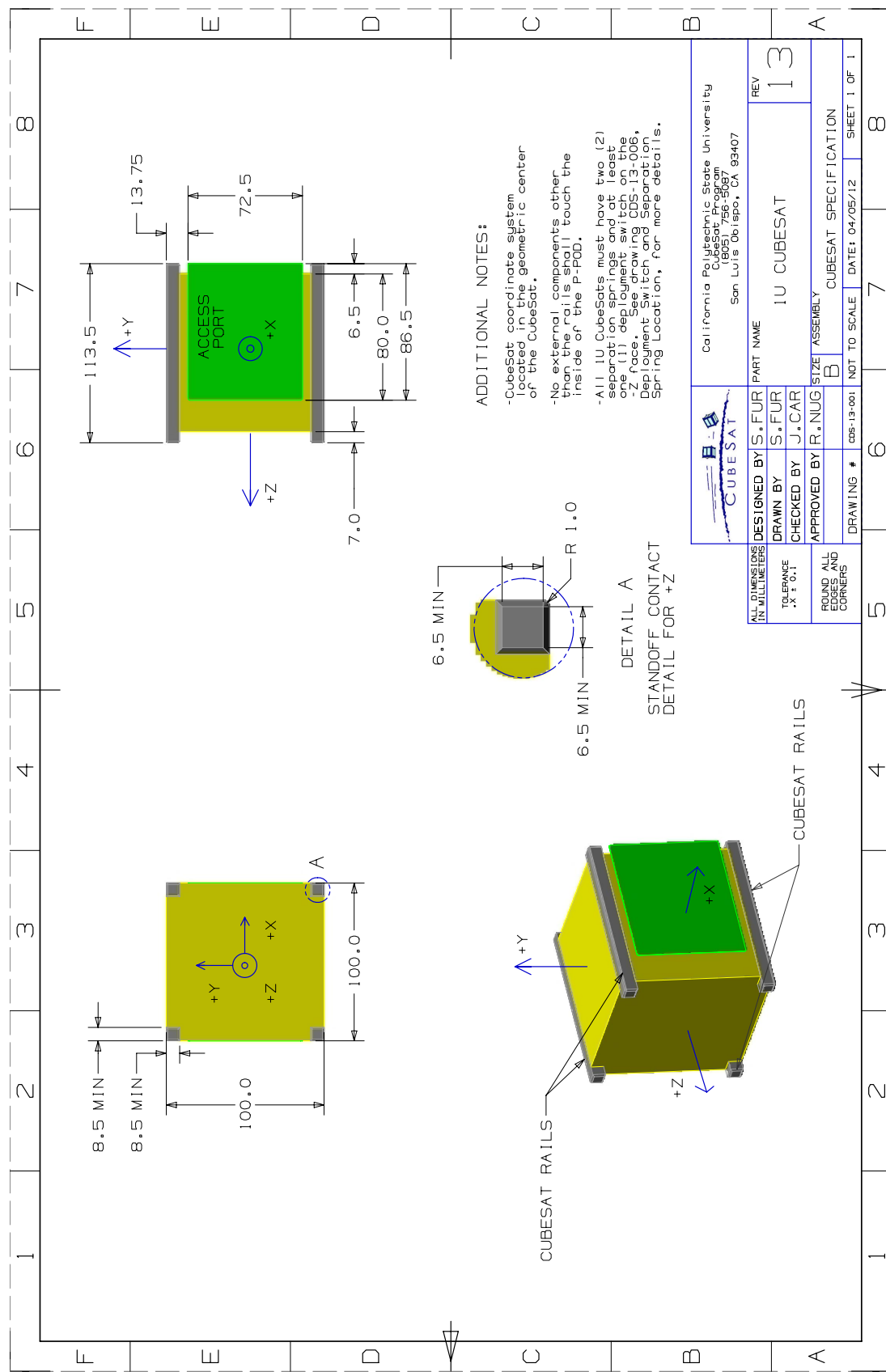
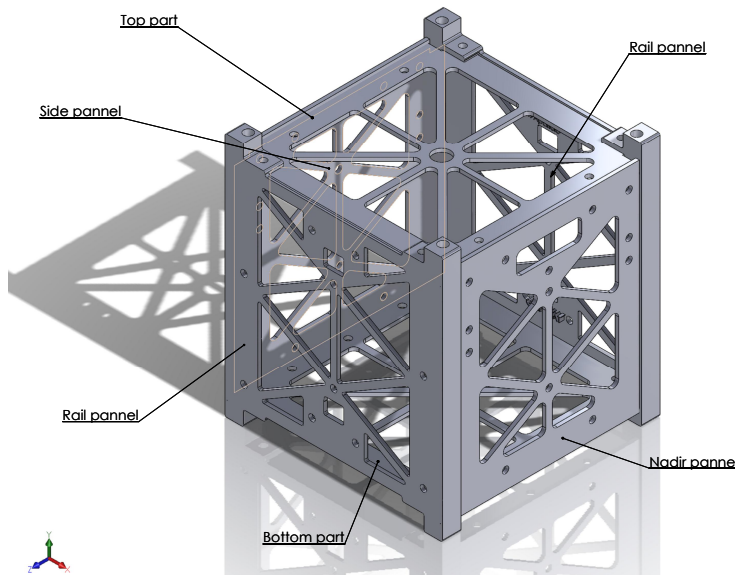


Figure 6.1 – Cubesat standard [10]

Using the software SolidWorks® it is possible to create a 3D model of the Cubesat for assembling purposes. As creating a new design from scratch is laborious and there is lots of information online, some of the drawings from CO3 (Colorado Space Grant Consortium Cubesat) were used for designing the model.

SolidWorks® allows to import Computer Aided Design (CAD) files or PDF files and recognise the model drawn. Using this capability each different piece was created allowing the final design to be as seen in Figure 6.2



**Figure 6.2 – Cubesat model (a) in SolidWorks®**

Once the model was designed it was possible to use the 3D printer available in the Electronic Laboratory for creating a prototype. The 3D printer available is a Prusa i3, with an impression volume of 20x20x20 mm. The final Cubesat printed can be seen in Figure 6.3.

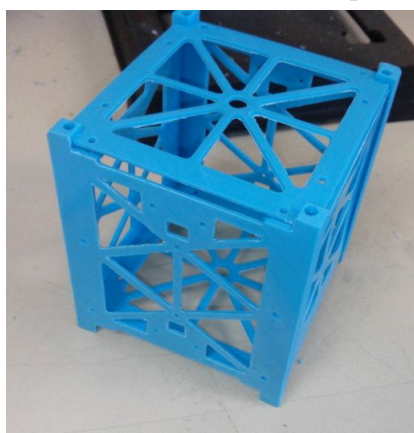


**Figure 6.3 – 3D printed Cubesat**

There are already some papers describing the possibility to send a plastic Cubesat made out of Acrylonitrile butadiene styrene (ABS) [18]. So this prototype can be considered as a

beginning for GranaSAT mechanical design.

After the model was designed and printed, the mechanical design of the top part was defined, and it will be used in the Electronic Design Automation Software Altium for defining the board shape of the PCB.

### 6.2.1.2 Antenna arrangement

One of the major problems with antenna design is its dimension. When talking about picosatellites this fact becomes critical because of its small size and low weight. A deployable antenna is the most common solution, but it can have problems related to pyrotechnical issues or the possible blocking of the deployment method. Tape measure is used in many solutions in this field for avoiding difficult mechanical methods of deployment. This material is flexible, getting to its original position when deployed as seen in Figure 6.4. In this Degree Thesis, this approach will be used for the turnstile antenna.

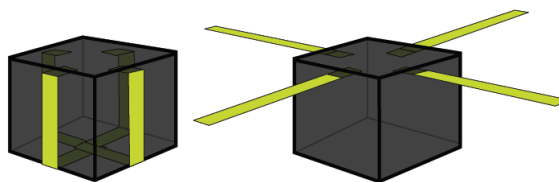


**Figure 6.4 –** On the left Cubesat before launch and on the right with antennas deployed [11]

Other solutions work for avoiding a deployment method in the aim of simplicity. This is the case of the bodipole. This antenna was designed to be equivalent to a dipole but without the unveiling, allowing to have a simpler mechanical design.

### 6.2.2 Matching networks and baluns

The input impedance of each antenna will be obtained with the help of Feko® simulations, allowing us to design a balun and matching network for each development.

6

#### 6.2.2.1 Bodipole

With Feko® the input impedance of the bodipole using the methodology detailed in the Appendix A.1 can be obtained. The PCB in which the system will be built is FR4, this can change the results of the antenna, so a simulation was performed with the FR4. The model designed is in Figure 6.5 and the model without the FR4 is the one presented in Figure 4.17. In Figure 6.6 the radiation pattern of each one is presented.

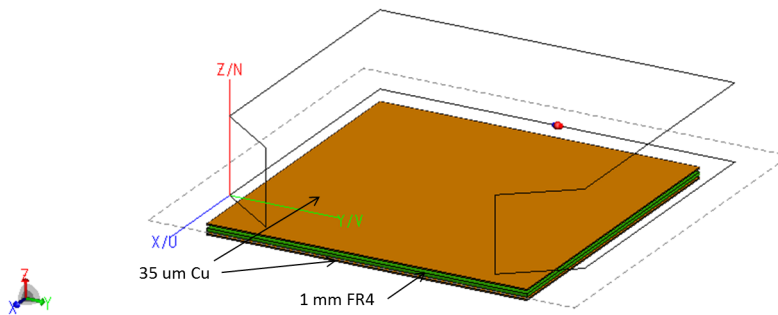


**Figure 6.5 – Bodipole with FR4 PCB in Feko®**

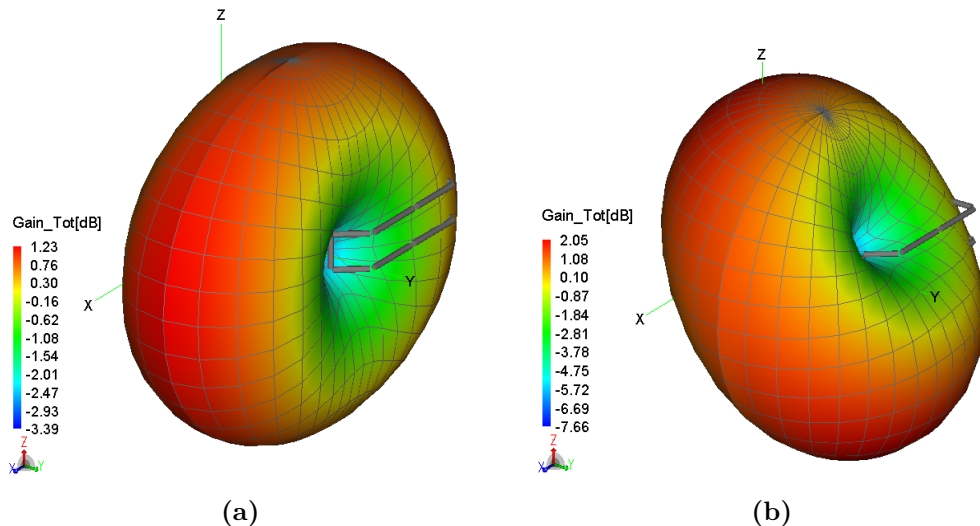


**Figure 6.6 – (a) Gain of the bodipole and (b) with FR4 substrate**

The input impedance changes because of the FR4 (Figure 6.7).

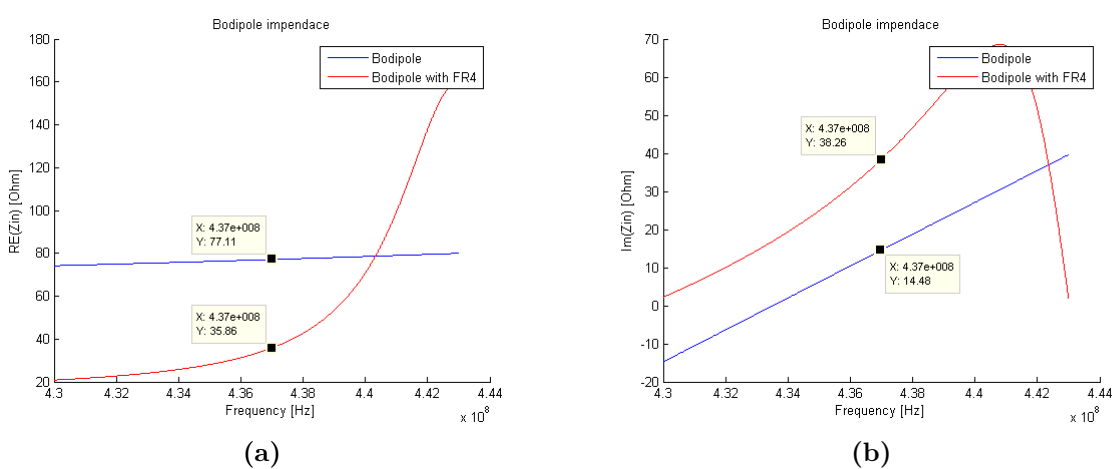


**Figure 6.7 – Bodipole impedance (a) real part and (b) imaginary part**

The SWR changes considerably with the FR4 fabrication on a PCB as it can be seen in

Figure 6.8.

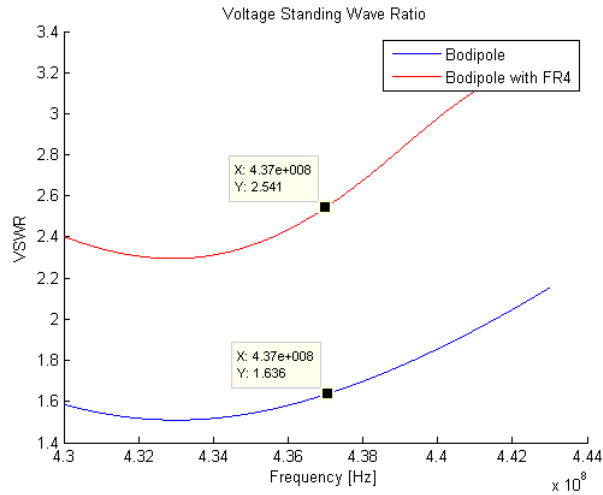


Figure 6.8 – Bodipole VSWR

### 6.2.2.1.1 Using a coaxial balun

The solution proposed by SNAPS is to use a choke balun [7]. This choke balun is based in the winding, creating an inductance that impedes common mode current. The choke allows normal mode current to pass, where normal mode current is a pair of currents that are equal and opposite in value. This choke balun is called transformer balun. They are normally implemented like coiled coaxial cable, as seen in Chapter 5.

As this is a solution that requires a lot of space, a  $\lambda/2$  balun will be tested. This balun works on the same principle as transformer baluns, in fact, it is a transformer balun. One side of the signal is transmitted as it is and the other side is produced by delaying the signal by half a wave length. This inverts the signal to produce the opposing one. These baluns work well enough but have the disadvantage of being restricted to a very narrow band of frequencies [8]. For computing the length of the  $\lambda/2$  coaxial line the propagation speed of the wave should be considered.

The coaxial used is RG58 with an attenuation between 1.7dB and 5.6 dB [19]. The velocity ratio is 0.666 from the speed of light.

### 6.2.2.1.2 Using passive components

The impedance that should be matched is  $Z_{inbodipole} = 35.86 + j38.26$  from Figure 6.7. This value should be matched achieving a balun, for feeding purposes. The software AppCAD by Avago Technologies allows this, obtaining the solution shown in Figure 6.9.

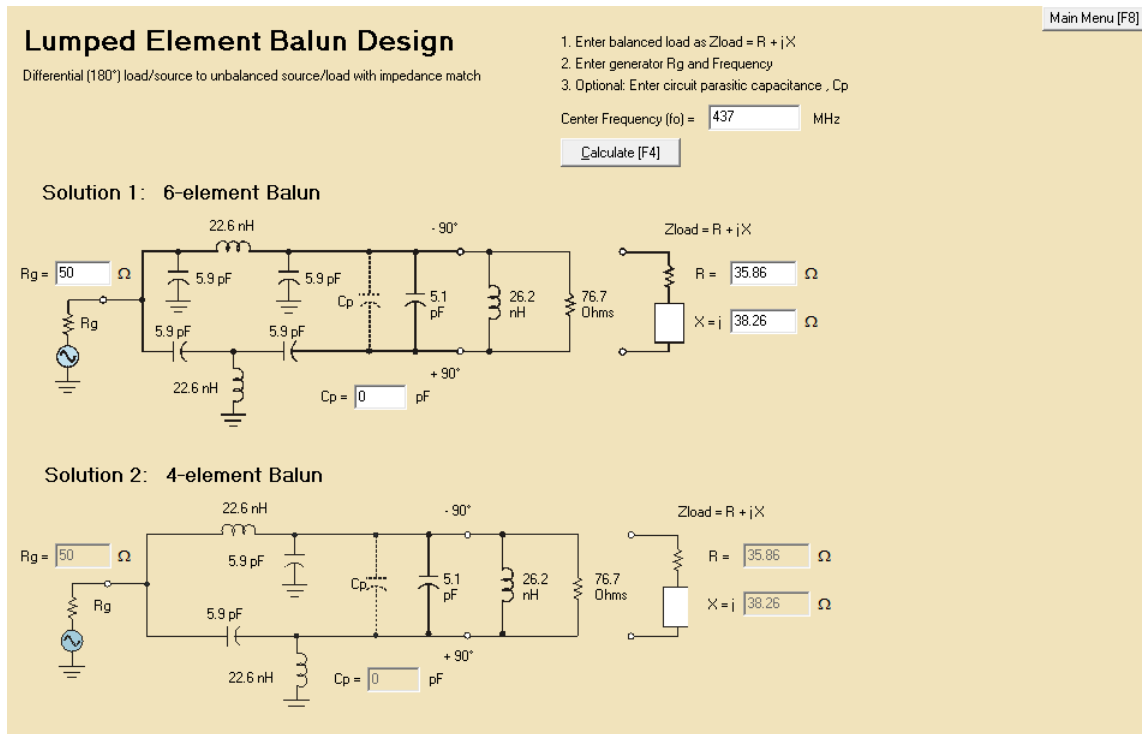


**Figure 6.9 – Balun with impedance matching in AppCAD**

### 6.2.2.2 Tunstile

The turnstile antenna based on crossed dipoles is frequently used in Cubesat applications. Ideally, the dipoles should be thin wires (around 2 mm) as seen in Figure 6.10, but because of mechanical reasons as seen in the subsection 6.2.1,a tape measure will be used. The results are shown in Figures 6.11 and Figure 6.12.

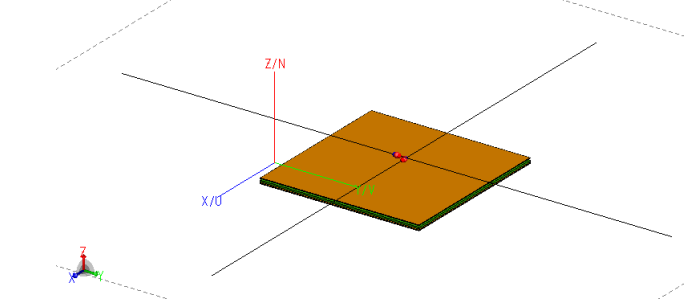


**Figure 6.10 – Crossed dipoles with FR4 PCB in Feko®**

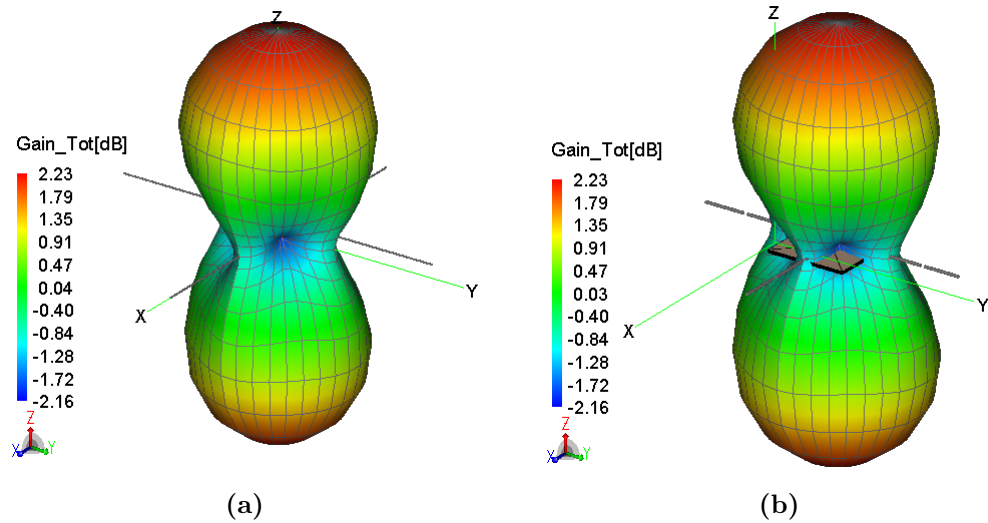


**Figure 6.11 – (a) Gain of the turnstile antenna (b) with FR4 substrate**

The input impedance changes because of the FR4 (Figure 6.7).

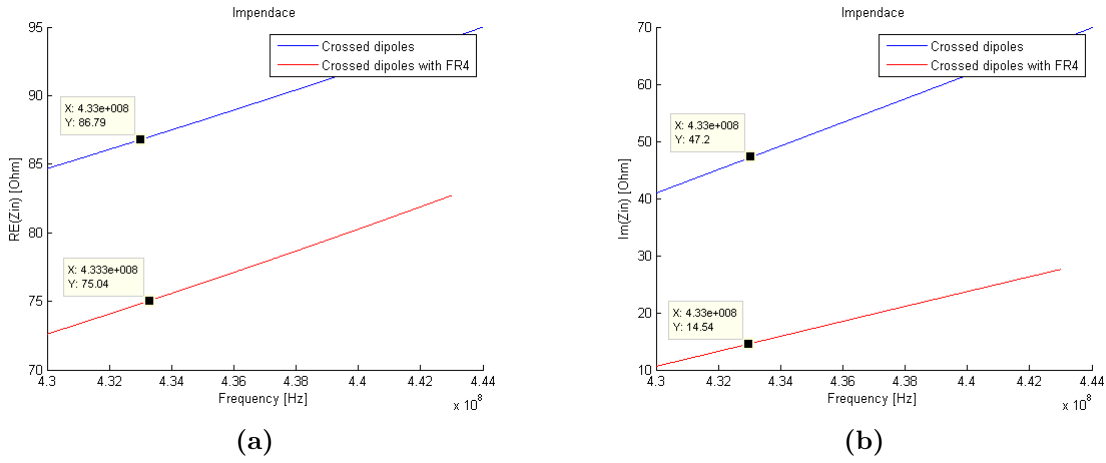


**Figure 6.12 – Impedance (a) real part and (b) imaginary part**

As before, the PCB changes considerably the SWR as seen in Figure 6.13.

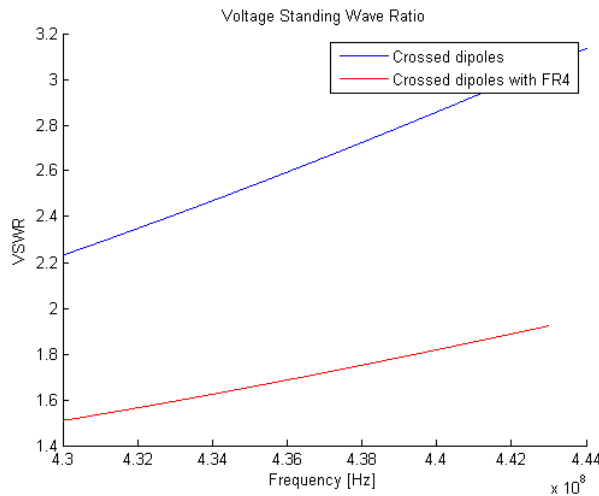


**Figure 6.13 – Turnstile SWR**

#### 6.2.2.2.1 Using a coaxial balun

This type of antenna is frequently used in amateur radio applications due to its easiness to build and its circular polarization. The balun normally used is the one shown in Figure 6.14.

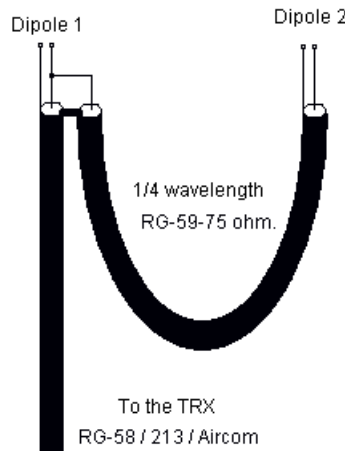


**Figure 6.14 – Balun normally used for turnstile configuration**

This configuration is based on the fact that a  $\lambda/4$  transmission line will produce a  $90^\circ$  phase shift. Transforming the impedance in a 4:1 relation, due to the fact that the RG59 cable is a  $75\ \Omega$  cable. The calculations on the cable length shall consider the velocity factor of the cable available on the datasheet [19] with a velocity ratio of 0.666 times the speed of light.

### 6.2.2.2.2 Using passive components

Once again it is possible to use passive components for achieving the phase shift. Circular polarization is needed, so the passive circuits need to create a phase shift of  $0^\circ, 90^\circ, 180^\circ$  and  $270^\circ$ . With a balun design a phase difference of  $90^\circ$  and  $-90^\circ$  can normally be achieved. With AppCAD this design can be made as seen in Figure 6.15.

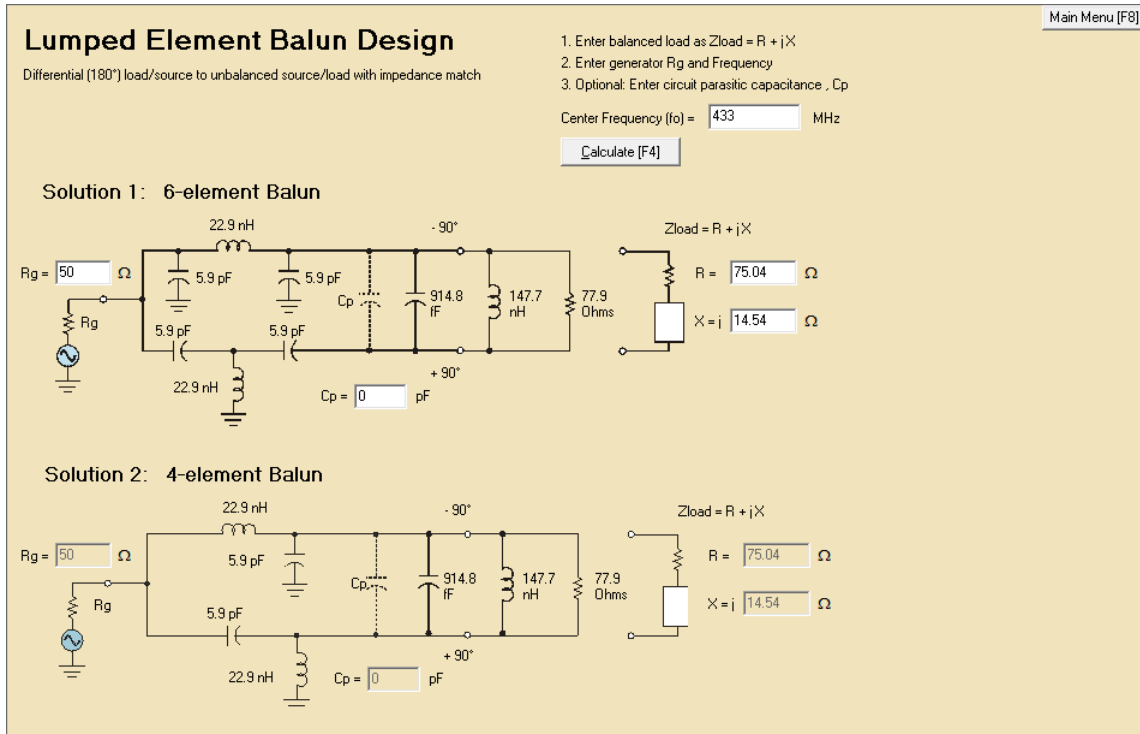


Figure 6.15 – Turnstile with impedance matching in AppCAD

In the market, there is a large variety of power splitters with a phase shift that work in a wide band. The phase shifter chosen was the QCN-5D+ by Minicircuits [20]. This components will allow to achieve the four quadrants of polarization. This device will be used in the PCB design.

### 6.2.3 PCB design for coaxial baluns

The solution with coaxial is chosen to be implemented first because it is flexible to changing the balun configuration. As the antennas developed will be a prototype, the objective is to economize the price of each prototype. Because of this, it is decided to develop a PCB that can integrate both solutions (bodipole & turnstile) on a double layer PCB. The PCB design is shown in Figures 6.16 and 6.17.

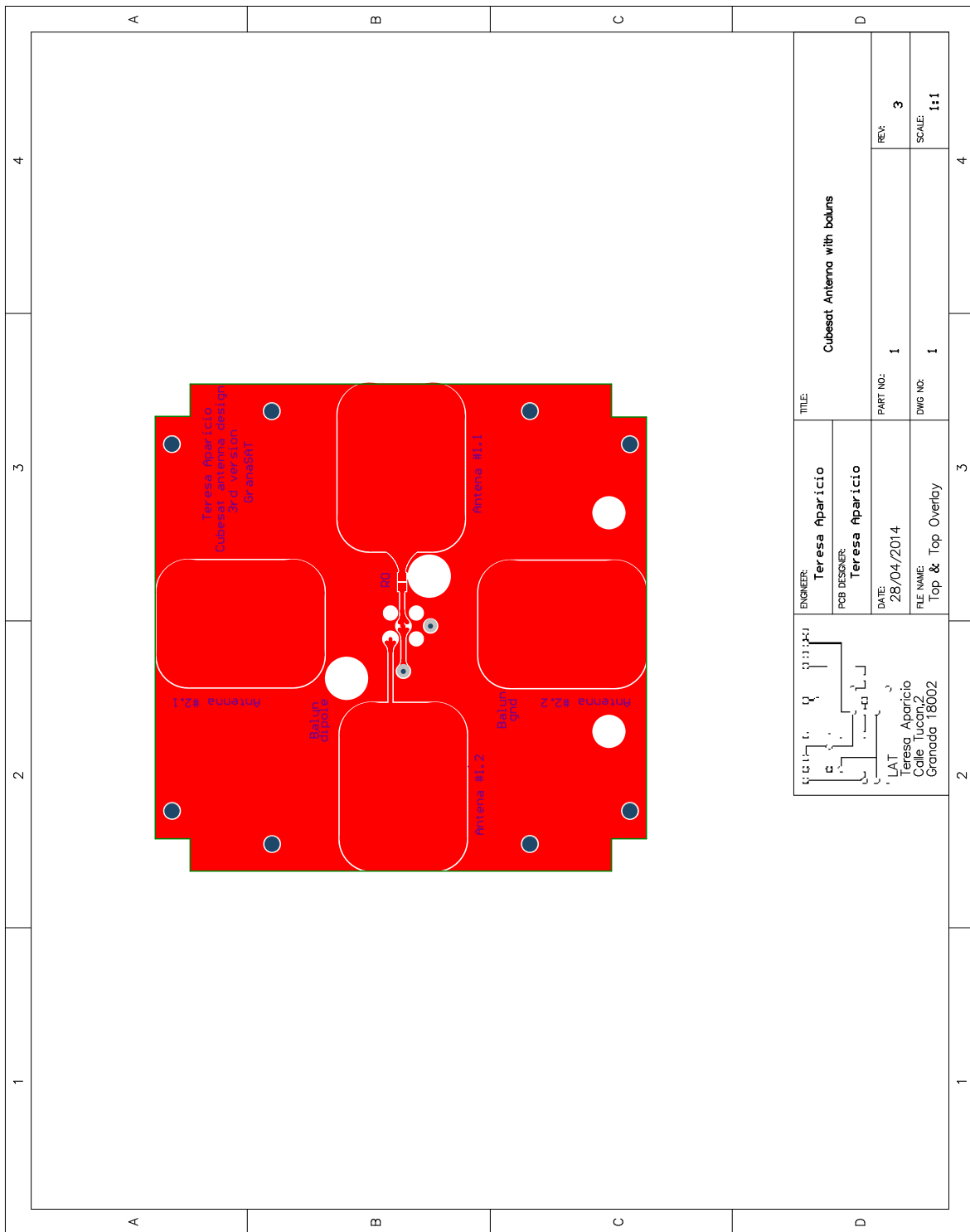
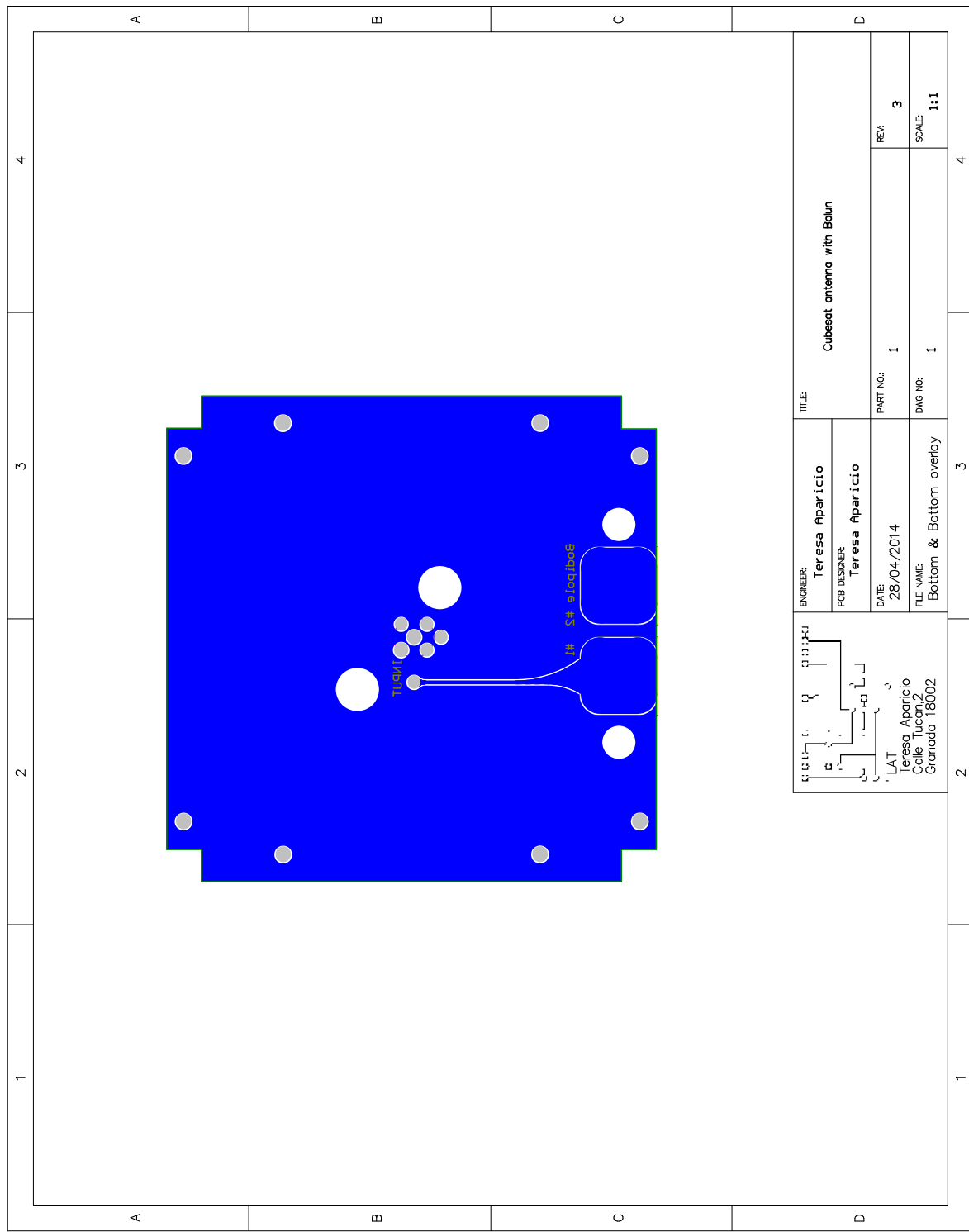


Figure 6.16 – Top layer of the PCB



**Figure 6.17 – Bottom layer of the PCB**

### 6.2.4 PCB design with passive components

With the AppCAD solution and the integration of a phase shifter with a high bandwidth, a double layer PCB can be designed. The design aims to have the flexibility to be used either with the boidipole or with the turnstile, including both solutions. The proposed circuit is shown in Figure 6.19. The use of two resistor of 0 ohms is for having the pads and being able to shortcircuit the feeding with the chosen solution.

The purposed PCB design is in Figure 6.20 and Figure 6.21. The impedance of the tracks can be obtained with AppCAD as well, obtaining the results in Figure 6.18.

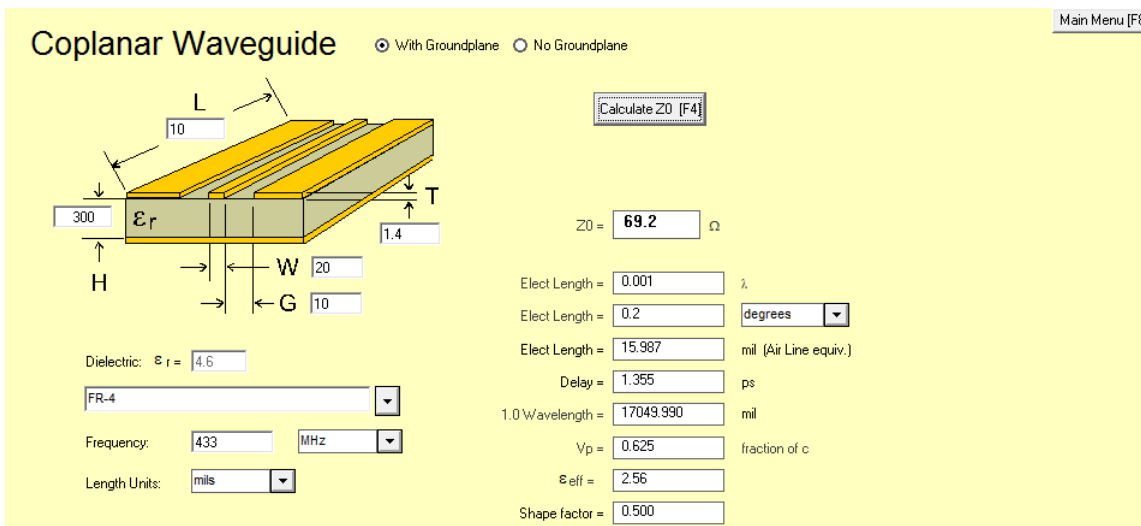


**Figure 6.18 – Impedance of the tracks with the design conditions**

For obtaining the correct phase difference, the distances between the phase shifting are the same for all antennas. The ground planes were made as small as possible for avoiding interferences and achieving the simulated behaviour.

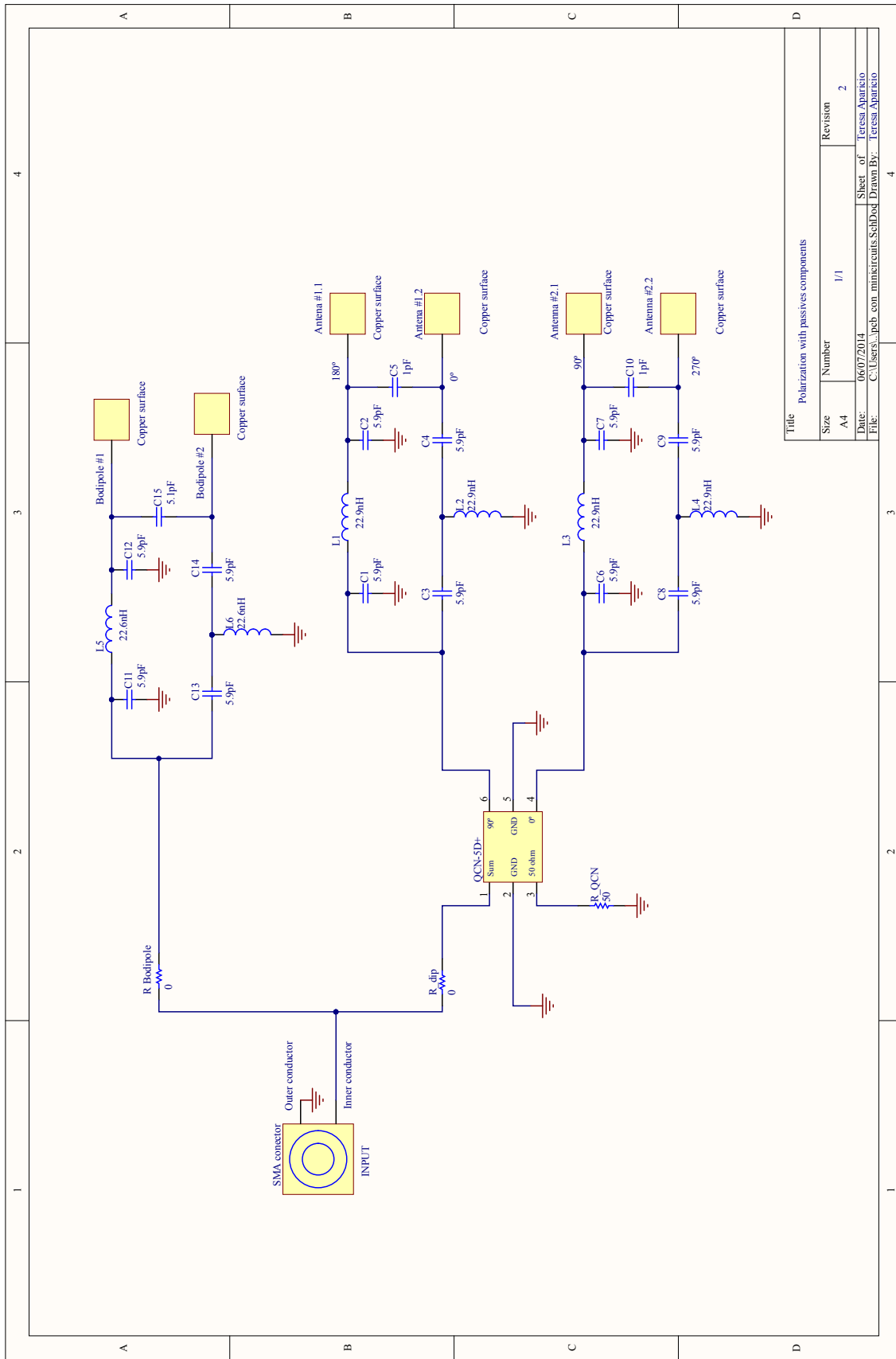


Figure 6.19 – PCB with passives

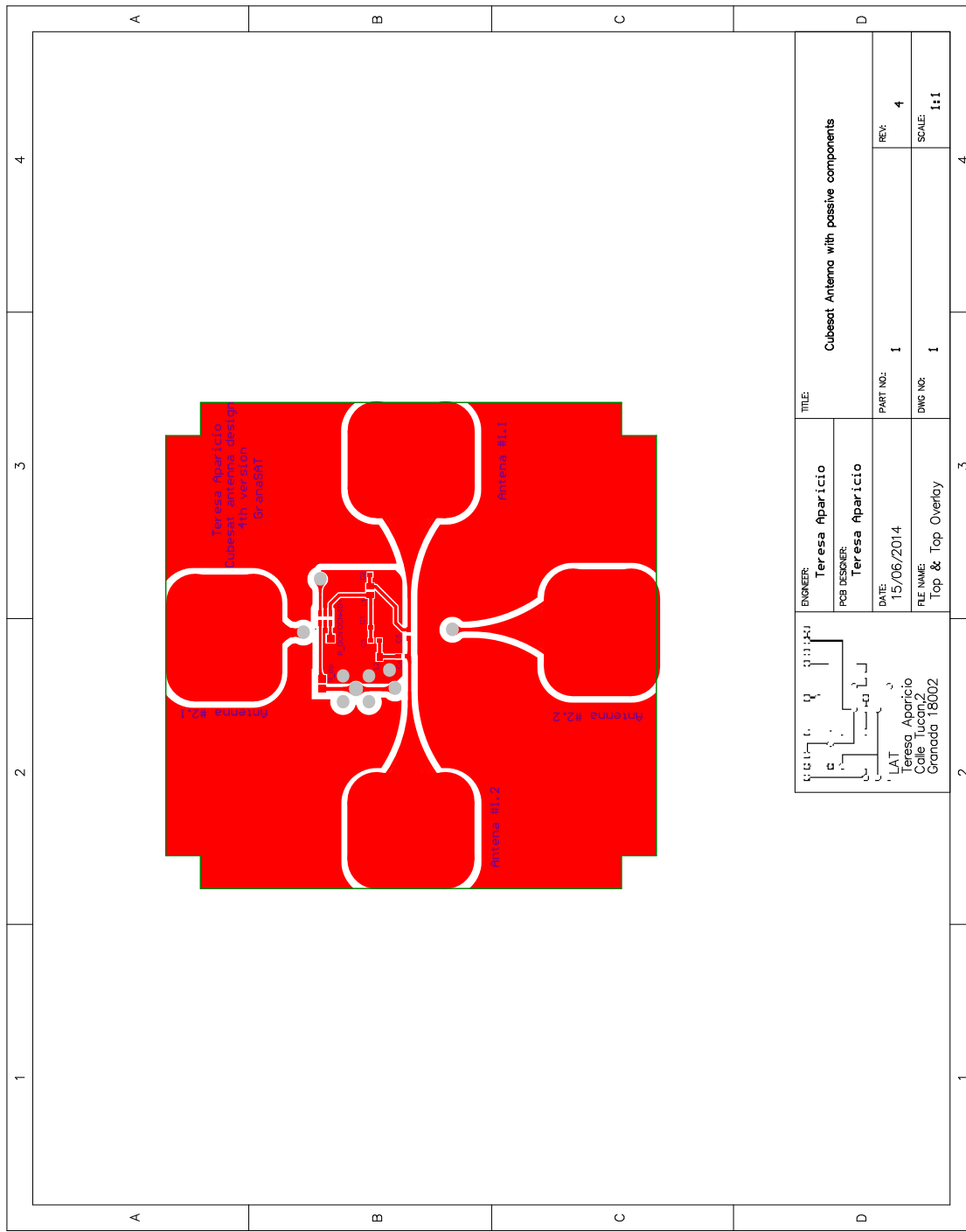


Figure 6.20 – Top layer of the PCB with passive components

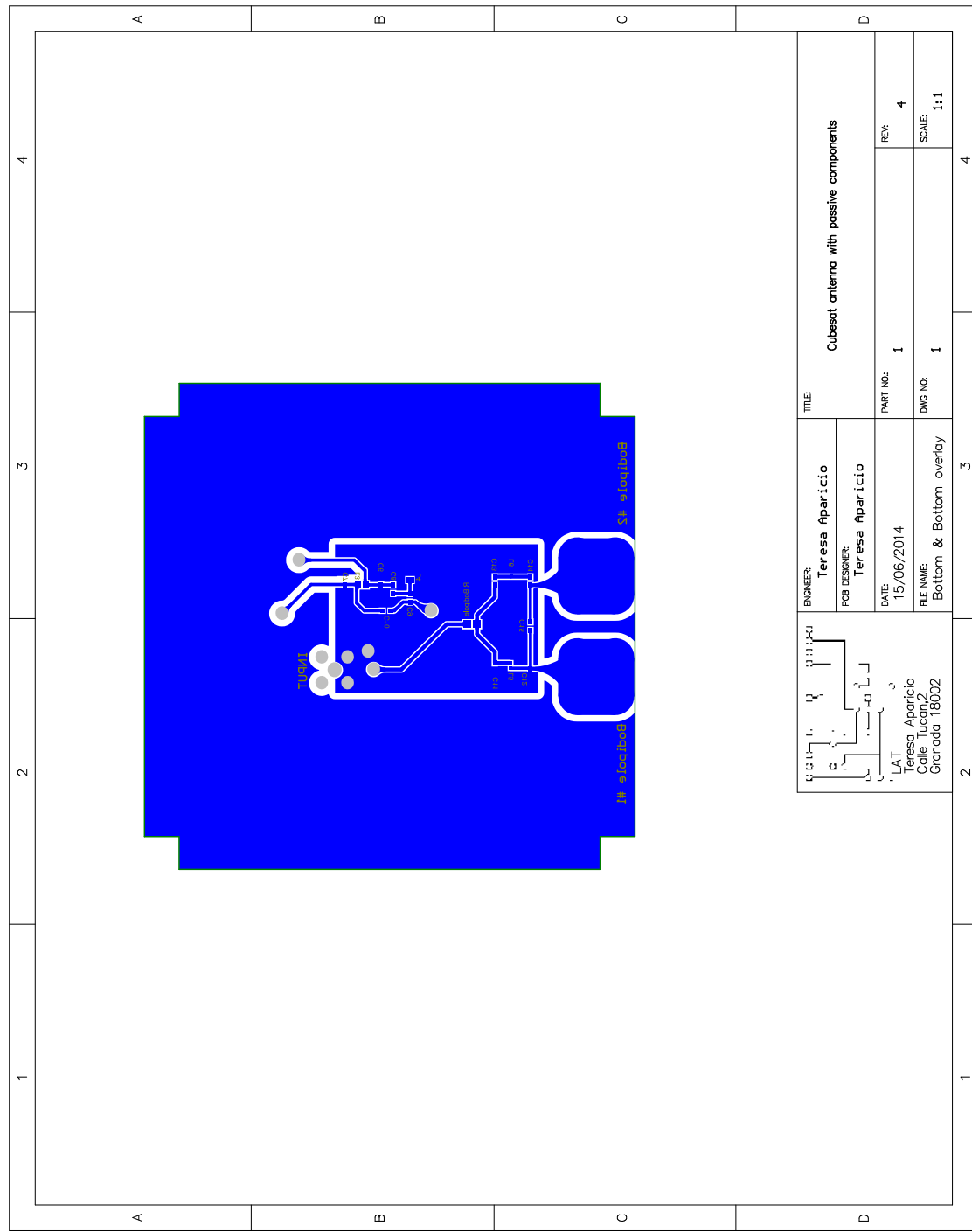


Figure 6.21 – Bottom layer of the PCB with passive components

## 6.3 Antennas fabrication

With the design of the prototype PCB defined, the fabrication of the antenna was undertaken. A milling machine from LPFK was used for producing the PCB. The antennas were built in measuring tape.

### 6.3.1 PCB fabrication

The first step for fabrication with a milling machine is to obtain the gerber files and NC drills in Altium. This can be done by creating an *Output job file* by clicking Right Mouse Button (RMB) on the project, and clicking Left Mouse Button (LMB) in add a new fabrication output as seen in Figure 6.22.

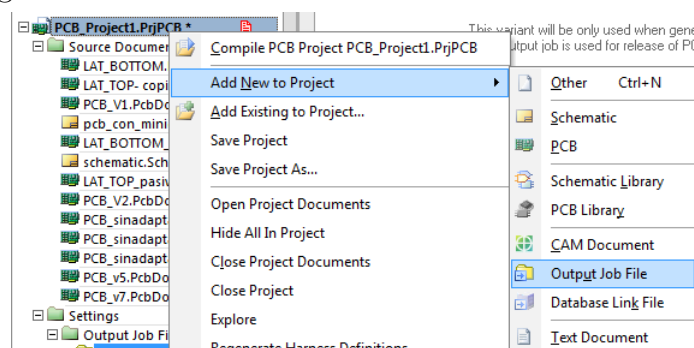


**Figure 6.22 – Creating a new fabrication output**

Adding the gerber files and the NC drills is achieved in Figure 6.23 by doing LMB into *Add New Fabrication Output*. The format should be 2:5 whenever possible (Figure 6.24).

Outputs			
Name	Data Source	Output Description	Enabled
Netlist Outputs			<input type="radio"/>
Documentation Outputs			<input type="radio"/>
Assembly Outputs			<input type="radio"/>
<b>Fabrication Outputs</b>			
Sir_adaptar	PCB_v7.PcbDoc	Gerber Files	<input type="radio"/>
NC Drill Files	PCB_v7.PcbDoc	NC Drill Files	<input type="radio"/>
[Add New Fabrication Output]			
Report Outputs			<input type="radio"/>
Validation Outputs			<input type="radio"/>
Export Outputs			<input type="radio"/>

**Figure 6.23 – Requesting the gerber files and NC drills**

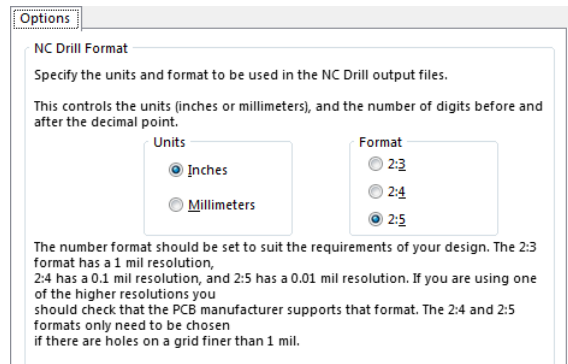


**Figure 6.24 – Selecting the minimum resolution available**

After obtaining all the required files, they should be imported in CCAM and proceed with the fabrication. Because of the material available at the laboratory at the fabrication moment, and as the layers are independent, it is decided to make a single layer PCB for each solution, even though the design was for doubled sided PCB.

### 6.3.2 Antenna implementation on the PCB

Finally, the arrangements of the antennas were made with their corresponding balun as seen in Figure 6.25 and Figure 6.26 .

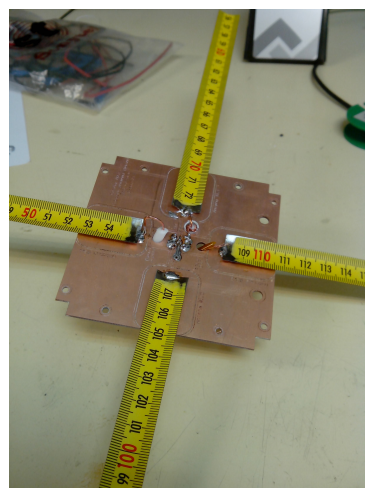


**Figure 6.25 – Turnstile antenna mounted with the coaxial balun**



**Figure 6.26 – Bodipole mounted with the coaxial balun**

## 6.4 Antenna tests

After building the antennas, it was necessary to perform some test in order to verify their behaviour.

### 6.4.1 Bodipole

The antenna was connected to the network analyser and its *SWR* was measured to find out the resonant frequency of the antenna. In Figure 6.27 the results of the measurement are shown.

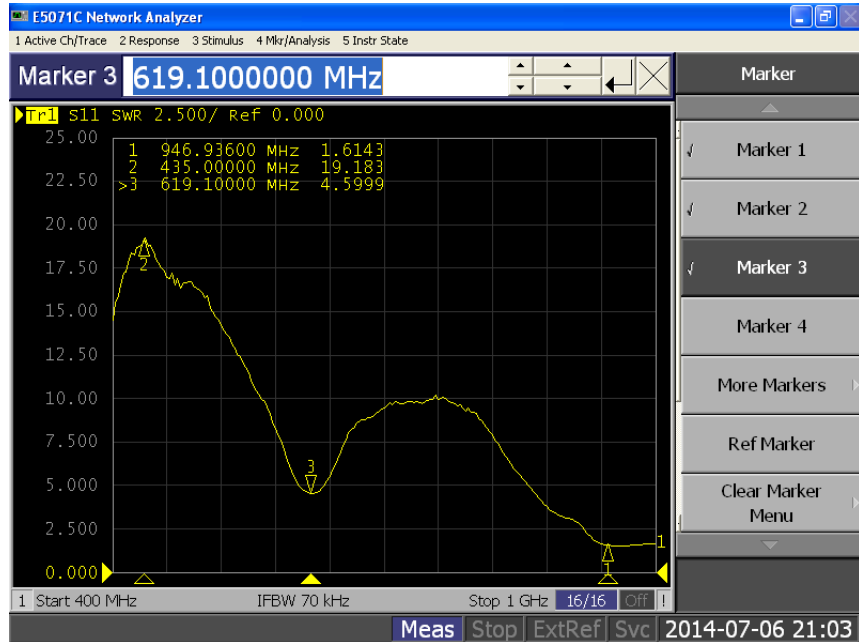


**Figure 6.27 – Bodipole SWR measurements**

It resonates at a different frequency than expected. After some research we could conclude that the  $\lambda/2$  balun does not provide impedance matching for this antenna, including as well some disturbances in the system. As the choke balun is too big for fitting in the antenna space proposed and this solution was thought to be implemented with passive components [7], it was decided to test this system in the future with the passive network.

## 6

### 6.4.2 Turnstile

The turnstile antenna made with tape measure with a length of  $\lambda/4$ . It was connected to the network analyser and the *SWR* was measured (Figure 6.28). There is a larger bandwidth than needed in order to characterise the different resonant points.

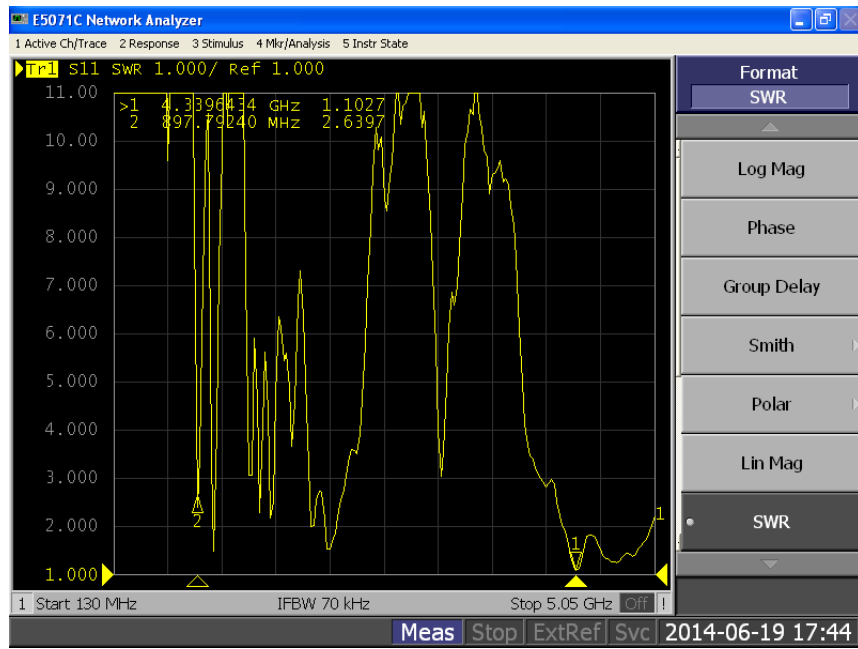


Figure 6.28 – Turnstile SWR measurements

As can be seen, the *SWR* at 433 MHz is over 10. The resonant frequency of the antenna is 897MHz, having a *SWR* of 2.63. As in simulation with thin wires the antenna works at 433 MHz, we decided to change the tape measure to copper wires and measure its *SWR*, the results obtained are in Figure 6.29.

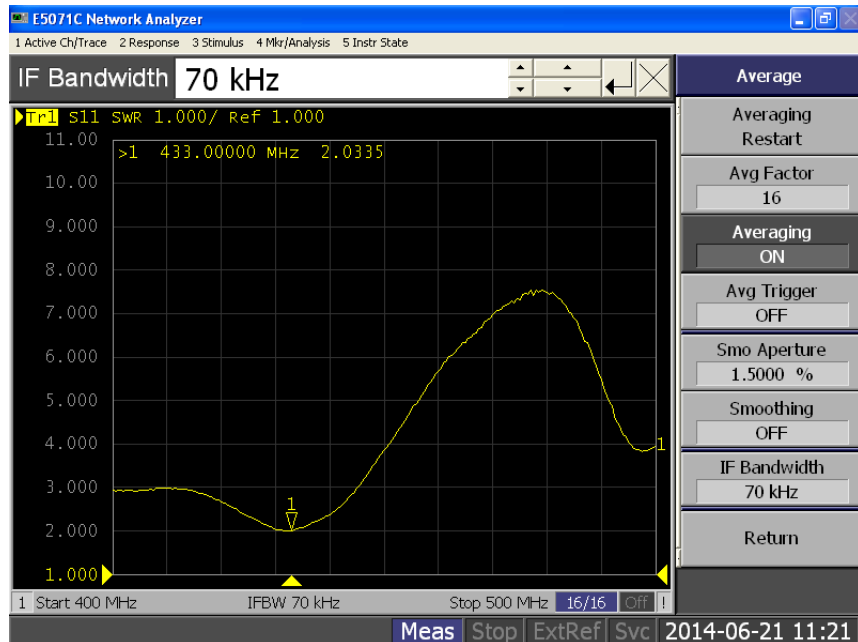
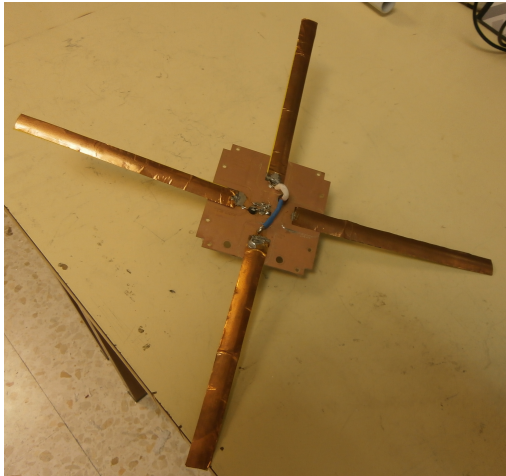


Figure 6.29 – SWR of the turnstile made with wires

The result obtained with the wires was that the antenna is resonant at 433 MHz. Therefore the PCB and the balun is working properly. Facing the problem of the tape measure, we faced different the fact that the metric tape is thinner than the wires (and from a different

material). This can increase its resistance of radiation, changing the resonant frequency. A copper pour was put in the antennas to increase its conductivity 6.30. The new *SWR* measured is in Figure 6.31.



**Figure 6.30 – Turnstile with copper pour**

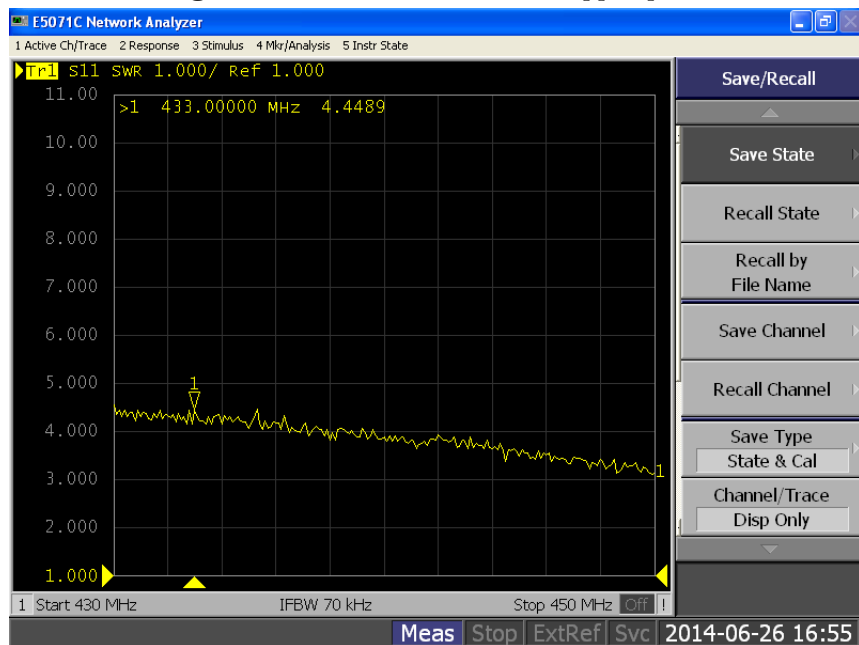


**Figure 6.31 – SWR of the turnstile with copper pour**

As the SWR decreases with the copper, we can conclude that the problem with the original tape measure is its conductivity, explaining the behaviour of the original antennas.

## 6.5 Turnstile antenna with different length

As in the test done in the section above, it shows the resonant frequency of the antenna in Figure 6.26 to be 897 MHz, which is exactly 2.07 times the resonant frequency desired, we can conclude that doubling the length of the antenna will decrease by a half the resonant

frequency [3]. Therefore, a new antenna was built with each part of metric tape equal to 31 cm ( $\lambda/2$ ). The antenna built is in Figure 6.32.

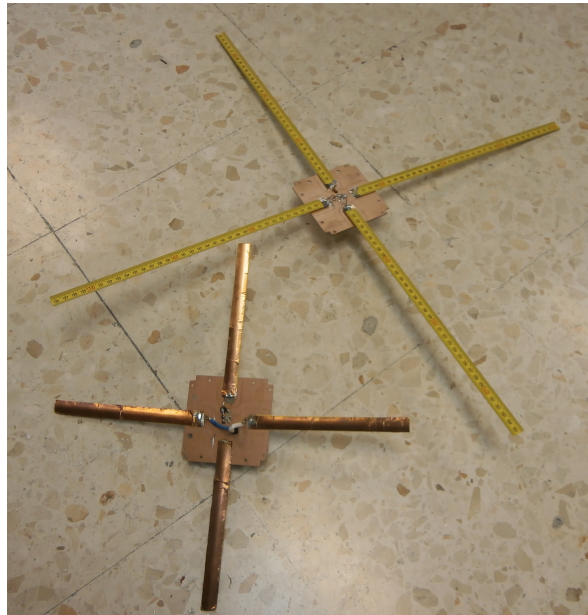


**Figure 6.32 – Original antenna with copper pour and double size antenna**

The new results obtained are in Figure 6.33.

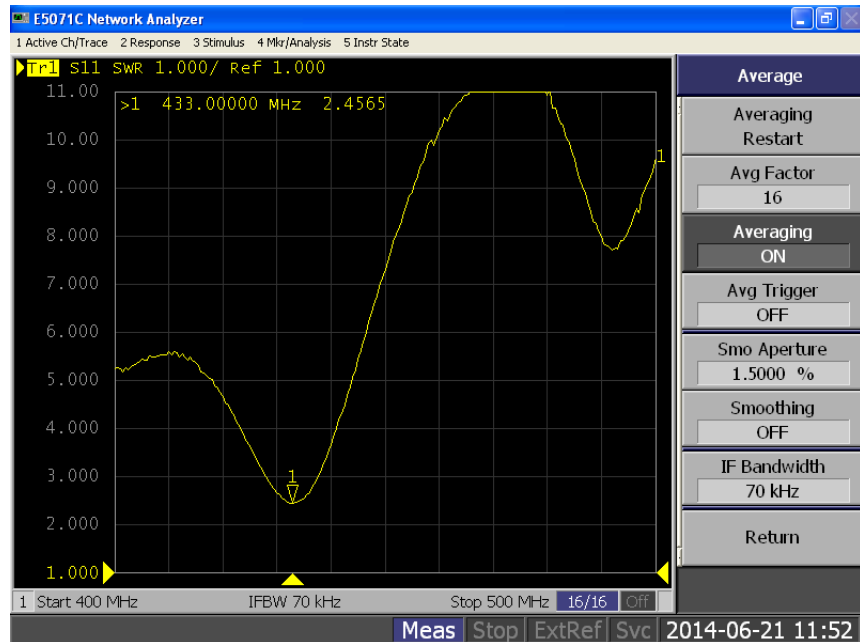


**Figure 6.33 – SWR of the double size antenna**

This antenna has a good  $SWR$ , to avoid losing power when receiving or transmitting. But the circular polarization must be confirmed as well for proper functionality.

### 6.5.1 Circular polarization

Circular polarization can be measured by using a monopole (with lineal polarization) to receive the signal generated with the circularly polarized antenna [2]. A monopole working at 433 MHz was built (Figure 6.34).

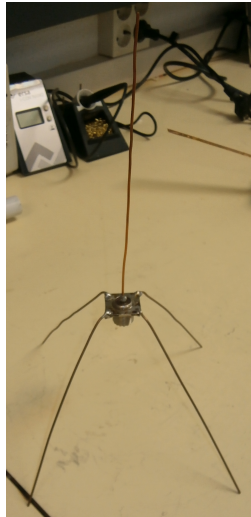


**Figure 6.34 – Monopole working at 433 MHz**

The setup used for measuring the polarization is in Figure 6.35.

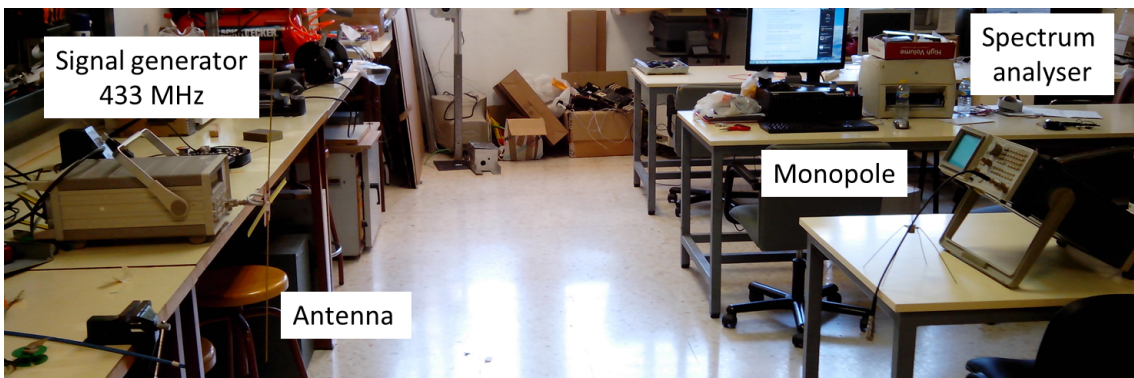


**Figure 6.35 – Setup for measuring circular polarization of the turnstile antenna**

The methodology consists of transmitting with the turnstile antenna, and having the monopole in front of it, make a rotation to observe if it continues receiving. The information shown in the Spectrum Analyser is in Figure 6.36.

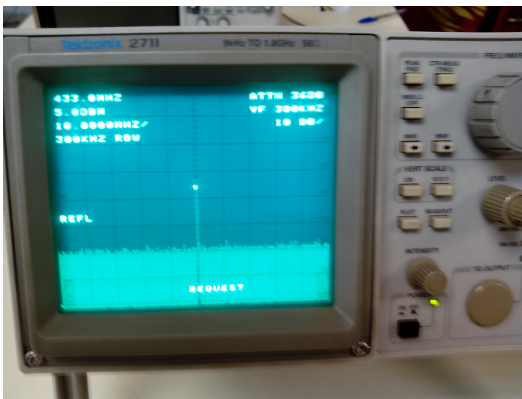


**Figure 6.36 – Spectrum analyser configured at 433 MHz and receiving through the monopole**

The reception works in all the angles of the monopole, achieving circular polarization as seen in Figure 6.37.

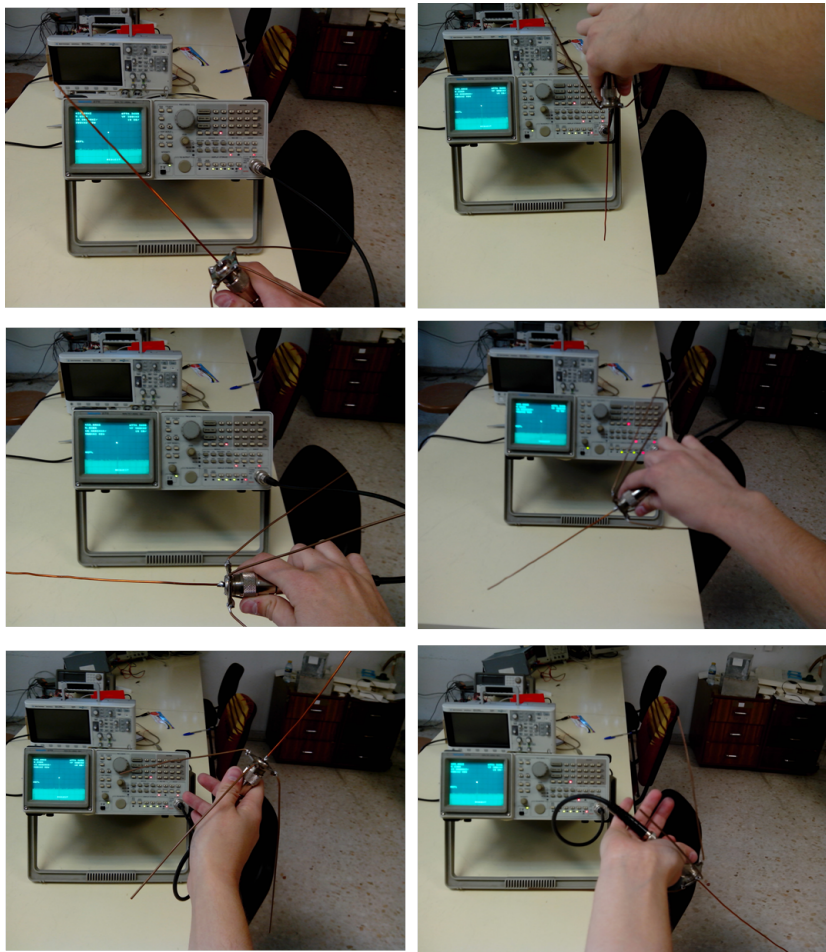


**Figure 6.37 – Monopole receiving in all angles at 433 MHz**

With this changes, a fully working antenna with circular polarization, good impedance matching and a method for an easy deployment is achieved.



## CHAPTER

### 7

# CONCLUSION AND PLANS FOR THE FUTURE

In this Degree Thesis and overview of UHF-VHF communications have been made, following step by step electromagnetic simulations with a professional tool such as Feko® and building different antennas to achieve a final working design of a Cubesat antenna. A small summary on antenna theory was made to be able to understand the different parameters and the comparison between antennas. After some research, a comparison between technologies was made and a receiving antenna was the first step to get the "know-how" about working with these type of electronic devices. At the end a prototype was tested, making changes until getting the desired solution, a fully working prototype with the necessary circular polarization.

The proposed future work is a main part of this project, as it aims to be the first step towards the design of a complete antenna system to implement in GranaSAT. The prototypes developed and this Thesis should allow the future developers of GranaSAT antennas to continue with the final implementation. The future guidelines for achieving a complete working system are the following:

- **Quadrifilar Helix Antenna:** the polarization should be tested with a walkie-talkie working at 137 MHz, analysing if the circular polarization is correctly achieved.
- **Cubesat Antenna Design:** Before the fabrication of the proposed PCB implemented with passive components for the Cubesat, a simulation with Feko should be performed

including the PSPICE models in Feko®. This will allow for confirmation of the behaviour of the circuit.

- **Readjust the parameters for integration:** Before integrating the antennas in the satellite, the solar panels and final configuration of the Cubesat should be taken into account, following the same methodology of simulation before the build stage.
- **Request radio license if needed:** Depending on the frequency of the final design, a radio license might be needed.

From a personal point of view, after doing this work I consider I have gained a deeper knowledge in how to effectively carry out an engineering project. This Thesis was a challenge for me as I did not study antenna theory on its own in the Telecommunications Technology Degree because of my specialization in Electronic Systems. Nevertheless, with this work I consider myself better prepared to face a job search, and understanding about a fundamental part of communications which are widely used today.

# APPENDIX

## A.1 Feko Guide step by step

In this appendix a short and intuitive user guide for creating the 3D models and simulating them in Feko® will be developed. An approach about the capabilities of this CAD will be made followed by an overview of the main software used during this Degree Thesis, CADFEKO and POSTFEKO. A free, fully featured version of Feko® but with limitations on the size of the problem that it can solve can be used for free.

For further information about the software please consult the *Reference Guide* [12].

### A.1.1 Feko® overview

Feko® is a comprehensive electromagnetic simulation software tool, based on state of the art computational electromagnetics (CEM) techniques. It enables users to solve a wide range of electromagnetic problems. Typical applications according to the Feko® website can include:

- Antenna designing
- Antenna placement
- Electromagnetic Compatibility (EMC)
- Bioelectromagnetics
- RF components analysis

-3D electromagnetic circuits

-Radomes

-Scattering problems

1

It allows to import and export CAD models, permitting the user to perform simulations about real problems.

The solution technique used is based on the Method of Moments (MoM) hybridised with other solutions techniques. This enables the software to use a different procedure depending on different parts of the same model.

### A.1.2 Feko® user interface

For a standard user there is a Graphical User Interface (GUI) composed of two main applications: CADFEKO for model definition, simulation and output specification and POSTFEKO for post-processing of simulated results. The standard Feko workflow is detailed in Figure A.1.

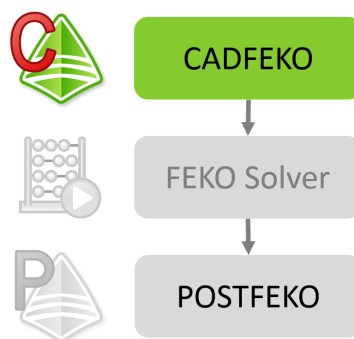
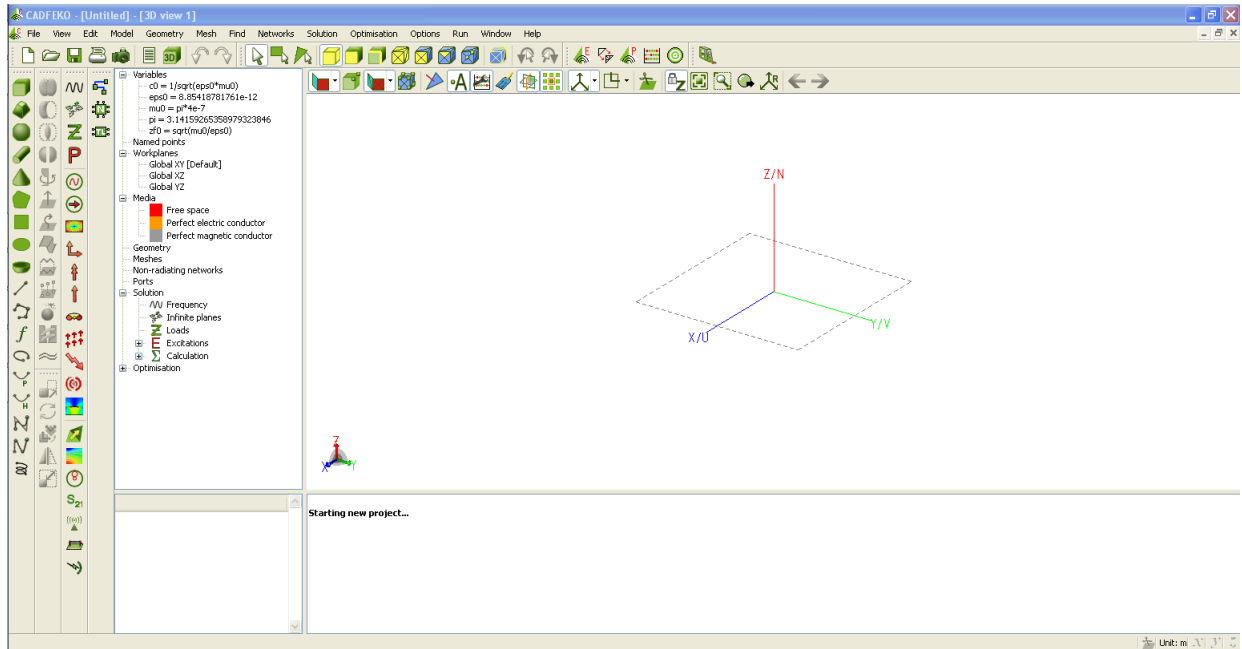


**Figure A.1 – Feko workflow**

#### A.1.2.1 CADFEKO

We can create 3D geometry using canonical structures, as well as import and modify CAD models. It has a large amount of parameters to define and a big number of options.



1

**Figure A.2 – CADFEKO screen on startup**

In this appendix, we will follow a step by step procedure for simulating a half wave dipole described in Chapter 4.

#### A.1.2.1.1 Selecting the model unit

Depending on the application, the unit might change. This can be changed by doing RMB on *Model Unit* and selecting the more convenient for us. In the dipole example the unit used is meters shown in Figure A.3.

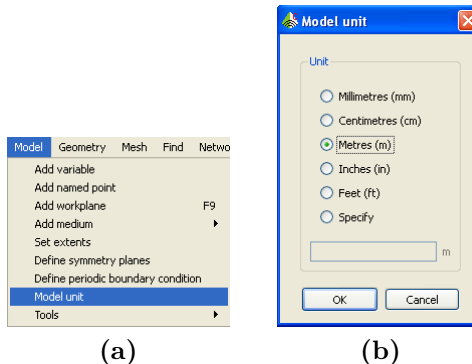


**Figure A.3 – Selecting the unit for the enviroment**

#### A.1.2.1.2 Creating variables

In the variables tree, we can create those variables that we consider important, using equations and other variables for computing. For example, we can define the frequency under

( $f_0$ ) study by doing (RMB) on *variables* and selecting *Add variable* (Figure A.4):

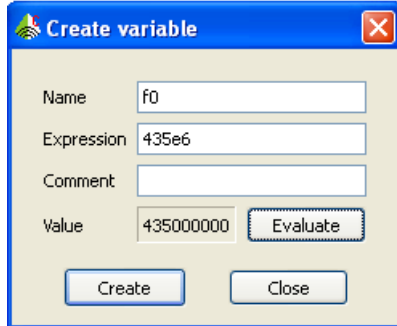


**Figure A.4 – Defining the frequency under study**

We can create variables depending on others previously defined by including the expression and using the (LMB) on *Evaluate*. In Figure A.5 the variable lambda is created.

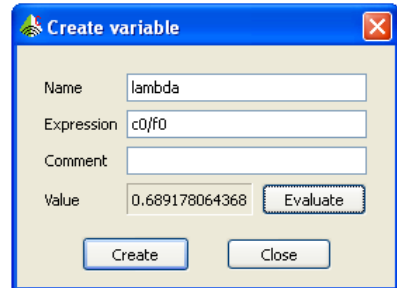


**Figure A.5 – Creating a variable from other variables**

#### A.1.2.1.3 Creating 3D models

The leftmost bar (where some different shapes can be seen) will be used for creating the 3D models . In this Final Degree Project, the line and polyline element were enough for creating all the models required in this work. We will define the line or polyline point by point (either with numbers or with variables) as depicted in Figure A.6 for a half wave dipole.

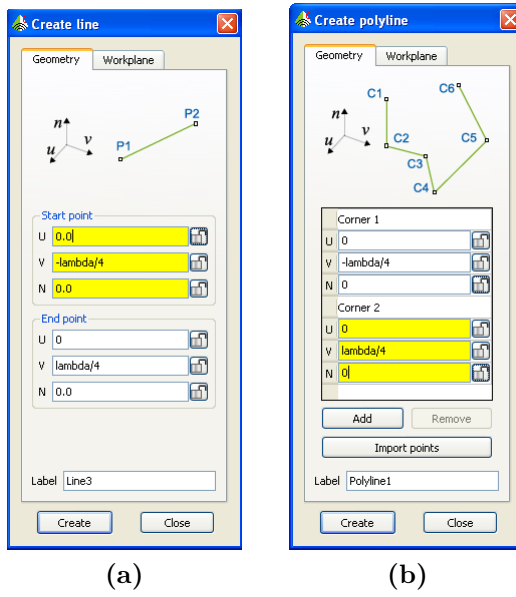


**Figure A.6 – Menu for creating a line and a polyline**

#### A.1.2.1.4 Creating ports

A port is needed for feeding the line. Using the RMB on *port* and selecting with LMB *add a wire port* will create a port:

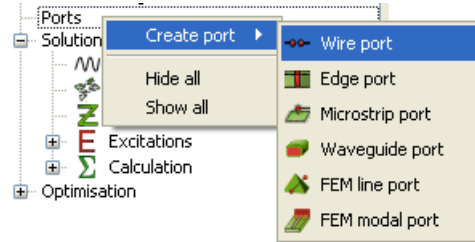


**Figure A.7 – Selection for defining a wire port**

Then we need to select the wire where the port will be and its position. The dipole will have the feeding at the centre of it, so we need to select middle of the segment and do RMB on the line as seen in Figure A.8. We can see a 3D placement of the port:

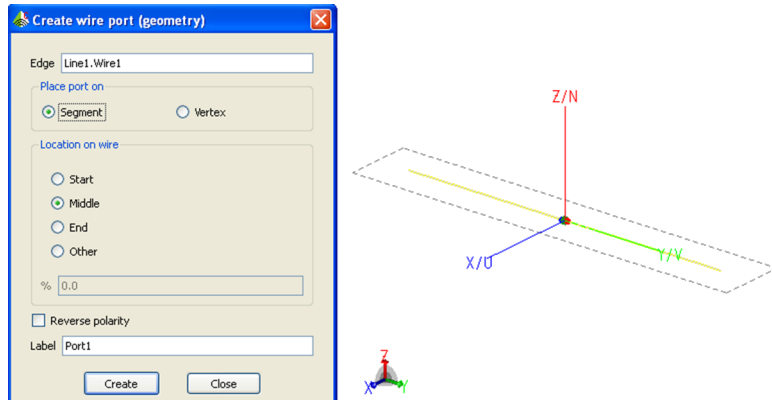


**Figure A.8 – Defining the wire port parameters**

#### A.1.2.1.5 Excitations

We can add many different type of sources, but in the models under analysis in this work the excitation used was the *Voltage source*. RMB on *Excitations* and LMB on *Voltage source*

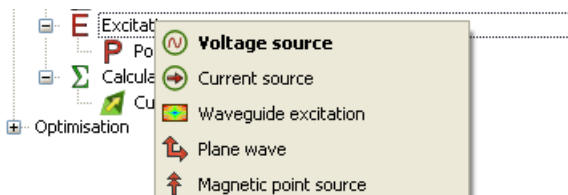


**Figure A.9 – Selecting a voltage source**

On the next screen the wire port where the source is should be selected. Set the parameters of the source include the voltage and the phase:

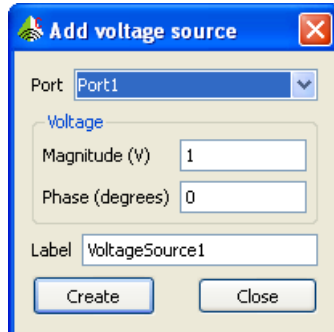


**Figure A.10 – Defining the voltage source parameters**

#### A.1.2.1.6 Solution frequency

The frequency can be a single one or a discrete interval for simulation purposes. Use RMB on *Frequency* as seen in Figure A.11 and Figure A.12 for setting the parameters. In the dipole example a single frequency analysis will be made for simpleness:



**Figure A.11 – Selecting the frequency analysis**

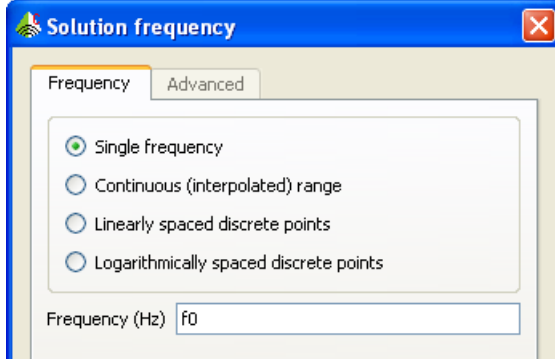


**Figure A.12 – Setting a single frequency**

#### A.1.2.1.7 Far field request

We can request a far field analysis using RMB on *Calculation* as seen in Figure A.13:



**Figure A.13 – Requesting a far field calculation**

On the Request Far Field window that appears, we should select the planes under study defining  $\Delta\theta$  and  $\Delta\phi$  as well as the number of points requested. In Figure A.14 a complete sphere for calculations was requested :

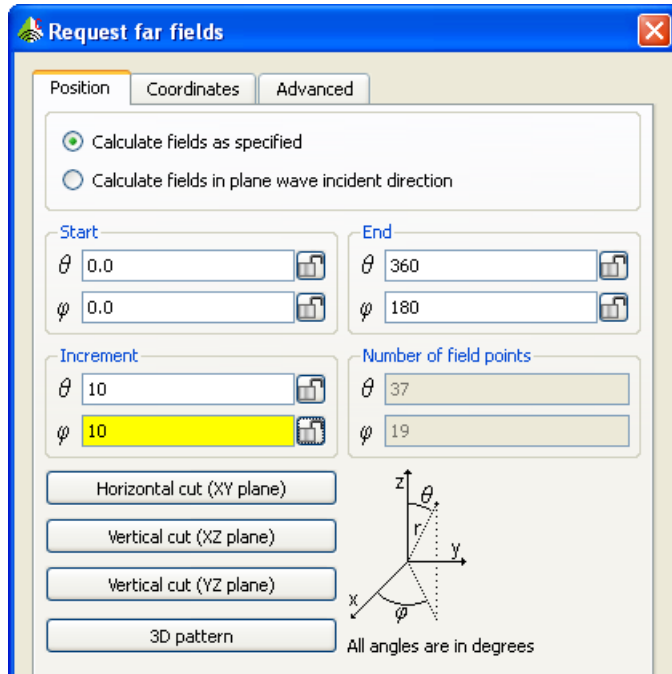


**Figure A.14 – Setting the far field request to cover all the points**

#### A.1.2.1.8 Meshing

We need to convert the model into an assembly of finite point mesh for simulation purposes. Therefore, we need to do RMB on *Meshes*:



**Figure A.15 – Accesing the mesh options**

We have to select the length of the wire segment as well as the radius. We should select a radius small enough for having a uniform current distribution on the conductor, for example 1 mm (A.16):

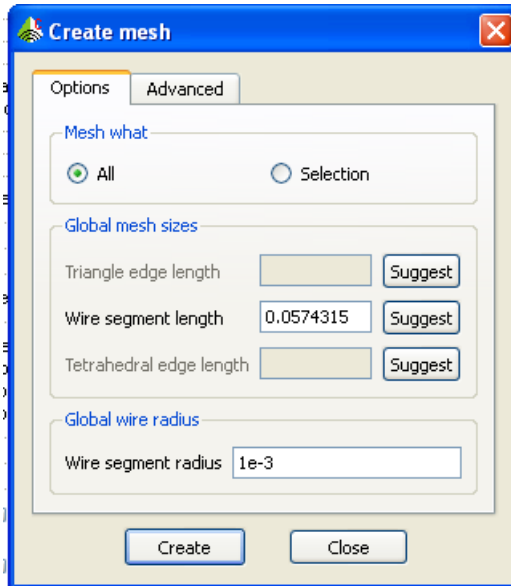


**Figure A.16 – Setting the mesh parameters**

#### A.1.2.1.9 Validating the model

Before the simulation starts, we have to validate that all the parameters needed are defined, for doing so we perform LMB on *Solution* and select *EM validate*:

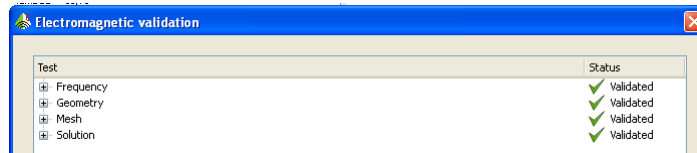


**Figure A.17 – Validation of the parameters**

#### A.1.2.2 Feko Solver

Once the model is created and defined, we can run the simulation by clicking on *Run Feko*.

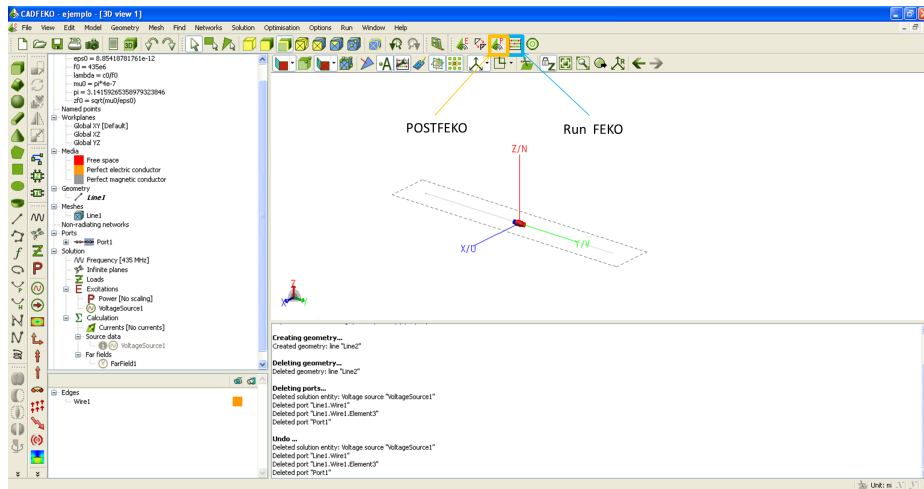


Figure A.18 – POSTFEKO and Run FEKO® button

### A.1.2.3 POSTFEKO

The standard FEKO workflow ends with result processing in POSTFEKO. Click on *Run POSTFEKO* shown in Figure A.18. The POSTFEKO application will start automatically with the results from the simulation. We will have to choose what to represent.

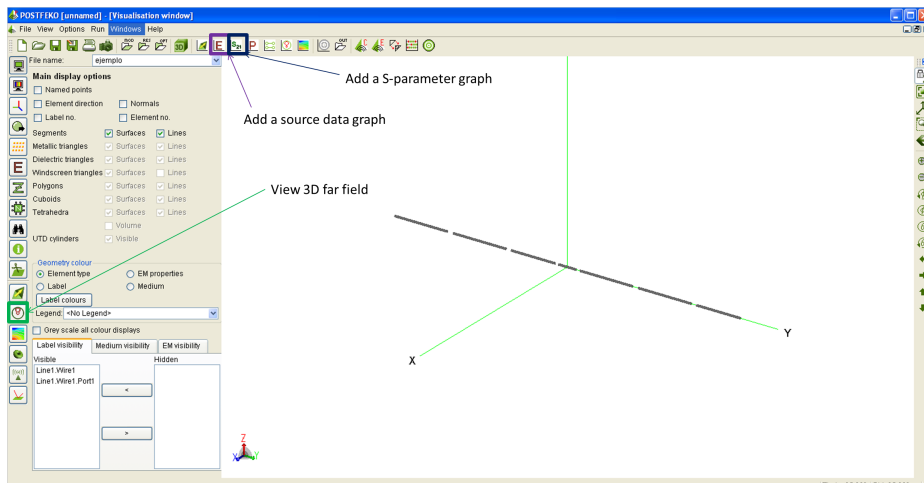
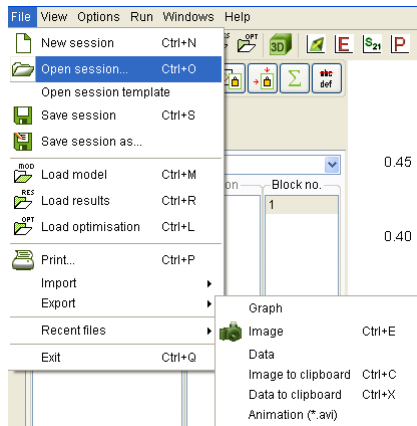


Figure A.19 – POSTFEKO main window

It is possible to export the data in .csv format for processing the information with other software such as MATLAB®. This can be easily done by using the RMB on *File*, *Export* and *Data* (Figure A.20).



**Figure A.20 – Exporting data from simulation**

#### A.1.2.3.1 3D Far field model

On the leftmost part of the POSTEFKO main window (Figure A.19) we can select *View 3D far fields*. We can select what to represent with the different options:

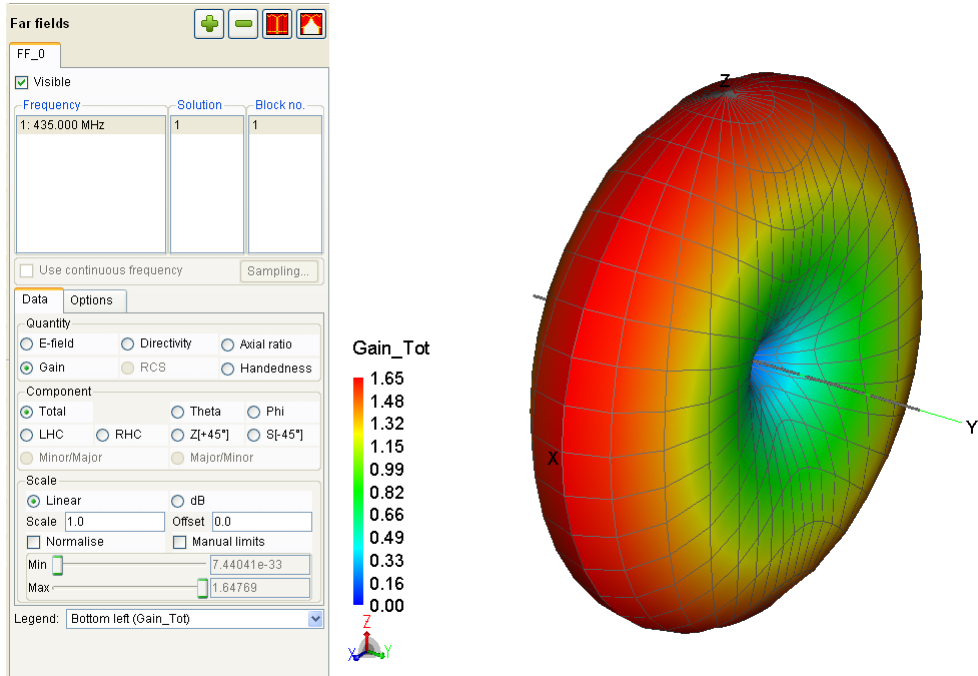


**Figure A.21 – Far field options and results**

With Feko® the polarization of an antenna can be known by plotting the axial ratio and the handedness of the antenna under analysis. The results for the dipole created are in Figure

1

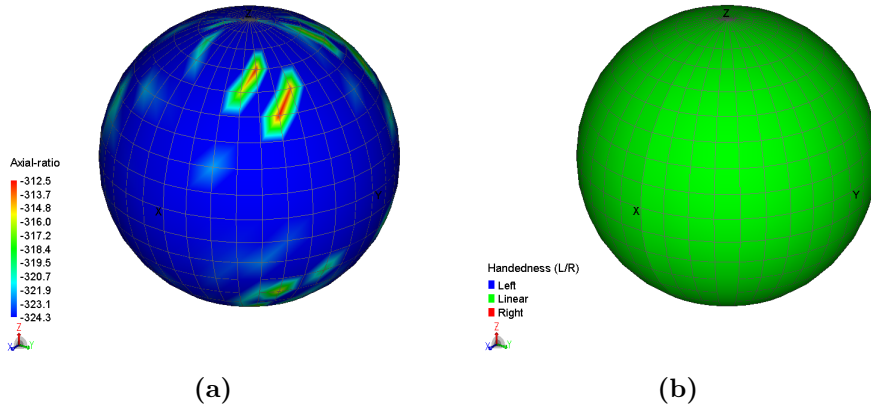


**Figure A.22 –** (a) Axial ratio and (b) handedness of a dipole

### A.1.2.3.2 Working with the scattering parameters

If we click on *Add a S-parameter graph* (Figure A.19) we can work with the S parameters by either obtaining a graphic of its value or either calculating other parameters from the S11 values.

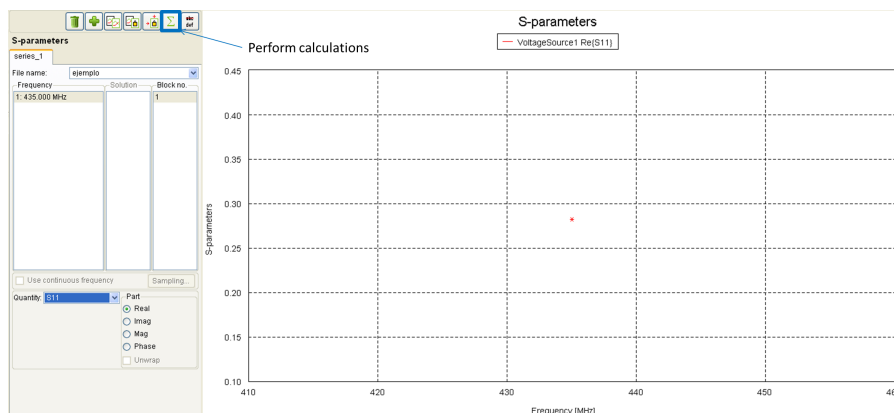


**Figure A.23 – S-parameter graph options**

We can make expressions with the values from the S11 parameters, for example we can obtain the VSWR defined by Equation 3.2.1:

Select with LMB the *Magnitude* option as seen in Figure A.23. Then LMB on *Perform calculations* button and set the calculations of the new series:

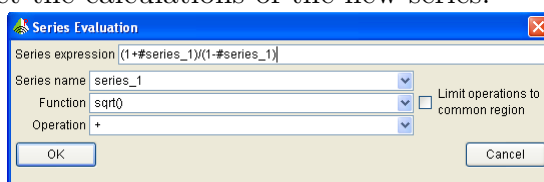


**Figure A.24** – Calculations for the VSWR

### A.1.2.3.3 Source data graph

Feko® has a large number of parameters that can be obtained, like:

- Impedance

- Admitance

- Voltage on the antenna

- Current on the antenna

- VSWR

- Source power

- Mismatch loss

- Active and loss power

- Efficiency of the antenna

RMB on *Add a source data graph* and select the parameter desired as seen in Figure A.25.

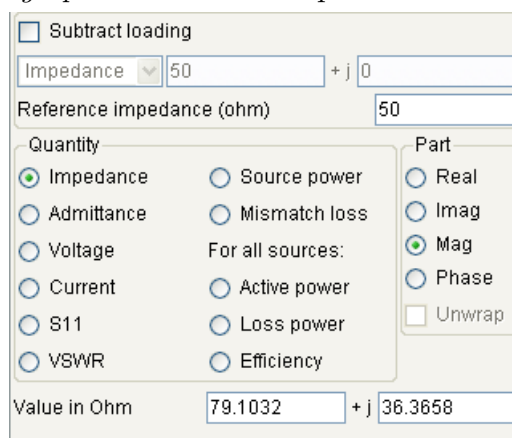


**Figure A.25 – Source data graph options**



# BIBLIOGRAPHY

- [1] Emily Clarke. An introduction to amateur satellite. *AMSAT*, AP-16(1):499 – 500, 1968.
- [2] Constantine A. Balanis. *Antenna Theory: Analysis and Design*. Wiley, 2005. ISBN 978-0471667827.
- [3] Lluís Jofre Roca Ángel Cardama Aznar. *Antenas*. Edicions UPC, 2002. ISBN 84-8301-625-7.
- [4] Wikipedia. *The Free Encyclopedia*. URL [www.wikipedia.org](http://www.wikipedia.org).
- [5] G. Thiele, E. Ekelman, and L. Henderson. On the accuracy of the transmission line model of the folded dipole. *Antennas and Propagation Society International Symposium*, 17:744–747, 2014. URL <http://cp.literature.agilent.com/litweb/pdf/E5071-90070.pdf>.
- [6] Kwai Man Luk Kai Fong Lee. *Microstrip Patch Antennas*. Imperial College Press, 2002. ISBN 1-84816-453-X.
- [7] Kaz Gunning Ana Tarano Niels Joubert, Theresa Johnson. Communications subsystem final report, snaps. 2014. URL [http://stanford.edu/group/ssdl1/SNAPS/files\\_distribution/reports/AA236B\\_20130323\\_COMM\\_Final\\_Report.pdf](http://stanford.edu/group/ssdl1/SNAPS/files_distribution/reports/AA236B_20130323_COMM_Final_Report.pdf).
- [8] American Radio Relay League. *The ARRL Antenna Book*. ARRL, 2000. ISBN 0-87259-804-7.
- [9] Agilent. Agilent E5071C ENA series RF network analyzers datasheet. 2014. URL <http://cp.literature.agilent.com/litweb/pdf/E5071-90070.pdf>.

## Bibliography

- [10] The CubeSat Program. Cubesat design specification. *3rd USAF Symposium on Antennas*, (13), 2014. URL [http://www.cubesat.org/images/developers/cds\\_rev13\\_final.pdf](http://www.cubesat.org/images/developers/cds_rev13_final.pdf).
- [11] A. Sánchez & J. Serra. *UPCSat-1. Analysis, Design and Breadboarding of a University Picosatellite*. PhD thesis, Universidad Politécnica de Cataluña, 2012.
- [12] Feko. Reference guide. 2014.
- [13] G. A. Deschamps. Microstrip microwave antennas. *3rd USAF Symposium on Antennas*, 1981.
- [14] ISIS. Cubesat antenna system. *Datasheet*, 2014.
- [15] C. Kilgus. Multielement, fractional turn helices. *IEEE Trans Antennas and Propagation (Communication*, AP-16(1):499 – 500, 1968. URL <http://ieeexplore.ieee.org/stamp/stamp.jsp?tp=&arnumber=1139459>.
- [16] Steve Blackmore. Quadrifilar helix antennas, 2009. URL [http://perso.wanadoo.es/dimoni/ant\\_qha.htm](http://perso.wanadoo.es/dimoni/ant_qha.htm).
- [17] GA (Us) Charles T. Rauch, Barnesville. Balun for an antenna. (Patent #: US 7,319,435 B2), 2008.
- [18] Giulio Pezzi Fabio Santoni Fabrizio Piergentili Jacopo Piattoni, Gian Paolo Candini. Plastic cubesats : An innovative and low cost way to perform applied space research and hands-on education. *Acta Astronautica*, 2012.
- [19] Pro-Power. Rg58/59 datasheet. 2012. URL <http://www.farnell.com/datasheets/84294.pdf>.
- [20] Minicircuits. Power splitter/combiner qcn-5d+ datasheet. 2012. URL <http://217.34.103.131/pdfs/QCN-5D+.pdf>.

# ACRONYMS

**ABS** Acrylonitrile butadiene styrene is a common thermoplastic used for 3D printing. 58

**CAD** Computer-aided design is the use of computer systems to assist in the creation, modification, analysis, or optimization of a design. 58, 83, 84

**LEO** A Low Earth Orbit is an orbit around Earth with an altitude between 160 kilometres , with an orbital period of about 88 minutes, and 2,000 kilometres , with an orbital period of about 127 minutes. 16, 35, 37

**LMB** Left Mouse Button. 72, 86–88, 91, 94

**MEO** is the region of space around the Earth above low Earth orbit (altitude of 2,000 kilometres) and below geostationary orbit (altitude of 35,786 kilometres. 16

**NOAA** National Oceanic and Atmospheric Administration is a federal agency from the United States focused on the condition of the oceans and the atmosphere. xxi, 6, 41, 48, 49

**PCB** A printed circuit board (PCB) mechanically supports and electrically connects electronic components using conductive tracks, pads and other features etched from copper sheets laminated onto a non-conductive substrate. viii, 4, 7, 55, 65, 73, 81

**RMB** Right Mouse Button. 72, 85–90, 92, 95

## Bibliography

**SNAPS** Stanford Nano Picture Satellite is engineered as an inspector satellite capable of imaging, photo processing and analysis, and downlink. Given the dimensions of the Containerized Satellite Dispenser (CSD), SNAPS will fit alongside a 3U satellite. The minimal intrusion and limited risk of launching SNAPS opens opportunities for photography of a deploying satellite or simply easier access to a launch. xx, 28, 29

**SWR** Standing Wave Ratio is the ratio of the amplitude of a partial standing wave at an antinode (maximum) to the amplitude at an adjacent node (minimum), in an electrical transmission line. xxii, xxiii, 11, 47, 60, 63, 64, 74–76

**UHF** Ultra High Frequency is the ITU-designated range of radio frequency electromagnetic waves from 300 MHz and 3 GHz. xv, 3, 28, 35, 37

**VHF** Very High Frequency is the ITU-designated range of radio frequency electromagnetic waves from 30 MHz to 300 MHz. xv, 3, 35, 37